1-2011

Investigating the Influence of Organic Acids on Uraninite Solubility and Uranyl Sorption onto Kaolinite

Michelle L. Barger
Western Michigan University

INVESTIGATING THE INFLUENCE OF ORGANIC ACIDS ON URANINITE SOLUBILITY AND URANYL SORPTION ONTO KAOLINITE

by

Michelle L. Barger

A Dissertation
Submitted to the
Faculty of The Graduate College
in partial fulfillment of the
requirements for the
Degree of Doctor of Philosophy
Department of Geosciences
Advisor: Dr. Carla M. Koretsky

Western Michigan University
Kalamazoo, Michigan
December 2011

INVESTIGATING THE INFLUENCE OF ORGANIC ACIDS ON URANINITE SOLUBILITY AND URANYL SORPTION ONTO KAOLINITE

Michelle L. Barger, Ph. D.

Western Michigan University, 2011

Within anoxic near surface aqueous settings where $UO_{2(s)}$ may be released an opportunity to encounter and complex with organic acids may occur. Reactions between $UO_{2(s)}$ and ligands may promote the solubility and mobility of uranium. Organic ligands investigated in the dissolution work include citric acid, NTA and EDTA. Exposure to the ligands had little effect on $UO_{2(s)}$ solubility. The log activity of $UO_{2(s)}$ hydrolysis under reduced conditions was -6.56. Under all measured conditions of ligand concentration, the data consistently show an increase in uranium concentration to a median log U activity of -4.89. The observed solubility of $UO_{2(s)}$ in the presence of chelating organic ligands is inconsistent with expected values based on literature data, possibly due to inefficient controls on oxidation. Although the solubilities values are higher than expected, these experiments suggest that strong chelating agents will have little effect on $UO_{2(s)}$ solubility.

The second part of this study concerned U(VI) sorption onto Georgia kaolinite (KGa1-b). Sorption was investigated as a function of ionic strength and pCO_2 concentration in the presence or absence of EDTA, citrate and fulvic acid. U(VI) sorption on kaolinite does not depend strongly on ionic strength, but a strong dependence on pCO_2 is observed, with less sorption of U(VI) occurring with increasing pCO_2. U(VI) sorption is enhanced by the addition of EDTA, citric acid or fulvic acid at low pH, likely due to

formation of ternary surface complexes. At high pH, U(VI) sorption decreases, presumably due to formation of competitive aqueous organic ligand-U(VI) complexes. Surface complexation of U(VI) as a function of ionic strength and pCO_2 is well described using a nonelectrostatic or a double diffuse layer model. However, neither model correctly simulates all of the U(VI) sorption edges in the presence of ligands, possibly due to incorrect estimates of $CO_2^{-3}{}_{(aq)}$ concentrations, inaccuracies in the predicted aqueous U(VI)-ligand speciation, partial dissolution of the clay by the organic ligands, or due to poor representation of the electrical double layer in the presence of the organic ligands.

ACKNOWLEDGEMENTS

My success in this work has come about from the support of several people. I want to express the most sincere gratitude to my friend and mentor, Dr. Carla M. Korestsky. Without her unflagging enthusiasm for this project my mental tenacity might never have survived. She has provided me with perspective and guidance when working through many difficult sections of this work. Her experience and attention quickly helped me overcome stumbling blocks and move on to the next phase, I would have stagnated without her direction. I am also very thankful for the summer research assistantships that I was provided. She is a tremendous example of a professor and was very willing to provide insight into the many positions an academic faculty member is expected to fill. I know working with Carla has given me a strong foundation to build my career upon.

Thank you to my other committee members, Dr. Johnson Haas, Dr. Patricia Maurice and Dr. Alan Kehew. Dr. Maurice provided access to Center for Environmental Science and Technology, allowing for TOC anaylses of my samples. I gratefully acknowledge support from the Gwen Frostic Doctoral Scholarship, the Patricia L. Thompson Doctoral Scholarship, the WMU Graduate College, the Department of Geosciences and the National Science Foundation (EAR-0348435). These awards and facilities provided me with the tools and funds to supplement the cost of research, travel, and tuition. It would have been a much harder road without this help.

Thanks to the department staff, Beth Cheeseman, Amy Stonerock and Kathryn Wright. I don't think any student could ever navigate out of this department without these diligent women watching over the details.

I would also like to give credit to my fellow lab mates. Ryan, Tom, Trevor, Andrew, Ann, Allie, and Batboy all made the lab, field and lunches quite fun. The group also made camping and conference trips an unforgettable blast. Carla was always a generous host and leader on these trips and I must thank her once more. I am especially happy to have caught the running bug and enjoyed the yearly relay races Team Geochemistry competed in.

Finally, to my friends and family, without the never-ending love and support of my parents it would have been impossible to get this far. I thank my father, Michael Barger, for teaching me you have to work hard, through his dedication to our family. I thank my mother, Arlene Barger, for her jubilant spirit and warm disposition. I thank you both for lifting me up to these heights through your love. Finally I must thank Roy Holmes, you've stayed with me through the distance and difficulties. If I had not had you as a confidant it may have been too hard. I have to say thank you so much for going through this with me, you stayed beside me during this testing trek.

Michelle L. Barger

TABLE OF CONTENTS

Table of Contents-Continued

Table of Contents-Continued

CHAPTER

LIST OF TABLES

LIST OF FIGURES

List of Figures-Continued

List of Figures-Continued

List of Figures-Continued

CHAPTER I

INTRODUCTION

Uranium (U) is an element of concern

Uranium dioxide ($UO_{2(s)}$) solid occurs naturally in the Earth's crust and is the most abundant uranium mineral on Earth (Ewing 1999). $UO_{2(s)}$ is a resource that is mainly used for fuel in nuclear power plants, military munitions and medical applications. Uranium (U) is classified as a heavy metal, and like most such metals, can be toxic to humans and harmful to the environment. From the front to the back end of the nuclear fuel cycle there are many opportunities for U release into the environment. Removing and processing U ore at the front end of the cycle introduces U to the critical zone where weathering can act on mill tailings resulting in acid mine drainage and subsequent mobilization of U. At the back end of the cycle, used spent nuclear fuel (SNF) presents a distinct management challenge due to the extremely long half-life of ^{238}U. Thus, responsible management of this waste necessitates storage in a long-term repository. However, such a facility has yet to be established in the United States. Morrison and Spangler (1992) report that approximately 35,000 metric tons of spent nuclear fuel is stored throughout the U.S. in temporary locations that present potential opportunities for U release into the environment. Documented cases of U migration from such facilities, such as have occurred at Hanford and Los Alamos (Ewing 1999), compel an understanding of the chemical properties that control and influence U migration and bioavailability.

Dissolution of $UO_{2(s)}$

Two processes that have a strong influence on U mobility and bioavailability are dissolution and sorption. The dissolution of a mineral causes a translocation of the elements that make up the bulk solid into the surrounding aqueous phase. In the solid state, uranium and other elements are considered to be relatively immobile. However, if ions in a mineral lattice are liberated into the aqueous phase, i.e. dissolved by groundwater or another solution, they will become more mobile and bioavailable, posing a greater potential risk to ecosystem and human health. Thus, to accurately predict the fate of U in environmental systems, it is necessary to quantify factors that could modify the solubility of U-containing solids. It is well established that the complexation of metals by organic acids in natural waters can significantly enhance mineral solubility (Pittman and Lewman 1994). However, the ability of commonly occurring natural and synthetic organic acids such as citric acid, EDTA and NTA to promote the solubility $UO_{2(s)}$ is not well understood.

In this study, the solubility of uraninite ($UO_{2(s)}$) in the presence of three organic acids (citric acid, EDTA and NTA) is investigated under anaerobic conditions as a function of pH. Citric acid is an organic acid that is found naturally in soil solutions and is known to form strong U-citric aqueous complexes (Drever and Stillings 1997, Jones 1998, Oburger et al., 2009). Ethylenediamine tetraacetic acid (EDTA) and nitrilotriacetic acid (NTA) are synthetic chelating agents used to remove U precipitates from instruments in nuclear power plants and have been identified as constituents of some spent nuclear fuel (SNF). A primary research aim of this study is to determine solubility equilibria for

$UO_{2(s)}$ in the presence of the EDTA, NTA and citric acid in order to provide a better overall understanding of $UO_{2(s)}$ behavior in near-surface anoxic systems.

Sorption

Sorption is another process that can greatly affect U mobility. The removal of U from the aqueous phase by complexation to a mineral surface can perturb U migration through soils. Atoms at the mineral surface will not be fully coordinated as atoms are in the bulk mineral, and these coordinately unsaturated surface sites can bind, or complex, metals such as U to the mineral surface. This study investigates how U may sorb onto the clay mineral kaolinite and how the presence of three organic acids may modify U sorption on this mineral. The effects of citric acid, EDTA and fulvic acid are quantified. Citric acid and EDTA are described above; fulvic acid is a naturally occuring acid that forms from the degradation of natural organic matter (NOM) and is found in virtually all soil solutions (Pittman and Lewman, 1994). Data from U adsorption edge experiments on kaolinite in the presence and absence of the organic acids are used to constrain surface complexation reaction stoichiometries and to derive stability constants for these reactions.

A brief history of uranium

Uranium was discovered in 1789 by the analytical chemist M.H. Klaproth. Before the radioactive properties of the element were known, interest in uranium was primarily academic. There was a small economic demand for uranium; some compounds were used for coloring glass and porcelain (Cordfunke 1969). The need for uranium and interest in

the metal changed dramatically with the discovery of radioactivity and the advent of the nuclear age. With the newfound properties of the metal, interest in uranium boomed and ore that bore the uranium-bearing minerals became in high demand. Discovery of nuclear fission and the outbreak of the Second World War contributed to a great surge in the need for uranium and uranium-bearing compounds (Cordfunke 1969).

Chemistry of uranium

Uranium, atomic number 92 with a mean atomic weight of 238.03, is classified as an actinide series element. Actinides share certain electronic and chemical properties as a result of their common property of an unfilled 5f orbital. As atomic number increases, an increasing number of electrons are required to neutralize the nuclear charge, and within the actinide family those electrons are characteristically shunted into the 5f orbital. The electronic structure of U allows it to exhibit several valence states.

Oxidation-reduction chemistry

Most uranium chemical species can be placed into two categories based on valence state: more reduced species that contain uranous (U(IV)) and more oxidized species that contain uranyl (U(VI)) (Figure 1.1; Burns 1999). Under reducing conditions in aqueous solutions and at very low pH U(IV) can exist stably as the lone U(IV) cation (Figure 1.1). As pH increases the cation will be hydrolyzed to UOH^{3+} and at circumneutral pH the neutral UO_2 complex dominates. In the presence of O_2 and other oxidizing agents, U can gain two electrons and be oxidized to U(VI). Upon formation in

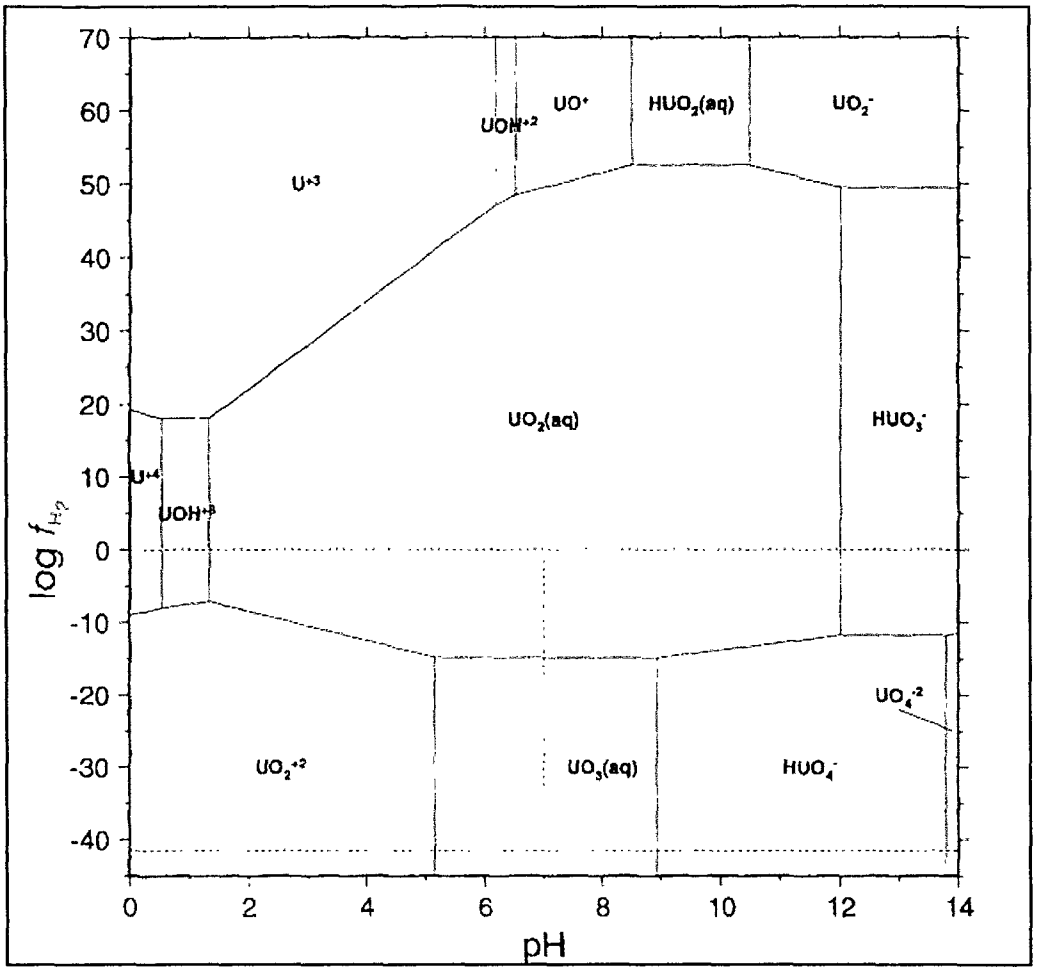

Figure 1.1. Plot of log fH_2 vs pH at 25°C and 1 bar showing fields of relative predominance of aqueous uranium species (after Shock et al., 1997).

aqueous solution or ambient atmosphere, U(VI) will immediately react with two water oxygens to form the uranyl molecule (UO_2^{2+}).

Crystal chemistry of UO_2

$UO_{2(S)}$ possesses the cubic fluorite structure with the U(IV) cation coordinated by eight O atoms in a cubic arrangement, and each O atom bound to four U(IV) cations (Burns 1999). Despite the importance of U minerals, and the considerable attention that they have garnered, our understanding of their crystal chemistry lags well behind that of

many other mineral groups (Burns 1999). U(IV) minerals are often more complicated than the simple $UO_{2(S)}$ fluorite structure would suggest. This complication is due in part to the tendency for U(IV) to partially oxidize. If the outer layer of a U(IV) mineral is in contact with an oxidizing environment it will be oxidized to the more soluble U(VI) (Figure 1.2), complicating the solubility behavior of the mineral. Burns further states that $UO_{2(s)}$ is probably always at least partially oxidized in natural systems.

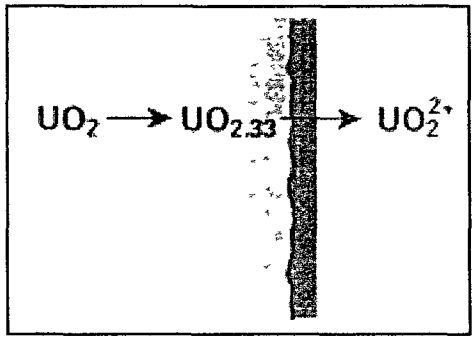

Figure 1.2. Schematic diagram illustrating the formation of oxidized rind on $UO_{2(s)}$ surface (after Shoesmith 2000).

Nuclear properties of uranium

The use of U for nuclear fission makes the element useful, desirable and profitable. There are also many uses for depleted uranium (DU), an industrial byproduct of U enrichment with the fissionable isotope ^{235}U. Uranium is long-lived and present in the Earth in significant amounts (Cotton 2006), with values ranging from 1.2 μg/g in sedimentary rocks to 120 μg/g in phosphate rocks (Langmuir 1997). Uranium exists as three naturally occurring isotopes, ^{238}U, ^{235}U and ^{234}U. ^{238}U is the most abundant, followed by ^{235}U and ^{234}U (Table 1.1).

Table 1.1. Naturally occurring isotopes of uranium (after Jiang and Aschner 2005).

Isotope mass	Atomic percentage
238	99.2745
235	0.720
234	0.0055

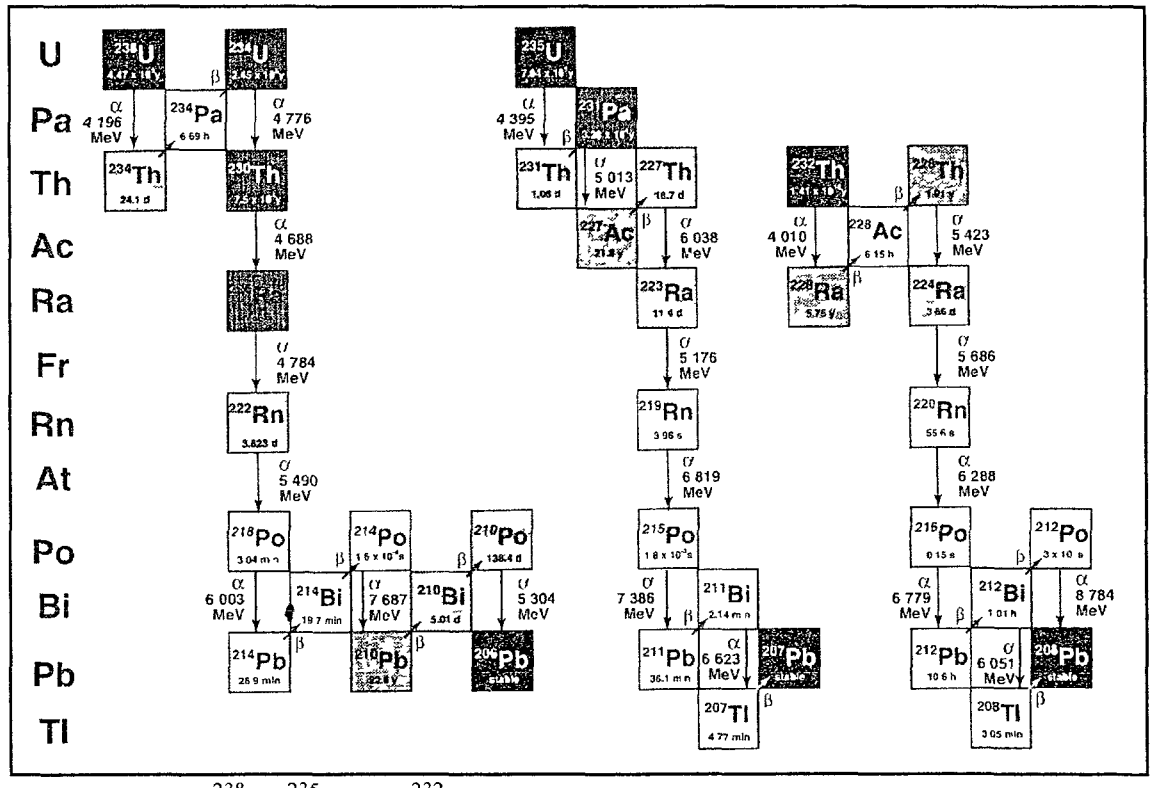

Figure 1.3. The ^{238}U, ^{235}U and ^{232}Th decay chains. The grayscale reflects half-life, with darker grays for longer half-lives (after Eby 2004).

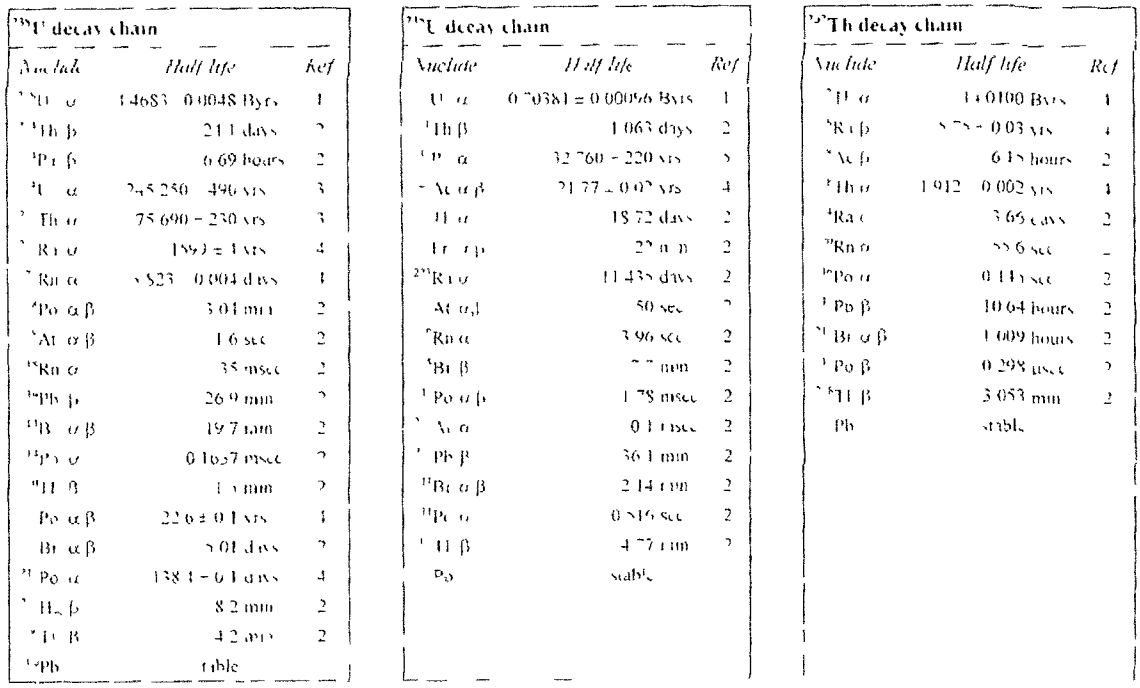

^{238}U decay chain		
Nuclide	Half life	Ref
^{238}U α	4.4683 ± 0.0048 Byrs	1
^{234}Th β	24.1 days	2
^{234}Pa β	6.69 hours	2
^{234}U α	245,250 ± 496 yrs	3
^{230}Th α	75,690 ± 230 yrs	3
^{226}Ra α	1599 ± 4 yrs	4
^{222}Rn α	3.823 ± 0.004 days	1
^{218}Po α β	3.04 min	2
^{218}At α β	1.6 sec	2
^{218}Rn α	35 msec	2
^{214}Pb β	26.9 min	2
^{214}Bi α β	19.7 min	2
^{214}Po α	0.1637 msec	2
^{210}Tl β	1.3 min	2
^{210}Po α β	22.6 ± 0.1 yrs	1
^{210}Bi α β	5.01 days	2
^{210}Po α	138.4 ± 0.1 days	4
^{206}Hg β	8.2 min	2
^{206}Tl β	4.2 min	2
^{206}Pb	stable	

^{235}U decay chain		
Nuclide	Half life	Ref
^{235}U α	0.7038 ± 0.00096 Byrs	1
^{231}Th β	1.063 days	2
^{231}Pa α	32,760 ± 220 yrs	5
^{227}Ac α β	21.77 ± 0.03 yrs	4
^{227}Th α	18.72 days	2
^{223}Fr α β	22 min	2
^{223}Ra α	11.435 days	2
^{219}At α β	50 sec	2
^{219}Rn α	3.96 sec	2
^{215}Bi β	7.7 min	2
^{215}Po α β	1.78 msec	2
^{211}At α	0.1 msec	2
^{211}Pb β	36.1 min	2
^{211}Bi α β	2.14 min	2
^{211}Po α	0.516 sec	2
^{207}Tl β	4.77 min	2
^{207}Pb	stable	

^{232}Th decay chain		
Nuclide	Half life	Ref
^{232}Th α	14.0100 Byrs	1
^{228}Ra β	5.75 ± 0.03 yrs	4
^{228}Ac β	6.15 hours	2
^{228}Th α	1.912 ± 0.002 yrs	1
^{224}Ra α	3.65 days	2
^{220}Rn α	55.6 sec	2
^{216}Po α	0.145 sec	2
^{212}Pb β	10.64 hours	2
^{212}Bi α β	1.009 hours	2
^{212}Po β	0.298 μsec	2
^{208}Tl β	3.053 min	2
Pb	stable	

Figure 1.4. Half-lives for the U and Th decay series (after Burdon et al., 2003).

Past efforts to characterize and understand the radioactive properties of U elucidated the phenomena not only of isotopes but also of radiation. The discovery of radioactivity, α-particles, β-particles and γ-rays resulted from unraveling the U and thorium (Th) decay series (Figure 1.3). The relatively long half-lives of U isotopes make these nuclides particularly suited to investigating many geological processes that occur over time scales similar to their decay period (Burdon et al., 2003) (Figure 1.4).

Inducing U fission results in the capture of energy used to produce electrical power and results in the production of SNF (Wronkiewicz and Buck 1999). U fuel for these processes is produced via U ore mining, which can result in leakage of U waste into the environment. Uranium can also enter near surface systems via leaching of mine tailings, military applications, power plant activities, and radioactive waste disposal. The potential release of U from crystalline $UO_{2(s)}$ into groundwaters and surface waters

necessitates an understanding of how the mineral will react in typical near surface aquatic systems.

The nuclear fuel cycle

The nuclear fuel cycle is typically divided into three types of processing. The "front-end" of the cycle involves exploration, development, mining, milling, conversion, enrichment, and fuel fabrication (Finch 1997). Currently in the United States more than 230 million tons of U mill tailings are stored at U mill sites (Morrisson and Spangler 1992). The "middle" division of the fuel cycle takes place at the nuclear power plant where energy production is derived from U fission. The "back-end" concerns the handling and reprocessing of spent fuel and disposal of the waste. Properly storing and disposing of spent fuel is an immense problem. It is estimated that by 2020 the quantity of spent nuclear fuel in the U.S will grow to nearly 80,000 metric tons (Ewing 1999).

Uranium mines, milling, and tailing pit

The great demand for uranium ore requires extraction of U from the Earth's crust, which contains an average U concentration of ~2.7 ppm (Blanpain 2005). Many locations in the U.S. contain significant U reserves or historical reserves. For example, American mining of U was once intense in the Colorado Plains and the South Texas Gulf Coast. In the 1980s, production dwindled and the U.S. lost the position as the world's leading producer to Canada (Finch 1997). Although production has peaked, U waste from past mining activity must still be managed.

Geographically, U resources are concentrated in a few places in the world; these are mainly located in Canada, Czech Republic, Germany, South Africa, Kazakhstan, Uzbekistan, Australia and the United States (Finch 1997). Finch (1997) states that in 1993 the world consumption of pitchblende (U_3O_8) was 150,000,000 pounds. U from mining activity is utilized for fissionable material in nuclear power plants, and depleted uranium (DU) resulting from the fuel enrichment results in byproducts, such as bullets, that are mainly used by the military. Furthermore, the resulting high density DU is used as weight ballast for airplanes and submarine, although due to the environmental concerns these uses of DU are being phased out (Uijt de Haag et al., 1992). The front end of the uranium cycle first involves removing and processing U from deposits in the subsurface. Uranium is mined by three basic processes: solution mining (in situ leaching), surface mining (open pit), and underground mining (Abdelouas 2006). Solution mining involves the subsurface removal of uranium from reduced ore minerals. Surface and underground mining are of great concern due to the storage and management practices of the resulting mill tailings. Surface pit mining consists of digging large holes in the ground to extract minerals that occur near the surface (Abdelouas 2006). Underground mining involves a shaft that reaches the ore deposit, which can then be extracted and removed from the underground system (Abdelouas 2006). After mining the rock, crushing or milling is a necessary first step for the processing of ore. One of the more environmentally troublesome by-products of the mineral processing operation are the tailings; they are usually finely divided and as a result, readily subjected to chemical weathering processes (Abdelouas 2006). Mill tailings are therefore a potent threat to environmental systems. Tailings from uranium mines often contain other radioactive

elements found in the uranium decay chain, including Th, Ra, Po and Rn, together with other heavy metals that can be leached from the tailings to produce contaminated runoff.

The inappropriate conditioning and disposal of tailings waste permit the contaminants to spread into air, soil, sediment, surface water, and groundwater. For example, if U in tailings comes into contact with organic acids in soil, sediments or aqueous solutions, U might be leached from the solid phase due to formation of organic complexes, greatly enhancing U mobility and bioavailability in the biosphere. Other processes that could mobilize U from the solid phase include: changes in pH and Eh resulting in changes of the U speciation and/or oxidation state, adsorption onto mineral or organic surfaces, formation of inorganic complexes with phosphate, carbonate or other anions and remineralization into secondary solids.

Each of these processes are potentially at work in the mine pits where tailings are contained. At the surface of the pits the tailings are exposed to oxidizing conditions, allowing the more soluble UO_2^{2+} species to form. Francis et al. (1991) reports that the predominant mechanism of dissolution of U from ores is oxidation of U(IV) to the more soluble U(VI).

Acid generation is also an issue affecting the solubility of UO_2 tailings. Pyrite is often associated with uraninite host rock and upon weathering, can contribute strongly to acidification of water in contact with tailings, via chemical reactions such as:

$$FeS_2 + 14Fe^{3+} + 8H_2O \rightarrow 15Fe^{2+} + 2SO_4^{2-} + 16H^+ \quad (1)$$

$$Fes_2 + 3.5O_2 + H_2O \rightarrow Fe^{2+} + 2SO_4^{2-} + 2H^+ \quad (2)$$

which are controlled by oxygen availability and the presence of bacteria such as *Thiobacillus ferrooxidans*, which enzymatically oxidize available Fe(II) to Fe(III). The

amount of Fe(III) produced by *Thiobacillus ferrooxidans* is a strong controlling factor on acid generation within tailings pits (Abdeluouas et al., 1999). The high acidity of the mine drainage enhances the dissolution of UO_2 from the solid phase to form the more souble and mobile aqueous UO_2^{2+}. Complexation of dissolved U with ligands such as carbonate, phosphate and organic ligands may further enhance U mobility in near surface aquatic systems.

Processing and enrichment of U ore

U resulting from ore milling is typically partially reduced and thus much less soluble than the oxidized form of U. However, processing of U ore typically includes industrial oxidation of U(IV) to U(VI) with hydrogen peroxide, ferric iron, or sodium chlorate to enhance the quantity of recoverable U (Blanpain et al., 2005). A base or hydrogen peroxide is then used to leach the "pregnant" solution of U, which is subsequently precipitated as $U_3O_{8(s)}$ or "yellowcake". Further processing is performed to isolate and purify the concentrated solution, resulting in $UO_{3(s)}$, which is then converted to UF_6 to prior to isotopic enrichment. Gaseous diffusion or gas centrifugation is used to separate the U isotopes. Between 3 to 5% ^{235}U is necessary for most currently-operating fission power plants in the U.S., which is significantly greater than the natural abundance of 0.7% ^{235}U (Table 1.1). The diffusion and centrifugation steps separate the isotopes based on mass differences resulting in "enriched uranium," which contains 3 to 5% ^{235}U for use in nuclear fuel. During isotopic separation UF_6 is converted to UO_2.

The back end of the fuel cycle

Spent nuclear fuel (SNF) will contain between 95 and 99% $UO_{2(s)}$ (Wronkiewicz and Buck 1999). The remaining portion will be made up of fission products and transuranic elements that form during fission, such as Cs, I, Ba and Sr (Shoesmith 2000). The fission products Cs and I have been recognized to separate from the bulk fuel and accumulate to the fuel sheath gap. Due to the high solubility of the precipitates in the gap, Shoesmith (2000) states that these deposits would dissolve instantly on exposure to groundwater. If a container is compromised, a major controlling process for $UO_{2(s)}$ escape will be the redox potential (Del Cul et al. 2000, Shoesmith 2000, Wronkiewicz and Buck 1999). Solution redox is a critical variable because the solubility of $UO_{2(s)}$ increases many orders of magnitude when the solid is oxidized.

The Hanford Site in Washington holds 231 million liters of waste material in 177 underground storage tanks (Huang 1996). It is estimated that 57 million liters were released in the 1970s, and during another accident in 1993 ~357,200 liters escaped. The sludge is known to contain plutonium (Pu), U, Cs, Sr and tritium. Included in this waste are organics used at the facility to remove metal precipitates from the machinery. Toste et al. (1995) conducted a study to identify organic compounds contained within Hanford waste containers. The work revealed that a complex mixture of organic compounds is present, ranging from commercial to defense waste. Toste et al. (1995) reported the presence of chelating agents including EDTA, NTA and HEDTA and the complexing agent citric acid. The compounds are likely present because they are extensively used in the nuclear industry as decontamination agents (as will be further discussed in the ligands section below). GC/MS analysis of the waste determined that it contained 64 mM citrate,

38 mM HEDTA, 31 mM EDTA and 7.3 mM NTA. Along with the "parent" organics, the presence of several other chemical classes, including mono- and dicarboxylic acids, alkanes and phthalate esters were found. These compounds are thought to be degradation products of the chelating and complexing agents. The presence of this complex mixture of chelating and complexing agents in the waste motivates better characterization of potential interactions between escaped U and these organics, so that waste migration can be better managed.

Organic ligands

Naturally occurring organic acids are biochemical compounds common to soils and natural waters including the plant canopy, forest litter, surface horizons, subsurface horizons, soil solutions, the rhizosphere and on rock surfaces (Stevenson 1967). These molecules are expected to play a dominant role in zones where microbial activity is intense; however, the amounts found at any one time represent a balance between synthesis and destruction by microorganisms. Organic acids perform many functions in soil including: root nutrient acquisition, mineral weathering, microbial chemotaxis and metal detoxification. In this study, several natural and anthropogenic organic acids found mainly in soil solutions and the subsurface horizon where U may escape from storage are considered. Four common ligands that are strong candidates to encounter SNF are NTA, EDTA, citric and fulvic acid.

Fulvic acid

The humic and fulvic content of natural organic matter (NOM) is made up of solid and dissolved organic matter that is a highly complex mixture of organic molecules

produced by incomplete breakdown of cellulose and lignin (Aiken et al., 1985). These compounds are typically categorized as naturally occurring, biogenic, heterogeneous organic substances that can generally be characterized as yellow to black in color, of high molecular weight, and refractory. Soil humic substances are divided into two major categories, the humic acid fraction and the fulvic acid fraction, based on solubility. The humic acid fraction is soluble in alkaline solution but will precipitate upon acidification and the fulvic acid fraction is soluble in alkaline and acidic solutions (Drever and Vance, 1994).

These acids are known to have a major influence on the translocation or mobility of many metals in soil profiles (McKeague et al., 1986). Fulvic acids are lower in molecular weight than humic acids and are the predominant form of dissolved organic carbon (DOC) in near surface aquatic systems (Drever and Vance, 1994). Fulvic acid is essentially ubiquitous, and as such is found in virtually every soil solution, surface water, or groundwater. Fulvic acid does not have a defined chemical composition or structure (Figure 1.5). The acid is acknowledged to have hydrophobic moieties that take the form of carbon chains, and hydrophilic functional groups (Maurice 2009). Functional groups such as phenol (-OH) and carboxyls (-COOH) have been observed (Figure 1.6). The high content of oxygen containing functional groups allows for the formation of stable complexes with polyvalent cations (Drever and Vance, 1994). Furthermore, because of its ubiquitous nature, it is possible that humic substances have a greater role than lower molecular weight acids in complexing and modifying metal mobility in soils. The concentration of humic and fulvic acid varies from soil to soil, but is generally controlled by the amount of organic matter contained in the soil. In well-drained soils levels can be

as low as 1.0 wt.%, increasing to up to 20 wt.% in wetlands, and peat can contain up to 30 wt. % humic and fulvic acid (Drever and Vance, 1994). Humic substances are capable of interacting with U resulting in several outcomes: (1) reactive sites on the acid can complex U resulting in an aqueous U-fulvic complexes; (2) reduction of the cation may take place causing precipitation of U(IV)-bearing solids; and (3) the formation of ternary complexes may modify sorption onto solids.

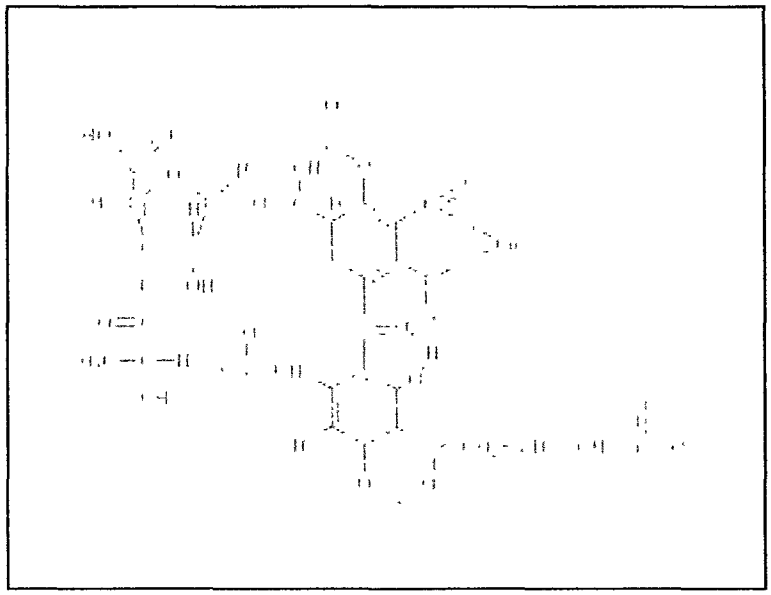

Figure 1.5. Proposed structure for fulvic acid (after Maurice, 2009).

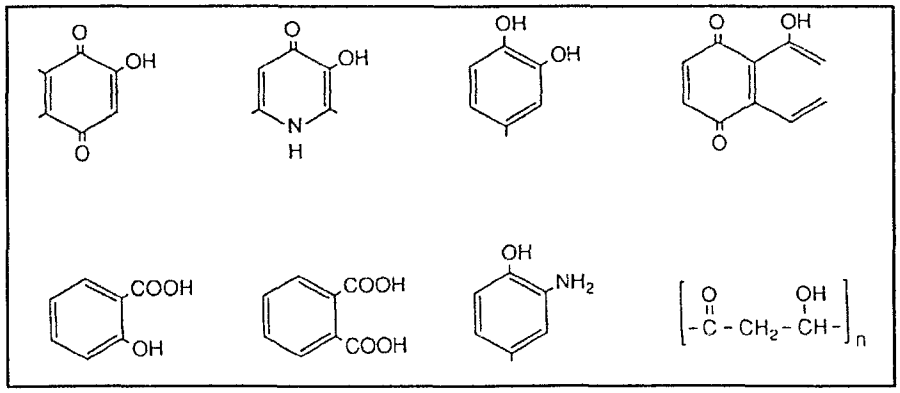

Figure 1.6. Potential binding sites on humic and fulvic acids (after Drever and Vance, 1994).

Citric acid

Citric acid ($C_6H_8O_7$) is a tricarboxylic acid (Figure 1.7) that occurs naturally in the environment and is also commonly used as a proxy to represent low molecular-weight (LWM) organics that are common in soils, and which are also strong chelators (Strobel, 2001). Citric acid is produced by plants, fungi and microorganisms, which are believed to exude it in order to help them take up metals from the environment (Jones, 1998). The concentration of LMW carboxylic acids, such as citric acid, are highest in soil solutions from the upper soil layers and can constitute up to 10% of DOC (Strobel, 2001). The concentration of aliphatic LMW di- and tricarboxylic acids (e.g., oxalic, malonic, malic, succinic, tartaric and citric) are usually in the range of 0-50 mM. In contrast, monocarboxylic acids typically occur in lower concentrations of ~0-1 mM (Strobel, 2001).

Citric acid contains three carboxyl functional groups that can deprotonate (Table 1.2) and form strong complexes with U in solution (Table 1.3). The complexation of U by citric acid can modify processes such as dissolution and sorption, which will be discussed further in chapters 2 and 5.

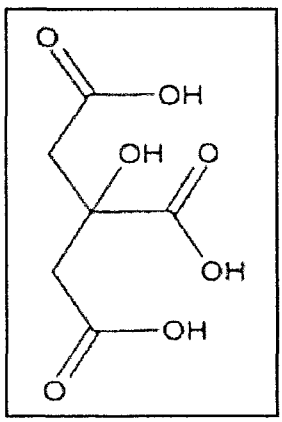

Figure 1.7. Citric acid structure (after Strobel 2001).

Table 1.2. pKa values for citric acid from MINTEQ default thermodynamic database (after Tomson 2004).

Reaction	pKa
$Citrate^{-3} + H^{+} \Leftrightarrow HCitrate^{-2}$	6.3
$Citrate^{-3} + 2H^{+} \Leftrightarrow H_2Citrate^{-}$	11.1
$Citrate^{-3} + 3H^{+} \Leftrightarrow H_3Citrate_{(aq)}$	-2.7
$Citrate^{-3} + H^{+} \Leftrightarrow HCitrate^{-2}$	6.3
$Citrate^{-3} + 2H^{+} \Leftrightarrow H_2Citrate^{-}$	11.1
$Citrate^{-3} + 3H^{+} \Leftrightarrow H_3Citrate_{(aq)}$	-2.7
$Citrate^{-3} + Na^{+} \Leftrightarrow NaCitrate^{-2}$	1.3
$UO_2^{+2} + Citrate^{-3} \Leftrightarrow UO_2Citrate^{-}$	8.6
$2UO_2^{+2} + 2Citrate^{-3} \Leftrightarrow (UO_2)_2Citrate_2^{-}$	21.3

Table 1.3. NEA selected thermodynamic data for reactions involving actinide compounds and complexes with selected organic ligands. All ionic species listed in this table are aqueous species. All data refer to the reference temperature of 298.15K and a pressure of 0.1 M Pa and I=0 (after Hummel et al., 2007).

Species	Reaction	$\log_{10} K^{\circ}$
$UO_2ox \cdot 3H_2O(cr)$	$UO_2ox(aq) + 3\ H_2O(l) \rightleftharpoons UO_2ox \cdot 3H_2O(cr)$	1.80 ± 0.27
$UO_2ox(aq)$	$UO_2^{2+} + ox^{2-} \rightleftharpoons UO_2ox(aq)$	7.13 ± 0.16
$UO_2(ox)_2^{2-}$	$UO_2^{2+} + 2\ ox^{2-} \rightleftharpoons UO_2(ox)_2^{2-}$	11.65 ± 0.15
$UO_2(ox)_3^{4-}$	$UO_2^{2+} + 3\ ox^{2-} \rightleftharpoons UO_2(ox)_3^{4-}$	13.8 ± 1.5
NpO_2ox^{-}	$NpO_2^{+} + ox^{2-} \rightleftharpoons NpO_2ox^{-}$	3.9 ± 0.1
$NpO_2(ox)_2^{3-}$	$NpO_2^{+} + 2\ ox^{2-} \rightleftharpoons NpO_2(ox)_2^{3-}$	5.8 ± 0.2
$Am(ox)^{+}$	$Am^{3+} + ox^{2-} \rightleftharpoons Am(ox)^{+}$	6.51 ± 0.15
$Am(ox)_2^{-}$	$Am^{3+} + 2\ ox^{2-} \rightleftharpoons Am(ox)_2^{-}$	10.71 ± 0.20
$Am(ox)_3^{3-}$	$Am^{3+} + 3\ ox^{2-} \rightleftharpoons Am(ox)_3^{3-}$	13.0 ± 1.0
UO_2cit^{-}	$UO_2^{2+} + cit^{3-} \rightleftharpoons UO_2cit^{-}$	8.96 ± 0.17
$(UO_2)_2(cit)_2^{2-}$	$2\ UO_2^{2+} + 2\ cit^{3-} \rightleftharpoons (UO_2)_2(cit)_2^{2-}$	21.3 ± 0.5
$UO_2(Hcit)(aq)$	$UO_2^{2+} + Hcit^{2-} \rightleftharpoons UO_2(Hcit)(aq)$	5.0 ± 1.0
NpO_2cit^{2-}	$NpO_2^{+} + cit^{3-} \rightleftharpoons NpO_2cit^{2-}$	3.68 ± 0.05
$Am(cit)(aq)$	$Am^{3+} + cit^{3-} \rightleftharpoons Am(cit)(aq)$	8.55 ± 0.20
$Am(cit)_2^{2-}$	$Am^{3+} + 2\ cit^{3-} \rightleftharpoons Am(cit)_2^{2-}$	13.9 ± 1.0
$Am(Hcit)^{+}$	$Am^{3+} + Hcit^{2-} \rightleftharpoons Am(Hcit)^{+}$	6.5 ± 1.0
$Am(Hcit)_2^{-}$	$Am^{3+} + 2\ Hcit^{2-} \rightleftharpoons Am(Hcit)_2^{-}$	10.8 ± 1.0
$Uedta(aq)$	$U^{4+} + edta^{4-} \rightleftharpoons Uedta(aq)$	29.5 ± 0.2
UO_2edta^{2-}	$UO_2^{2+} + edta^{4-} \rightleftharpoons UO_2edta^{2-}$	13.7 ± 0.2
$(UO_2)_2edta(aq)$	$2\ UO_2^{2+} + edta^{4-} \rightleftharpoons (UO_2)_2edta(aq)$	20.6 ± 0.4
$UO_2(Hedta)^{-}$	$UO_2^{2+} + Hedta^{3-} \rightleftharpoons UO_2(Hedta)^{-}$	8.37 ± 0.10
$Np(edta)(aq)$	$Np^{4+} + edta^{4-} \rightleftharpoons Np(edta)(aq)$	31.2 ± 0.6
NpO_2edta^{3-}	$NpO_2^{+} + edta^{4-} \rightleftharpoons NpO_2edta^{3-}$	9.23 ± 0.13
$NpO_2(Hedta)^{2-}$	$NpO_2^{+} + Hedta^{3-} \rightleftharpoons NpO_2(Hedta)^{2-}$	5.82 ± 0.11
$NpO_2(H_2edta)^{-}$	$NpO_2^{+} + H_2edta^{2-} \rightleftharpoons NpO_2(H_2edta)^{-}$	4.47 ± 0.14
$Pu(edta)^{-}$	$Pu^{3+} + edta^{4-} \rightleftharpoons Pu(edta)^{-}$	20.18 ± 0.37
$Pu(Hedta)(aq)$	$Pu^{3+} + Hedta^{3-} \rightleftharpoons Pu(Hedta)(aq)$	1.84 ± 0.26
$Am(edta)^{-}$	$Am^{3+} + edta^{4-} \rightleftharpoons Am(edta)^{-}$	19.67 ± 0.11

NTA and EDTA

NTA and EDTA are synthetic organic acids that were first manufactured in 1936 and 1939, respectively. These acids are considered complexing agents and are used for many purposes in industry. Because almost all processes conducted in aqueous solution will experience interferences by metal ions, i.e., the formation of highly insoluble precipitate of alkaline-earth or heavy-metal salts (Knepper 2003), complexing agents such as NTA and EDTA are used to remove problem metals and/or to bind and "mask" metal ions in industrial processes. These ligands have a broad area of application as complexing agents, but are mainly used for the complexation of Ca^{2+} and Mg^{2+} ions. Specifically, these acids are used as additives in washing and cleaning agents, in textile and pulp paper industry to mask heavy-metal ions, in the photo industry (now mostly phased out), in plating enterprises as inhibitors during the elimination of nickel from galvanic wastewater, in dairy processing to eliminate formation of "milk-stone linings", in remediation of contaminated soils or sludges, in agriculture as fertilizer auxiliary materials and as a source of nitrogen, and in the pharmaceutical cosmetics and food stuffs industries as stabilizing agents.

NTA and EDTA are both amino polycarboxylates that have a tertiary nitrogen atom in a central position in the molecule and acidic groups bound at alkyl residues around them (Figure 1.8). EDTA has four functional groups, which possess donor properties, spatially arranged in such a way that they can usually form 1:1 complexes with many metals, including U(VI) (Table 1.3) (Hummel et al., 2007). In the environment, complexing agents are usually present as complexes and not, as shown in Figure 1.8, in their acidic form. In a metal (M)-EDTA complex, the metal ion can be

located in the center of the complex whilst being coordinately bound to nitrogen and oxygen atoms (Figure 1.9; Knepper, 2003). This configuration is termed chelation and is very effective at masking the positive charge of the metal, causing enhanced metal mobility in the environment. Both EDTA and NTA are highly stable and can be removed only with extreme difficulty from the wastewater produced in industrial processes. The stable configuration of these complexes has lead to increased mobility of heavy metals. The complexes are usually highly stable because of the enclosure of the central ion by the complexing agent.

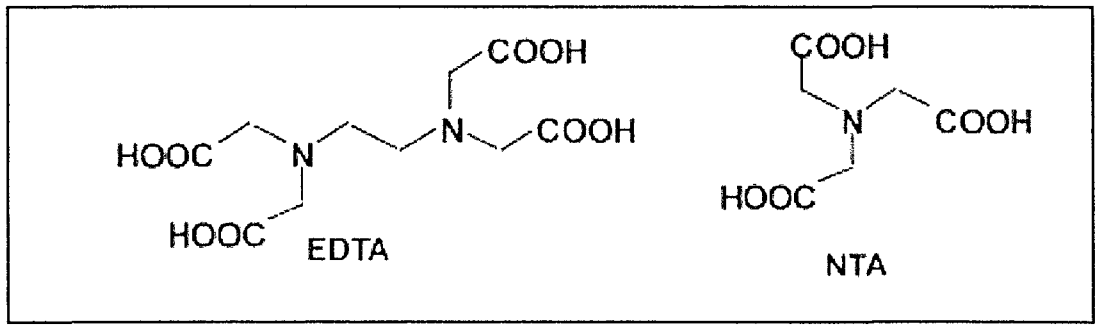

Figure 1.8. Structures of EDTA and NTA (after Knepper, 2003).

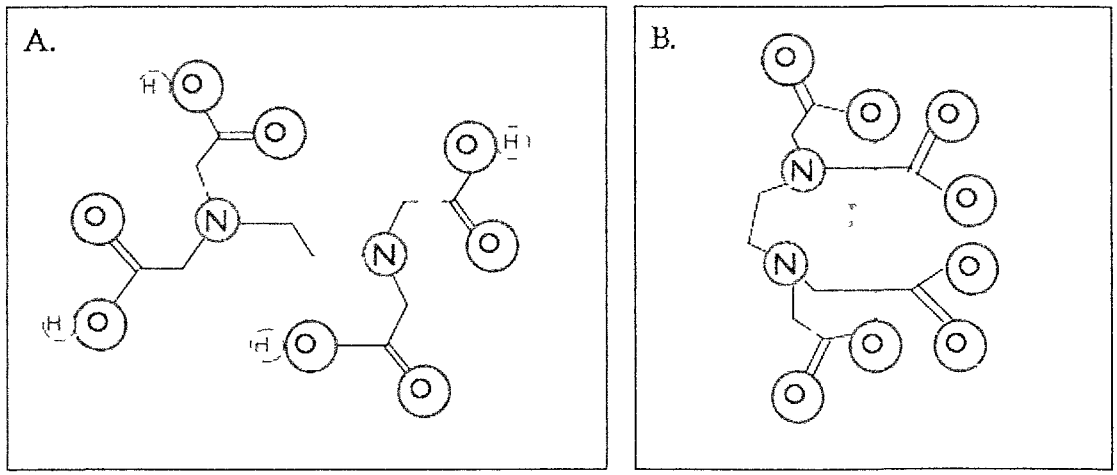

Figure 1.9. The EDTA molecule (A) and a schematic of EDTA chelating around a metal cation (B).

Objectives and hypothesis

The dissolution portion of this study investigates the influence of organic acids on the solubility of $UO_{2(s)}$. Data derived from this research helps to elucidate how organic ligands such as citric, oxalic and NTA acids affect the distribution and stability of UO_2 in near surface environments. It is hypothesized that:

(1) In the absence of oxygen and organic acids the solubility of UO_2 will depend on pH, with increasing solubility at pH < 4 and > 11.

(2) Upon the addition of organic acids, $UO_{2(s)}$ solubility will increase.

Bulk adsorption experiments conducted under a broad range of solution conditions are used to investigate UO_2^{+2} sorption on kaolinite, a mineral found in many near surface earth system. Data from this study is used to constrain reaction stoichiometries and thermodynamic stability constants to describe UO_2^{+2} adsorption on kaolinite with double diffuse layer and non-electrostatic surface complexation models, These models can be used to calculate UO_2^{+2} partitioning onto kaolinite under a range of possible solution conditions (pH, ionic strength, solution composition). The following hypotheses are tested with the investigations of the UO_2^{+2}-kaolinite-organic acid systems:

(1) In the absence of organic acids, UO_2^{+2} adsorption on kaolinite will be greatest at circumneutral pH and will decrease below 7 and above 8, with little ionic strength dependence.

(2) Organic acids will increase UO_2^{+2} adsorption at pH values <7 when compared to UO_2^{+2} adsorption onto kaolinite in the absence of organic acids, due to the formation of ternary surface complexes.

(3) At high pH, addition of organic acids will result in less adsorption of the UO_2^{+2} on kaolinite, due to the formation of aqueous U-organic acids, desorption of the organic acids from the kaolinite surface and/or because organic acids may outcompete UO_2^{+2} for mineral surface sites.

Overall this research will contribute fundamental thermodynamic data regarding interactions of UO_2^{+2} with a common clay mineral and three natural and synthetic organic acids found in many near-surface environmental systems.

CHAPTER II

$UO_{2(s)}$ SOLUBILITY BACKGROUND

Mechanisms of dissolution

This study investigates the solubility of uraninite, under reducing conditions, when exposed to citric acid, NTA and EDTA. In a closed system, with a fixed temperature and pressure, a saturated aqueous solution consisting only of water, $UO_{2(s)}$, and an organic acid will have two major dissolution mechanisms at work. The first mechanism is controlled by pH, i.e. the concentration of H^+ and OH^- ions in solution and is termed "proton-promoted" or "hydroxide-promoted" dissolution. H^+ and OH^- ions can form a complex with O and U atoms at the mineral surface, weakening bonds to the internal mineral lattice, resulting in desorption of surface atoms to form aqueous species. The second mechanism that may act to dissolve UO_2 in the system described above is "ligand-promoted" dissolution. During ligand-promoted dissolution, mineral solubility is enhanced by the complexation of ligands with ions at the mineral surface. The following sections offer a detailed explanation of chemical interactions that occur during both types of dissolution.

Effects of pH on $UO_{2(s)}$ solubility

In a system of UO_2 and water, the dissolution of uraninite will be promoted by H^+ and OH^- ions in solution. For the uraninite solid the O=U=O atoms at the mineral surface will be less stable relative to atoms that are embedded further within the solid because U

and O atoms located on the surface of the mineral lattice will have unsatisfied bonds (Morel and Herring, 1993). The uraninite structure consists of eight O atoms in a cubic arrangement, with each O atom bonded to four U(IV) cations (Burns 1999; see Chapter 1). O and U atoms located at the mineral are coordinatively unsaturated and, as a consequence, will be reactive toward species in the aqueous solution. Reactions between atoms at the mineral surface and H^+ and OH^- ions in solution can result in enhanced dissolution of the UO_2 solid.

Proton-promoted dissolution

Mineral surfaces exposed to aqueous solutions will hydrolyze; U cations attract hydroxyls, while O atoms at the mineral surface will be protonated to form >UOH surface groups, where > indicates binding to the mineral lattice (Figure 2.1). Under acidic conditions ($\leq$ 4), proton-promoted dissolution occurs. In this case, protons in solution bind to the mineral surface, forming a protonated surface group. This weakens the underlying bond between the U-O in the mineral lattice, promoting release of the U into the aqueous solution. This effectively results in an exchange between the H and the U cations at the surface of the metal-oxide crystal lattice (Figure 2.2), resulting in the dissolution of UO_2 and subsequent formation of U-OH aqueous species (Rai 1990). Proton-promoted dissolution is controlled by the activity of protons present in solution. Thus, lower pH promotes greater proton-promoted mineral solubility (e.g. Figure 2.2).

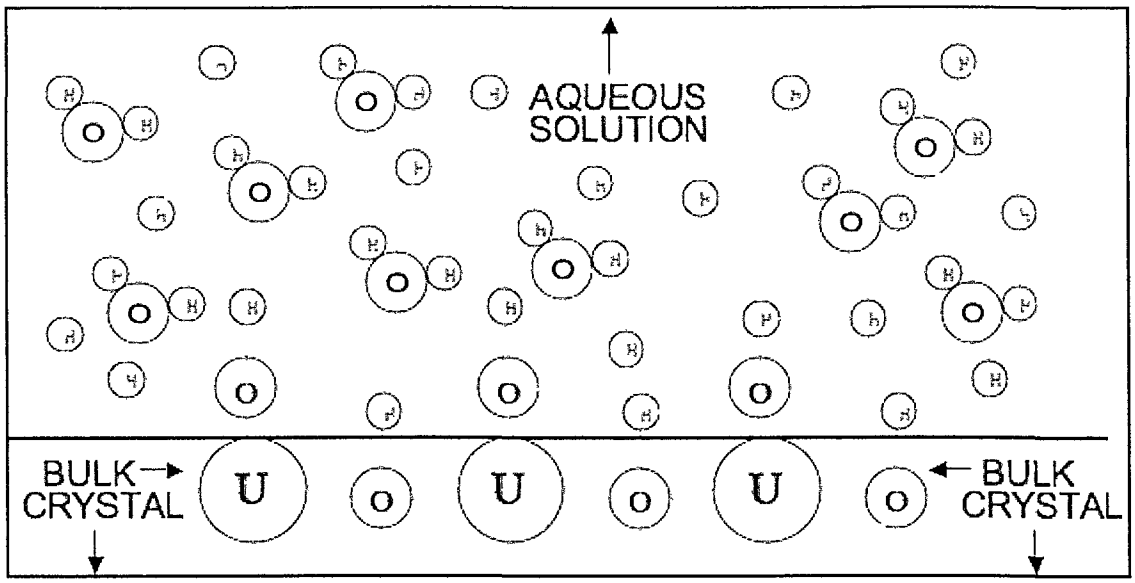

Figure 2.1. In an aqueous system the UO_2 mineral surface is hydrolyzed.

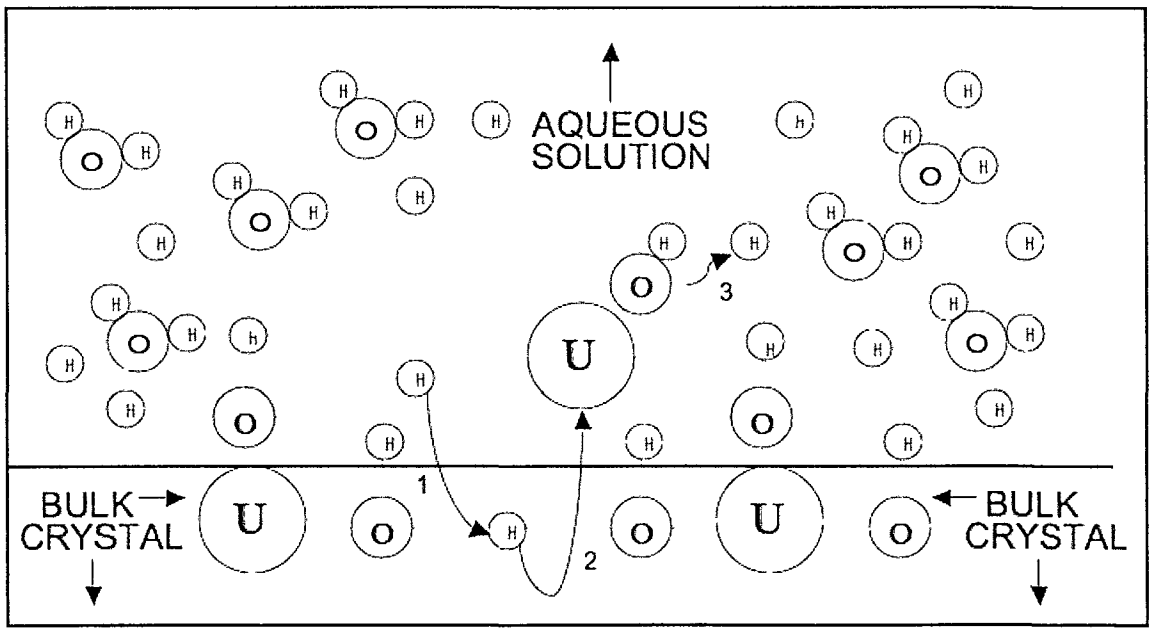

Figure 2.2. Proton promoted dissolution of UO_2. Protons in solution effectively compete with the U cation in the mineral structure (1). The U atom is removed as a hydrolyzed species and the proton substitutes for the U (2). The hydrolyzed U is deprotonated, resulting in U-OH species (3).

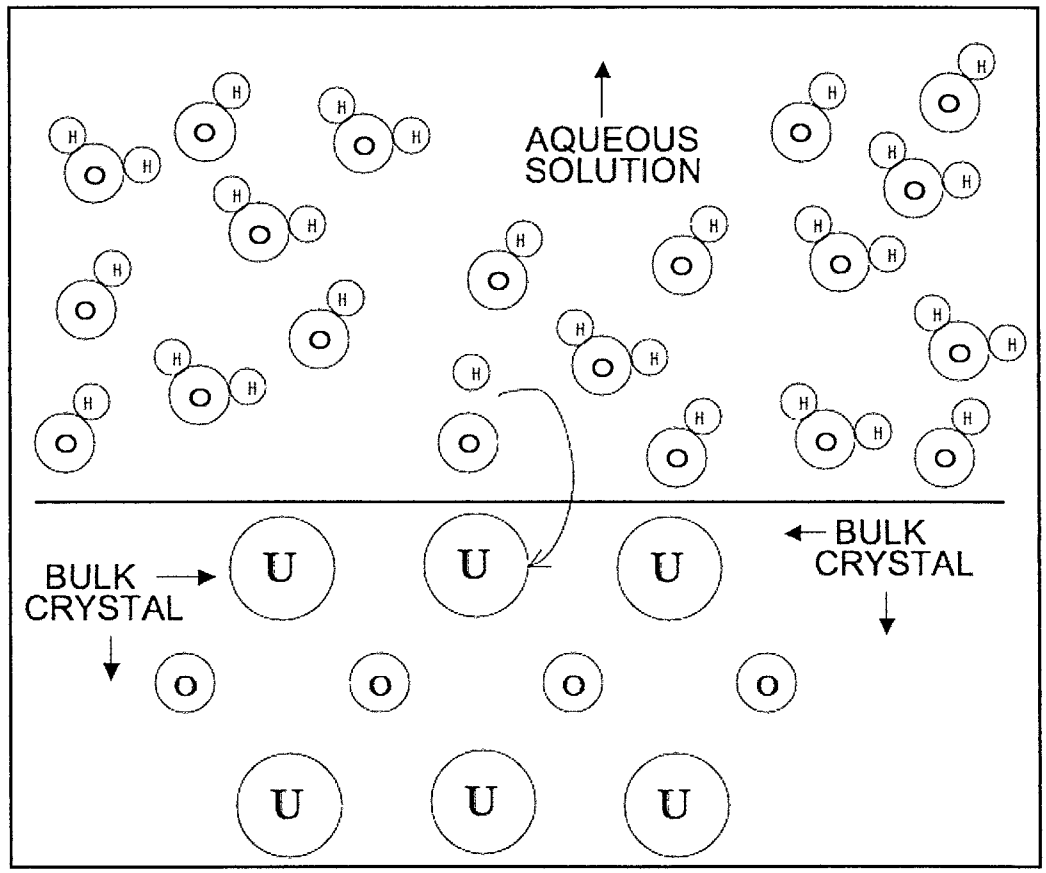

Figure 2.3. Hydroxide promoted dissolution. At high pH OH^- ions are attracted to the metal resulting in a weakening of U-O bonds within the mineral structure and enhanced solubility.

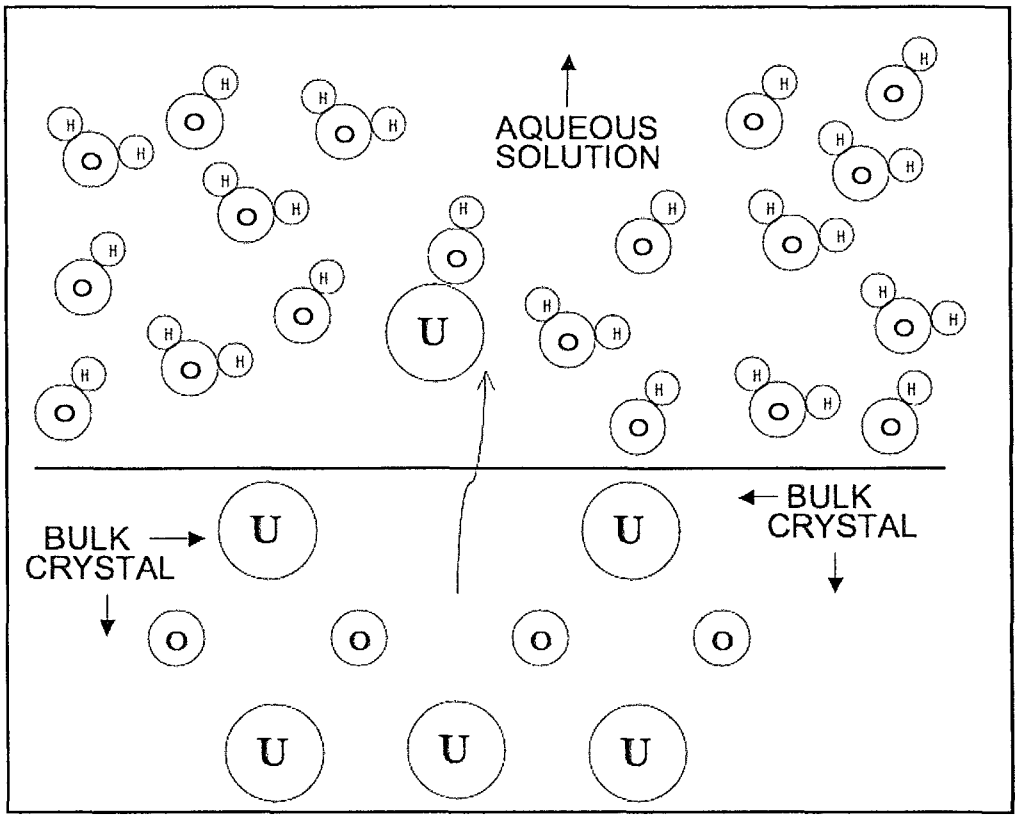

Figure 2.4. Hydroxide promoted dissolution results in removal of U from the mineral as a U-OH complex.

Hydroxide promoted dissolution

In neutral to alkaline aqueous solutions, a complex will form between the surface U and the OH^- anion, weakening the bonds between U at the surface and O atoms in the mineral lattice. The bonds are polarized allowing for the removal of a U-OH complex into solution (Figure 2.4). Because U is removed from the solid to the aqueous phase the mineral is dissolved and solubility is promoted.

Dissolution promoted by ligand chelation

In the natural environment the degradation of organic matter by microorganisms results in the formation of organic acids. As these acids are transported through near

surface environments they may encounter mineral constituents of the soil. Organic acids are implicated in mineral-surface interactions where they can act in ligand exchange reactions to increase the rate of mineral dissolution (Casey and Ludwig 1995). When the solubility of a mineral is affected by ligand complexation, resulting in a metal-ligand species, it is termed "ligand promoted dissolution" (Casey and Ludwig 1995).

Pittman and Lewan (1994) state that there are three fundamental rate-controlling steps in ligand promoted dissolution. First, ligands must migrate to the mineral surface. Once in contact with a cation, negatively charged reactive sites on the ligand may then form a complex with the metal cation located on the mineral surface. Complexation to the mineral can occur by several mechanisms, including: water bridging, electrostatic (coulombic) attraction, coordinate linkage with a single donor group, and chelation (Figure 2.5). These interactions with the mineral surface may promote the dissolution of the mineral in much the same way as protons or hydroxyls, as described above. The complex weakens the preexisting bonds of the metal and allows for the newly formed complex to be desorbed from the crystal. Finally, the third step is for the newly formed complex to diffuse away from the mineral surface, moving down the concentration gradient (Casey and Ludwig 1995). By removing the U metal from the crystal lattice and forming a stable aqueous complex organic acids enhance the dissolution of UO_2.

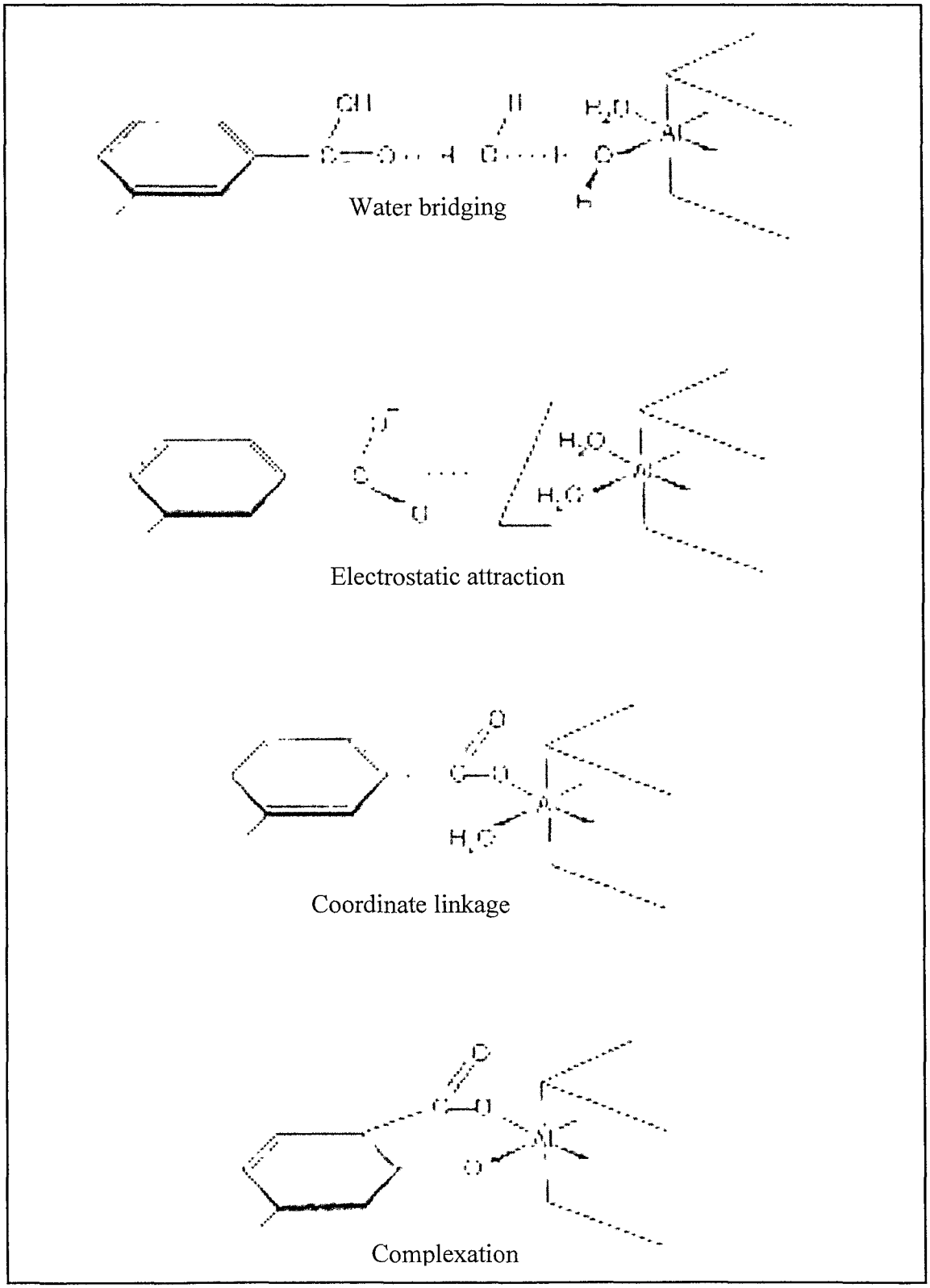

Figure 2.5. Adsorption mechanisms between organic acids and mineral surfaces (after Drever and Vance 1994).

Law of mass action and equilibrium constant

Chemical reactions are described using mathematical equations, for example, a simple chemical reaction might be stated as:

$$a\,A + b\,B \Leftrightarrow c\,C + d\,D \qquad (2.1)$$

where: *a*, *b*, *c*, and *d* are the stoichiometric coefficients of reactants and products in the balanced chemical reaction, and A, B, C, and D are the concentrations or activities of reactants and products at equilibrium. The double arrow symbolizes reversibility; at equilibrium conditions the forward reaction rate is equal to the reverse rate. Reactions can be expressed using the Law of Mass Action:

$$K = \frac{[C]^c[D]^d}{[A]^a[B]^b} \qquad (2.2)$$

where the brackets [ ] represent the activity of the products and reactants and K symbolizes the equilibrium constant. For a reaction in a state of equilibrium, the concentrations of the reactants and products will not change with time. Molecular motion and diffusion continue at equilibrium, but the activities of the products and reactants remain constant. Hence, the Law of Mass Action when expressed as equation 2.2 states that the energy of the system is equal to the energy of the products over the energy of the reactants.

The law of mass action can be applied to solubility reactions, such as those described above. For a reaction occurring at a constant pH, temperature and pressure, the complexation of reaction constituents with ligands and removal of U or O from the mineral lattice will continue to occur at a constant rate. In other words, organic acids, H^+ and OH^- species continue to react with uraninite, however, the activity of U in solution

will not change at equilibrium. Concentrations of constituents in solution will remain constant for as long as conditions are unchanged.

The equilibrium constant (K_{eq}) for a dissolution reaction represents the activity of ions in solution (products/ reactants) at saturation (Eby 2004). The Law of Mass Action (Equation 2.2) can be used to extract the equilibrium constant for a reaction if the activities of the products and reactants at equilibrium are known, simply by rearranging the expression. An example reaction such as

$$UO_2 \bullet xH_2O_{(am)} + 3H^+ \Leftrightarrow UOH^{3+} + (x+1)H_2O \quad (2.3)$$

has a corresponding mass law of

$$K_{eq} = [UOH^{3+}]/[H+]^3 \quad (2.4)$$

because the activities of pure solids (UO_2) and liquids (H_2O) are assumed to be equal to one. Taking the logs of each side and rearranging yields a linear expression:

$$\log_{a(UOH^{3+})} = \log K - 3pH \quad (2.5)$$

where the activity of UOH^{3+} in the system is the y variable, m (the slope of the line) is the stoichiometric coefficient, the x variable is the pH of the system and b (the intercept of the line) is the equilibrium constant (K_{eq}).

In experiments conducted in this study, UO_2 activity in solution is measured as a function of organic ligand activity and pH. At equilibrium, all components of the line, with the exception of b, are known. The activity, or the y variable, of the aqueous U species is found by analyzing the concentration of U in samples taken from experiments. The x variable, pH, measured using a pH electrode. By plotting the aqueous U activity as a function of pH, with a slope given by the stoichiometric coefficient, K_{eq} can be calculated from the intercept of the line (Figure 2.6).

For example, Figure 2.6 shows data from Rai (1990). Rai (1990) carried out solubility experiments of $UO_2 \cdot xH_2O_{(am)}$ in a glove box, from the point of undersaturation in deoxygenated water at STP for 1 – 8 days. The aqueous concentration of U in equilibrium with $UO_2 \cdot xH_2O_{(am)}$ was measured as a function of pH. The data clearly delineate two lines of differing slope, from which it is evident that two reaction mechanisms take place. By graphing a line through the two linear portions of the data, the K_{eq} for each of these two reactions can be extracted from the data.

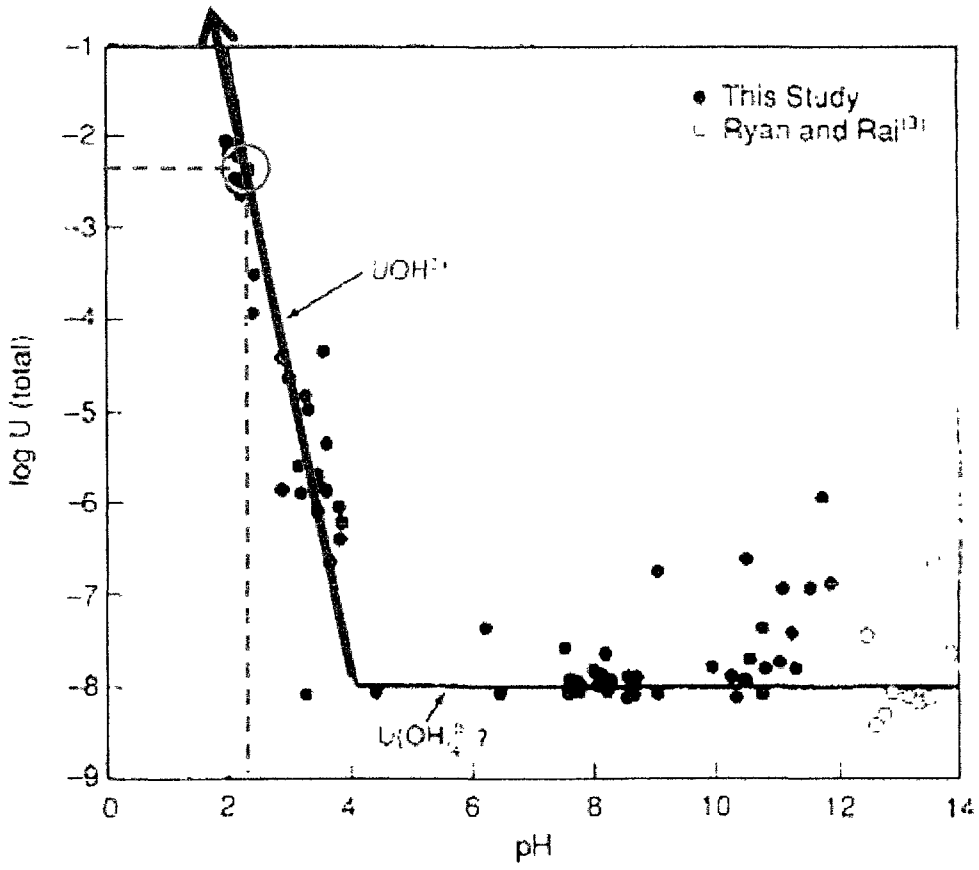

Figure 2.6. The solid lines are best-fit lines to data from aqueous U concentrations in equilibrium with $U0_2.xH_20$(am) (after Rai 1990).

By using the coupled nonlinear least-squares and chemical equilibrium program (NONLIN) Rai (1990) determined the equilibrium constants for the first hydrolysis constant (the blue line) to be log K = 3.5 ± 0.8 for reaction 2.3. Data from Figure 2.6 can be used with equation 2.5 to solve for the log K of the reaction. Picking a data point (e.g., red circle, Figure 2.6) and inserting the activity of UOH^{3+} and pH into equation 2.5,

$$-2.3 = \log K - (3*2.2) \quad , \tag{2.6}$$

yields a log K of 4.3, which is within the error of Rai's equilibrium constant (3.5 ± 0.8). By manipulating the mass law equations for solubility experiments in this study the equilibrium constants for $U(IV)O_{2(s)}$-ligand dissolution reactions can be determined in this manner.

Inconsistency of K_{eq} values in the literature

Although the solubility of depleted uranium has been investigated extensively, there is a great deal of scatter in the data reported in the literature (Neck and Kim 2001). More than four decades of past studies focusing on spent nuclear fuel disposal have aimed to quantify the solubility of $UO_{2(s)}$ dissolution, but significant gaps in the quantitative understanding of $UO_{2(s)}$ reactivity remain (Neck and Kim 2001). Reported equilibrium constants for $UO_{2(s)}$ hydrolysis vary by approximately 8 orders of magnitude. There are several complicating factors that may account for the enormous discrepancies among the reported values:

(1) Neck and Kim (2001) suggest that a major contributor to the observed scatter in solubility data for $UO_{2(s)}$ is that the constants do not refer to a unique material, but rather to a range of poorly defined solids with different thermodynamic stabilities.

The starting material for $UO_{2(s)}$ solubility experiments are often inadequately described and reported simply as either crystalline samples of a given stoichiometry or as "amorphous" materials (Fuger 1993). However, a crystalline mineral containing just 1% of an amorphous impurity phase, may yield tremendously skewed K_{sp} values, due to the extreme difference in solubilities of the crystalline and amorphous $UO_{2(s)}$ phases. In addition to the complexities of properly identifying the starting material, difficulties also exist in ascertaining that no structural transformation or secondary phase precipitation occurs during solubility experiments, which are sometimes quite lengthy (Fuger 1993). For experiments in which saturation is approached from undersaturation, as in this study, the Gibbs free energy of the reaction is dependent on the degree of crystallinity of the starting solid-phase of the mineral. In order to obtain meaningful equilibrium constants the initial $UO_{2(s)}$ mineral phase must be well defined.

(2) In addition to the problems of obtaining well characterized solids, uraninite may also have partially, or even entirely, oxidized surface layers containing a mixture of U(IV) and U(VI) (Rai 1990, Shoesmith 2000). Neck and Kim (2001) state that crystalline $UO_{2(s)}$ can be entirely coated by amorphous hydroxide layers. These oxidized surface phases are highly soluble relative to the reduced crystalline phase, thus, the presence of even a small amount of amorphous material at the surface or a partially oxidized surface layer U will greatly skew solubility results.

(3) Because of the high solubility of oxidized surface layers, the redox conditions in the $UO_{2(s)}$ solubility experiments must be strictly controlled. The lack of suitable

techniques and reducing agents to effectively sustain U(IV) over a wide range of pH values and temperatures is a major issue in measuring U(IV) solubility (Rai 1990). Redox reactions due to oxidizing agents, such as O_2, interacting with surface U or aqueous U will greatly raise U activity in solution (Fuger 1993). Because U(IV) is readily oxidized to U(VI), reducing conditions must be carefully maintained. O_2 is a strong and rapid oxidant for U(IV) and Rai (1990) states that keeping redox potentials low is absolutely critical for maintaining uranium in the tetravalent state. If U(IV) in the mineral lattice is even partially oxidized to the more soluble U(VI) species, the activity of U in solution will be greatly elevated and not reflective of U(IV) solubility.

(4) The low activity of U(IV) at equilibrium is also a complicating factor. Because the solubilities of tetravalent uranium oxides are low, it can be difficult to accurately detect low levels of uranium in solution in order to adequately constrain mineral solubility constants (Neck and Kim 2001).

CHAPTER III

$UO_{2(s)}$ DISSOLUTION METHODS

Materials

All chemicals used in the study were reagent grade and included $UO_{2(s)}$ purchased from International Bio-Analytical Industries, $EuCl_{2(s)}$ purchased from Strem Chemicals, $NaHCO_3$ purchased from Acros Organics, NaOH pellets purchased from Acros, NaCl purchased from Mallinckrodt Chemicals, nitrilotriacetic acid (NTA) and citric acid trisodium salt dihydrate purchased from Sigma, HCl and electrophoresis grade ethylene diamine tetraacetic acid (EDTA) disodium salt purchased from Fisher Scientific. Water for all experiments was purified with a Barnstead E-pure (Model D4641) water system to >18.2 mΩ•cm.

All experiments involving UO_2 were carried out inside a Coy (®) type B glove box anaerobic chamber, which was filled with a gas mixture of 95% N_2 and 5% H_2. Oxygen concentrations in the anaerobic chamber were monitored using an internal oxygen sensor and maintained below a working level of 10 ppm using catalytic desiccant packs combined with recirculating fans inside the chamber. For some experiments pH was controlled using an automated digital titration apparatus (Mettler-Toledo ® DL-58), which was maintained within the anaerobic chamber. Dissolved concentrations of U were measured in experimental samples using a Perkin Elmer, Optima 2100 DV inductively-coupled plasma optical emission spectrometer (ICP-OES) and a Therme Finnigan Element 2 High-Resolution Double Focusing Magnetic Sector inductively-coupled plasma mass spectrometer (ICP-MS). UO_2 crystallinity was determined by a Scintag, X1

diffractometer with powder diffraction done on zero background quartz slides with Cu radiation. A Sentro Tech STT-1700-2.5-12 High Temperature Tube Furnace was used to ensure all U(VI) was driven off UO_2.

Preparation of $UO_{2(s)}$ for solubility experiments

Because the goal of this study is to determine the solubility product (K_{sp}) of U(IV) and not U(VI) oxide, it is essential to remove all U(VI) from the mineral surface. U(VI) has a much higher K_{sp} when compared to U(IV) (Burns 2000), therefore, moderate to highly-soluble U(VI) alteration products on the mineral surface are preferentially dissolved, resulting in higher K_{sp} values. To ensure removal of surface U(VI), several methods were employed.

To maintain strictly anoxic and reducing conditions throughout experimental procedures all aqueous solutions were sparged with internal air within the anaerobic chamber for at least 24 h prior to use. Sparging solutions within the anaerobic chamber displaces dissolved atmospheric gases such as O_2 and CO_2, replacing these with N_2 and H_2. Exsolved O_2 is actively removed within the chamber, as described above, while exsolved CO_2 is eliminated using a dry reservoir of periodically refreshed NaOH within the chamber.

Fine-grained synthetic UO_2 was used for all solubility experiments. Prior to using UO_2 it was necessary to remove any U(VI) oxide or hydroxide alteration products on grain surfaces that may have developed by exposure of the fresh $UO_{2(s)}$ to air. To remove unwanted U(VI) from particulate surfaces, solids were exposed to a solution of 0.5 M $NaHCO_3$ to extract soluble U(VI) as uranyl carbonate complexes in solution. Clark et al.

(1995) states that uranyl carbonate complexes in solution are quite stable and are probably the most important dissolved complexes responsible for U(VI) migration in oxidizing environments. The strong affinity for U(VI) to form stable aqueous carbonate species preferentially removes U(VI) from the mineral surface. To perform the U(VI)-carbonate extraction 1 gram of raw $UO_{2(s)}$ was introduced into 50 mL of a degassed 0.5 M $NaHCO_3$ solution. All steps involved in this procedure took place within the anaerobic chamber. The bicarbonate solution was allowed to equilibrate with UO_2 for 24 hours on a Barnstead Labquake shaker. This extraction technique was repeated two more times, for a total of three extractions. Every 24 hours the supernatant was removed and replaced with another 50 mL of fresh 0.5 $NaHCO_3$ solution. The supernatant from the first 24 hours had a conspicuous lemon yellow tint indicating that U(VI) dissolution had occurred. The following two supernatants removed were clear in color indicating that the major fraction of U(VI) was removed in the first $NaHCO_3$ wash. Supernatant solutions from the $NaHCO_3$ wash were analyzed to determine the total U(VI) removed via ICP-OES. Once the bicarbonate wash was complete, treated UO_2 was then rinsed three consecutive times with 50 mL of sparged DDI water inside the anaerobic chamber, prior to being used in solubility experiments.

Treatment of $UO_{2(s)}$ with HCl

An acid wash was performed to ensure removal of any U(VI) left from the bicarbonate extraction and to remove anomalously reactive surface areas because moderate to highly-soluble U(VI) alteration products on the mineral surface are preferentially dissolved. The $UO_{2(s)}$, particulates were exposed to 50 mL of a 0.1 M HCl

acid solution to complex U(VI) and remove it from the mineral surface. Solutions were agitated on a Labquake platform for 24 hours. The supernatant was removed and the UO_2 was then rinsed three times with degassed DDI water. Finally, the UO_2 was dried within the anaerobic chamber for two days by leaving the 50 mL tube open and securing a kimwipe around the top to keep matter out of the tube, but still allow the particles to air dry.

High temperature heating of $UO_{2(s)}$

To ensure that no U(VI) remained at the mineral surface, a fraction of the treated particulates were heated inside a Sentro Tech STT-1700-2.5-12 High Temperature Tube Furnace with $MoSi_2$ heating elements. UO_2 is pyrophoric and can spontaneously ignite in air, consequently, the furnace is kept devoid of oxygen and contains 4% H_2 gas. UO_2 was heated to 1600 °C so that any oxidized material at the mineral surface would be driven off, leaving a surface with only reduced UO_2. Because a highly reducing atmosphere is used during the heating process, no oxidization will occur in the furnace.

$UO_{2(s)}$ solubility experiments under pH-stated conditions

This study examined the dissolution of UO_2 when exposed to citric acid, NTA or EDTA using solubility experiments conducted from pH of 5 to ~11. pH was controlled using a Mettler-Toledo digital titration instrument to obtain and maintain an assigned pH. If the solution pH drifted from the assigned point, the titrator would deliver a small volume dose of titrant stock solution (0.01 M NaOH or 0.01 M HCl) to counter the pH drift. Standard solutions of the acid and base were prepared from a 37% HCl solution and

97% NaOH pellets in the anaerobic chamber. All experiments were conducted with an 0.01 M NaCl background solution within the anoxic chamber with an atmosphere of 95% N_2 and 5% H_2.

To begin each experiment, 50 mL of sparged solution containing 0.01 M NaCl and $2.6 \cdot 10^{-3}$ M $Eu(II)Cl_2$ was added to a titration cup that contained 0.1 g of the treated UO_2. NaCl was used as a background electrolyte and $Eu(II)Cl_2$ was added to help maintain a low redox potential in solution (Rai 1990). The solution was stirred and titrant was added to obtain the assigned pH. Experiments were conducted for a pH range of 5 to 12. After the pH remained stable for ~7-10 minutes, the desired ligand was added for experiments investigating the effects of NTA, EDTA or citric acid on uraninite solubility.

Initial solubility experiments in the absence of organic acid were monitored for 32 hours to confirm that equilibrium had been achieved. During the first seven hours, a 1 mL sample was removed every hour, after which a 1 mL sample was removed at 24 hours and 32 hours. Samples were filtered through a 0.2 μm Whatman Schleicher & Schuell syringe filter into clean 15 mL Fisherbrand® centrifuge tubes with 5% HCl for subsequent analysis of total dissolved U by ICP-OES. 5% HCl is used to prevent adsorption of uranium onto the tube wall.

Organic acids used in solubility experiments - citric acid, NTA and EDTA

A 1 M stock solution of each ligand was prepared in the glovebox and then sparged in the anaerobic chamber. Stock solutions were diluted to the desired concentrations (100, 200 and 500 mM organic acid) as needed for a given experiment. After addition to the $UO_{2(s)}$ each solution was allowed at least two hours for pH

equilibration, after which, the pH was recorded and the suspension allowed to equilibrate for three days. At the conclusion of this period, the pH was again recorded and 10 mL of the supernatant was removed for analysis as described above for the experiments without added organic acid.

Solubility experiments conducted under ambient atmosphere

Solubility experiments were also conducted under ambient atmosphere to allow oxidation to occur. Data from these experiments provide a comparison of the solubility of UO_2 in an oxidizing environment to that in the reduced chamber atmosphere. The same methods as above were employed except that $Eu(II)Cl_2$ was not added to the solutions. Batch experiments were covered with parafilm with a hole to allow for gas exchange and placed on a Lab-Line, model number 4626, oscillating platform and rotated at 200 rpm for three days.

CHAPTER IV

$UO_{2(s)}$ DISSOLUTION RESULTS

XRD analysis

Powder diffraction of the uraninite solid showed sharp peaks indicating crystalline phase $UO_{2(s)}$. Peaks correlate well to results from Rai 2003 and expected peaks for crystalline phase $UO_{2(s)}$. Results confirm that the solid is crystalline and not amorphous.

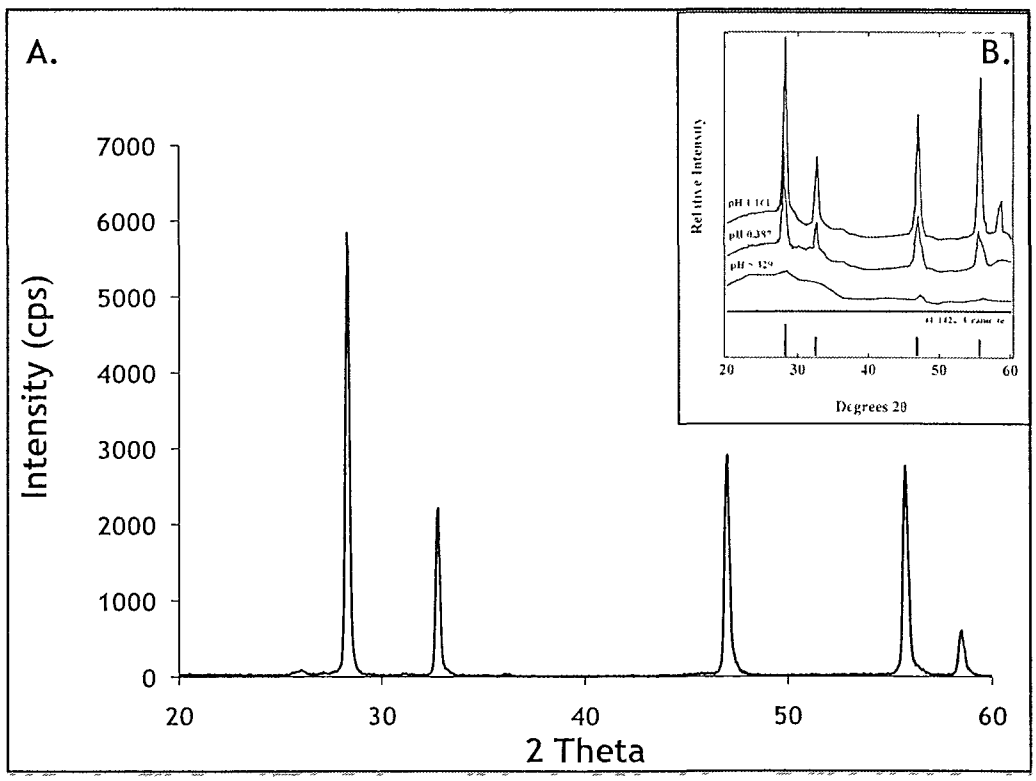

Figure 4.1. (A) XRD analysis of $UO_{2(s)}$ from this study compared to (B) XRD analysis of $UO_{2(s)}$ (Rai et al., 2003).

X-Ray powder diffraction of the kaolinite solid was comparable to baseline XRD studies for KGa1-b performed by the Clay Minerals Society (Chipera and Bish 2001). Peaks correlated to those established for kaolinite, including a high intensity peak that is caused by a known anatase impurity (Figure 4.2). This confirms the presence of TiO_2 sites that are included in the nonelectrostatic surface complexation model (see Chapter 8).

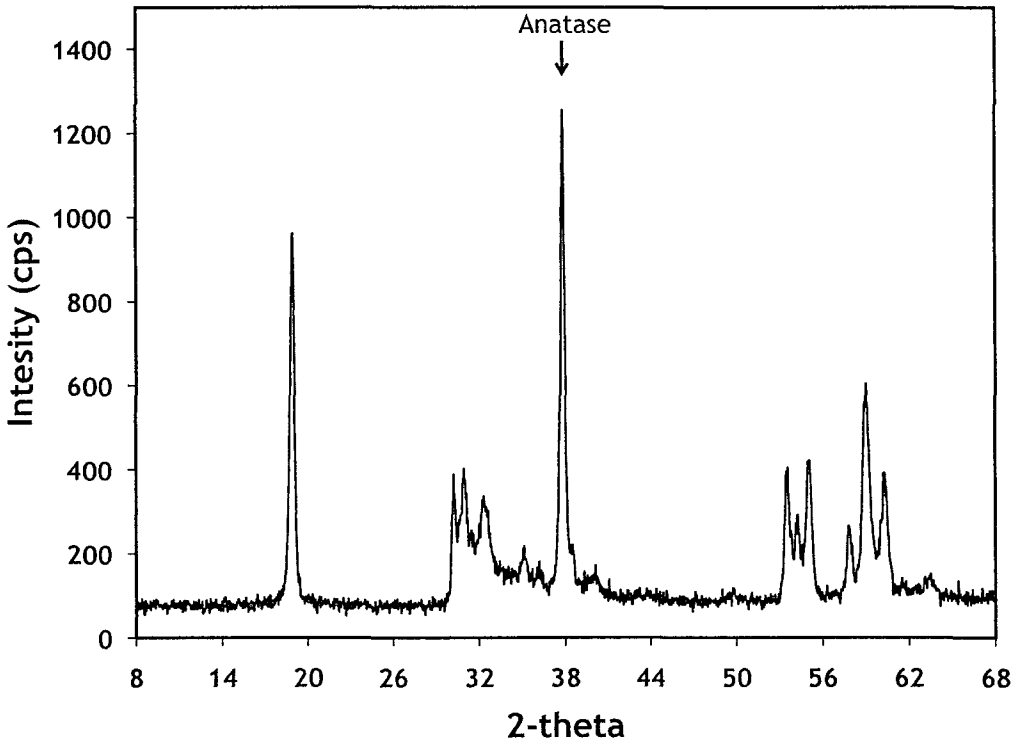

Figure 4.2. XRD analysis of kaolinite (KGa1-b) used in this study.

Removing U(VI) from uraninite surface

$UO_{2(s)}$ particulates used in this study were exposed to atmospheric oxygen. Under atmospheric conditions a thin layer of U(VI) will develop on the mineral surface. In order to remove this oxidized coating, a 0.5 M $NaHCO_3$ wash was performed, as discussed in

the Materials and Methods section (Chapter 3). $UO_{2(s)}$ was exposed to a 0.5 M $NaHCO_3$ solution for 24 hours, after which the solution was refreshed and the wash repeated a total of three times.

Samples were taken hourly for the first eight hours and then every eight hours to confirm equilibrium (Figures 4.3). The first wash shows an initial U(VI) concentration of ~ 20 ppm and after 5 hours the concentration of U(VI) in solution plateaus to ~12 ppm for the remaining 20 hours of the wash. Samples taken from the second wash show a great decrease in U(VI) complexed from the solid surface: U(VI) recovered is < 0.25 ppm and remains at this low concentration for the 24 hour period. The first hour sample of the third wash also contained < 0.25 ppm U(VI), with U below the detection limit in subsequent samples. Thus, after the third wash it was assumed that all possible U(VI) that could be removed by $NaHCO_3$ complexation had been achieved.

To further ensure removal of any remaining U(VI) that might be below ICP-OES detection limits, a 0.1 M HCl wash was next performed. Washing with HCl is assumed to preferentially solubilize the more soluble U(VI), allowing for complete removal of U(VI) from the solid surface. Approximately 7 hours into the first wash dissolved U concentrations reach ~600 ppm (Figure 4.4) This high level of U is likely reflective of steps or kinks on the mineral surface that are reactive and easily dissolved. The second and third wash result in similar concentrations of ~10 ppm dissolved U, leading to the conclusion that highly reactive surfaces as well as any remaining U(VI) is removed in the first wash. Uranium concentrations in the second and third wash are thought to be reflective of U(IV) solubility in the presence of HCl.

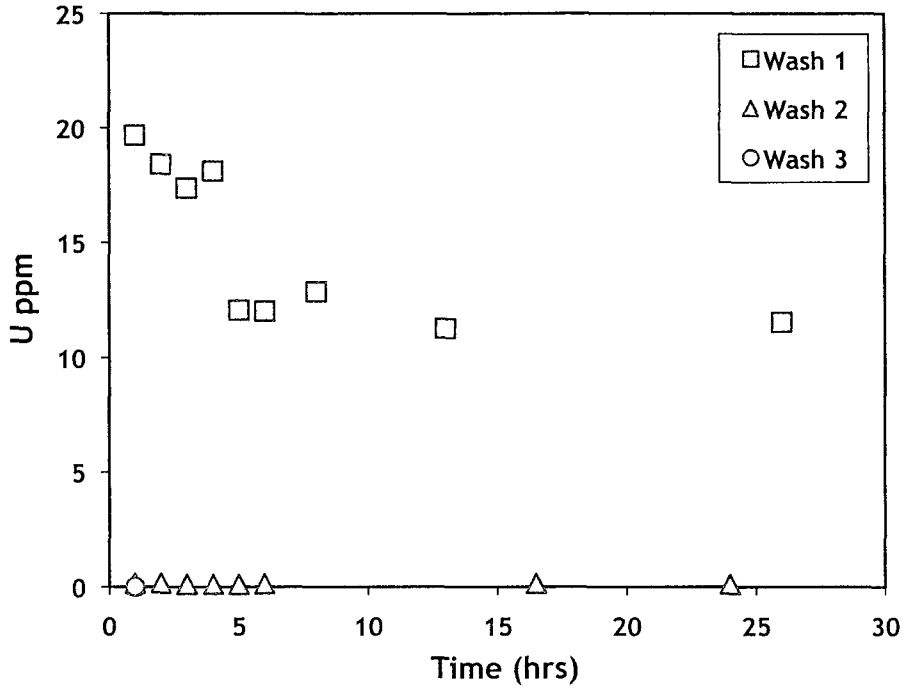

Figure 4.3. Removal of U(VI) over time by washing with 0.5 M $NaHCO_3$.

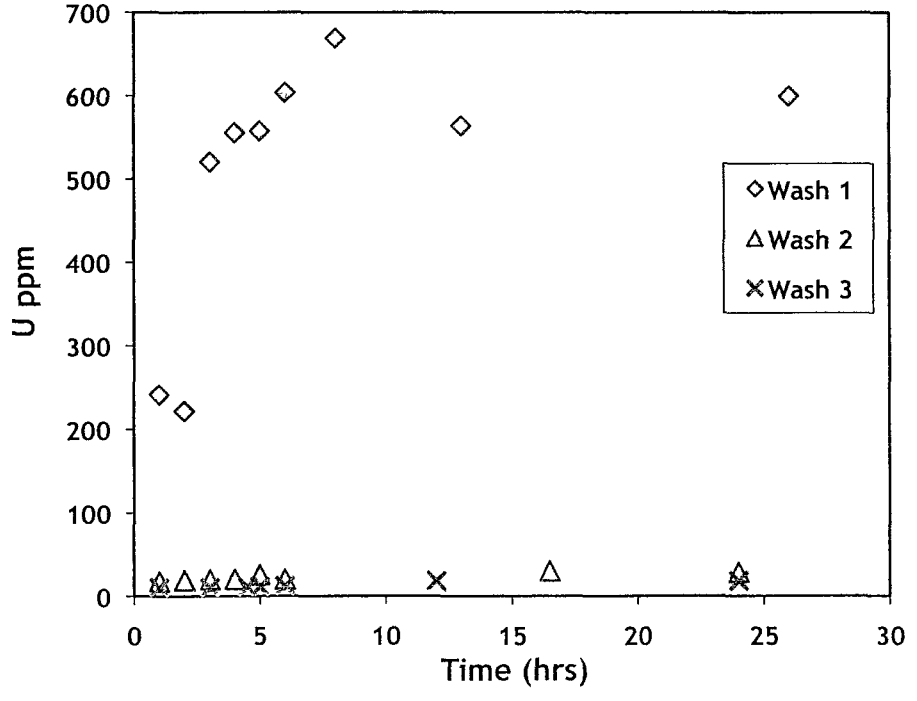

Figure 4.4. Removal of U over time by washing with 0.1 M HCl.

Kinetics experiments

A kinetic experiment was carried out to determine the equilibration period for the hydrolysis of $UO_{2(s)}$. Inside the glovebox, the solid was exposed to 50 mL deionized water in the presence of 0.01 M NaCl for 32 hours. Results show that after an initial peak in the first 3 hours, within 5 hours the concentration of dissolved U declines and then for some samples peaks again (Figure 4.5). To ensure equilibrium was investigated in the solubility experiments, the equilibration period was lengthened to three days.

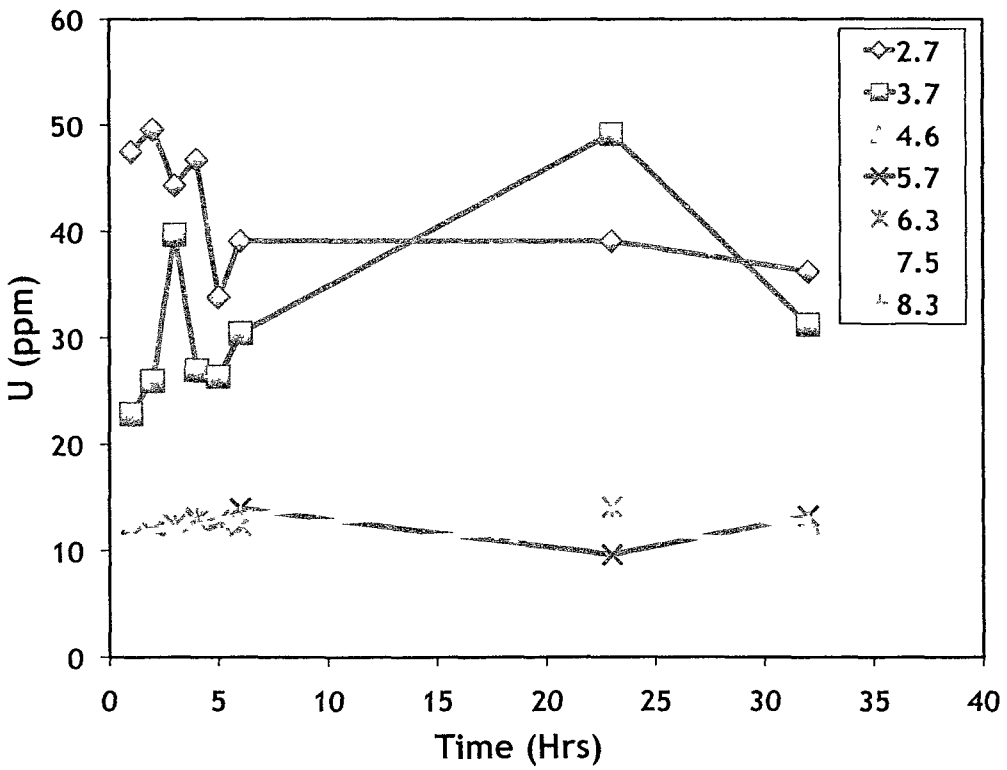

Figure 4.5. Hydrolysis of $UO_{2(s)}$ in the presence of 0.01 M NaCl at various pH, inside glovebox, STP.

$UO_{2(s)}$ hydrolysis experiments

After treating $UO_{2(s)}$ to remove U(VI), hydrolysis experiments were performed at room temperature with 0.01 M NaCl used as a background electrolyte over a pH range of 5 to ~11. For experiments conducted in the glovebox, $2.6 \cdot 10^{-3}$ M $Eu(II)Cl_2$ was added to control redox potential in the solution. The $UO_{2(s)}$ hydrolysis experiment shows that the log activity of U in solution is ~ - 6 over the pH range investigated, and no pH dependence is observed (Figure 4.56).

To compare solubility of the solid under oxidizing conditions, an identical experiment was also performed outside of the glovebox in ambient atmosphere. Experiments carried out under oxidizing conditions produce a two orders of magnitude increase in $UO_{2(s)}$ solubility (Figure 4.6). As for the hydrolysis experiment completed under reducing conditions, little or no pH dependence is observed.

Solubility of $UO_{2(s)}$ with addition of citrate, NTA or EDTA under reducing conditions

The solubility of $UO_{2(s)}$ was examined in 0.01 M NaCl with $2.6 \cdot 10^{-3}$ M $Eu(II)Cl_2$, in the presence of 100, 250 and 500 mM citrate in an N_2/H_2-filled glovebox (Figure 4.7). There is no difference in $UO_{2(s)}$ solubility, within the uncertainty of the experiments, compared to results obtained in the absence of citrate. As for data measured in the absence of organic acids, there is little or no pH dependence, and no discernible dependence on the concentration of organic acid added. The addition of 100, 250 and 500 mM NTA does slightly enhancement $UO_{2(s)}$ solubility, by ~ half an order of magnitude (Figure 4.8). However, as was the case for citric acid, there does not appear to

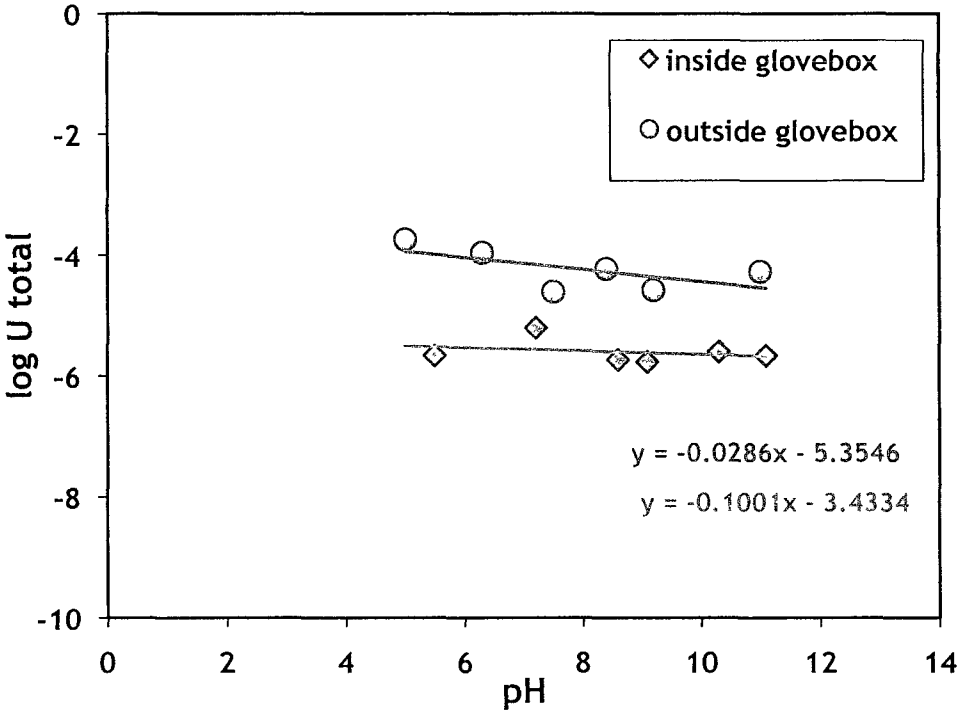

Figure 4.6. Hydrolysis of $UO_{2(s)}$ under reducing (blue) and oxidizing (red) conditions, in 0.01 M NaCl with $2.6 \cdot 10^{-3}$ M $Eu(II)Cl_2$ to control redox potential under reducing conditions.

be any discernable dependence on the added ligand concentration or the pH. In contrast, the addition of 100 or 250 mM EDTA does cause an increase in $UO_{2(s)}$ solubility. There is more than an order of magnitude increase in $UO_{2(s)}$ solubility observed with the addition of 100 mM EDTA (Figure 4.9). However, addition of more EDTA (250 mM) actually results in less solubilization of the U. This suggests either a significant error in the experimental data (possible oxidation), or an indication that high concentrations of EDTA might actually stabilize the $UO_{2(s)}$, reducing its solubility.

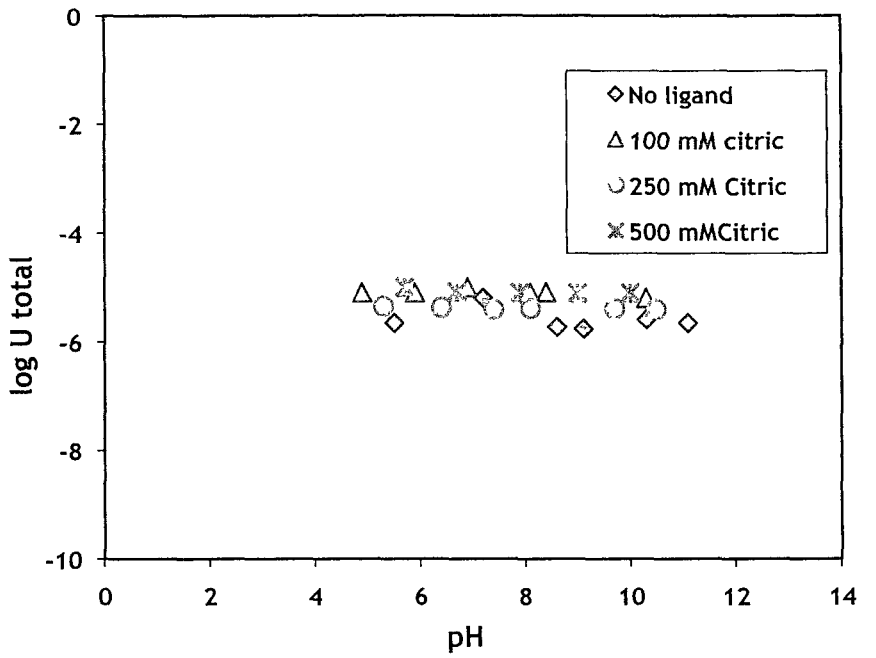

Figure 4.7. Exposure of UO_2 to ligands under reducing conditions with 0.01 M NaCl and $2.6 \cdot 10^{-3}$ M $Eu(II)Cl_2$ at STP and in the presence of varying concentrations of citrate.

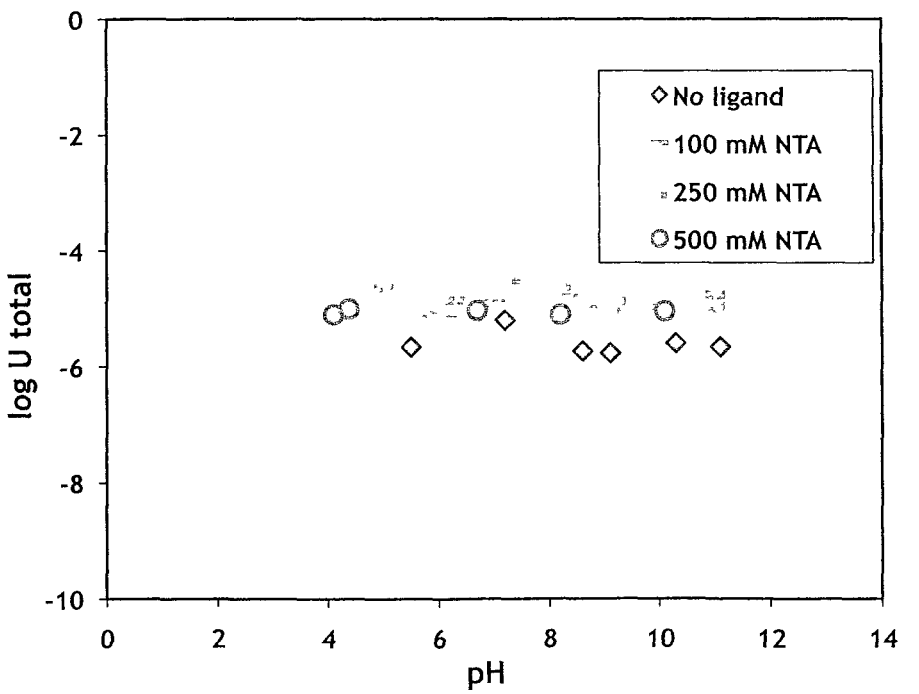

Figure 4.8. Exposure of UO_2 to ligands under reducing conditions with 0.01 M NaCl and $2.6 \cdot 10^{-3}$ M $Eu(II)Cl_2$ at STP and in the presence of varying concentrations of NTA.

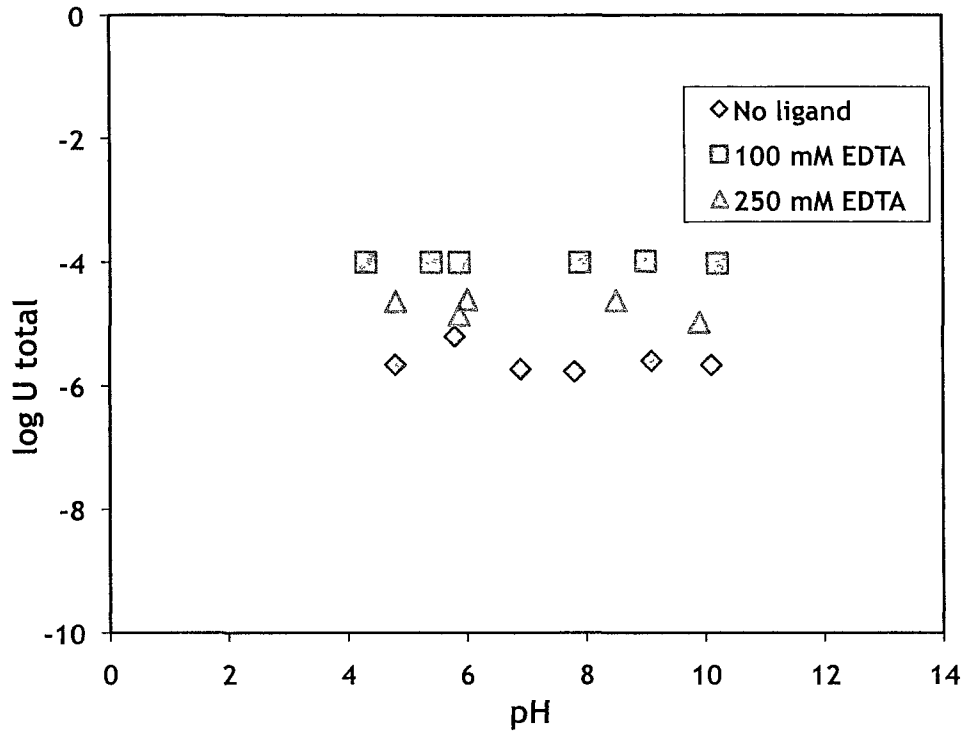

Figure 4.9. Exposure of UO_2 to ligands under reducing conditions with 0.01 M NaCl and $2.6 \cdot 10^{-3}$ M $Eu(II)Cl_2$ at STP and in the presence of varying concentrations of EDTA.

Solubility of $UO_{2(s)}$ with addition of citrate, NTA or EDTA under ambient atmosphere

It was not possible to confirm the oxidation state of U for experiments conducted with organic acids inside the glovebox. With the extensive methods applied to remove U(VI) from the surface, and by adding a reducing agent to the solution, U at the solid surface is expected to be entirely in the tetravalent state. However, to provide further constraints on experiments performed in the glovebox, identical experiments were conducted outside of the glovebox under ambient atmosphere. These experiments provide a comparison with $UO_{2(s)}$ solubility when U(VI) is expected to exist at the surface and to allow for a better interpretation of results from the reducing tests.

Solubility experiments investigating the effect of U(VI) on U-citric complexation under ambient atmosphere show a pronounced pattern of citrate concentration dependence (Figure 4.10). Increasing the citrate concentration results in a corresponding increase in U activity in solution. The highest concentration of citrate added, 500 mM, produces distinctly elevated U concentrations compared to experiments with lower concentrations of citrate added. In contrast, no dependence on citrate concentration was observed for experiments conducted in the glovebox under reducing conditions. It should also be noted that the data obtained under reducing conditions in the glovebox clusters around the data obtained under ambient atmosphere, suggesting that the results obtained in the glovebox reflect $UO_{2(s)}$ tainted with U(VI), as will be further discussed in Chapter 5.

Experiments investigating the dissolution of UO_2 in the presence of NTA under oxidizing conditions show a ligand concentration dependence similar to that observed for citrate (Figure 4.11). The addition of 100 mM NTA produces the lowest solubilization effect and also plots within the range of data obtained in the reducing atmosphere of the anaerobic glovebox. Increasing NTA concentrations to 250 or 500 mM causes an enhancement in UO_2 dissolution relative to that obtained under reducing conditions or in the absence of organic acids under ambient atmospheric conditions. Less scatter is seen for the data from the experiments conducted under oxidized conditions for the individual ligand strengths, and a clear concentration dependence is also evident. The activity of U in solution obtained in glovebox experiments plots at the lower limit of the oxidized data, suggesting that U(VI) contamination is present for experiments inside the glovebox.

Experiments investigating the effect of EDTA on $UO_{2(s)}$ dissolution under oxidizing conditions do not show the same concentration trends as observed for citrate and NTA experiments. Citrate and NTA solubility studies showed an increase in U activity with increasing organic ligand concentrations. However, for experiments in ambient atmosphere with EDTA, no dependence of solubility on the ligand concentration is observed (Figure 4.12). Furthermore, the data for atmospheric experiments plots between the data obtained under reducing conditions, again implying that these experimental results may reflect the presence of U(VI) in the $UO_{2(s)}$

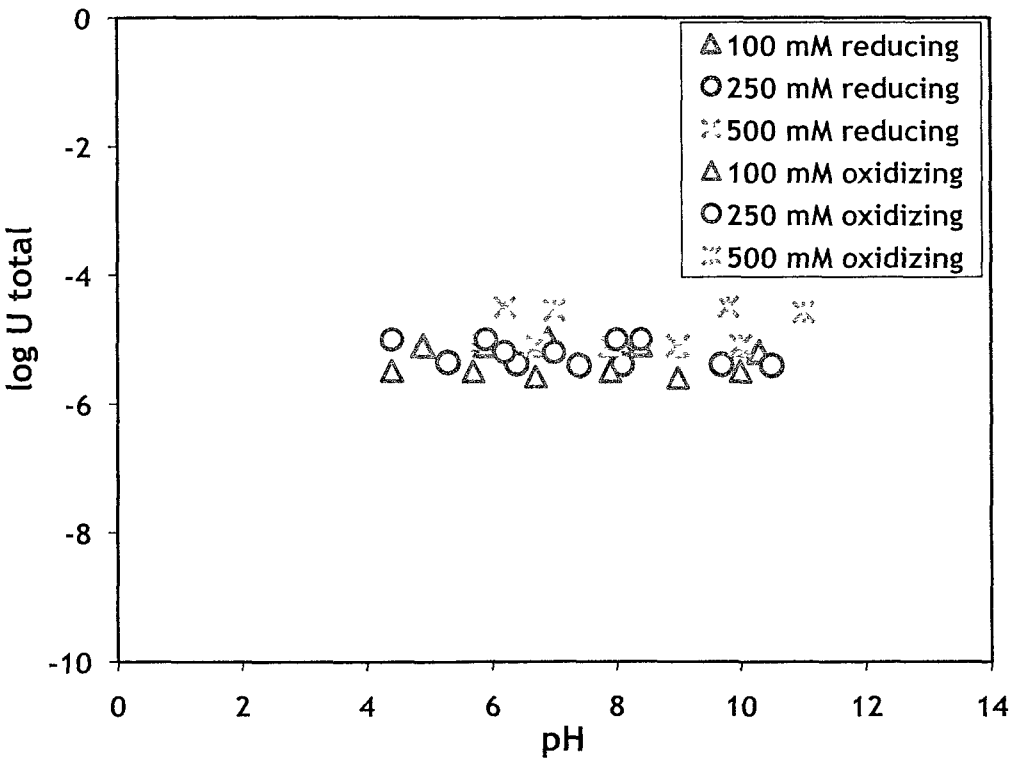

Figure 4.10. Exposure of UO_2 to ligands under ambient atmosphere (oxidizing) or in a glove box with $2.6 \cdot 10^{-3}$ M $Eu(II)Cl_2$ added (reducing) with 0.01 M NaCl and in the presence of varying concentrations of citrate.

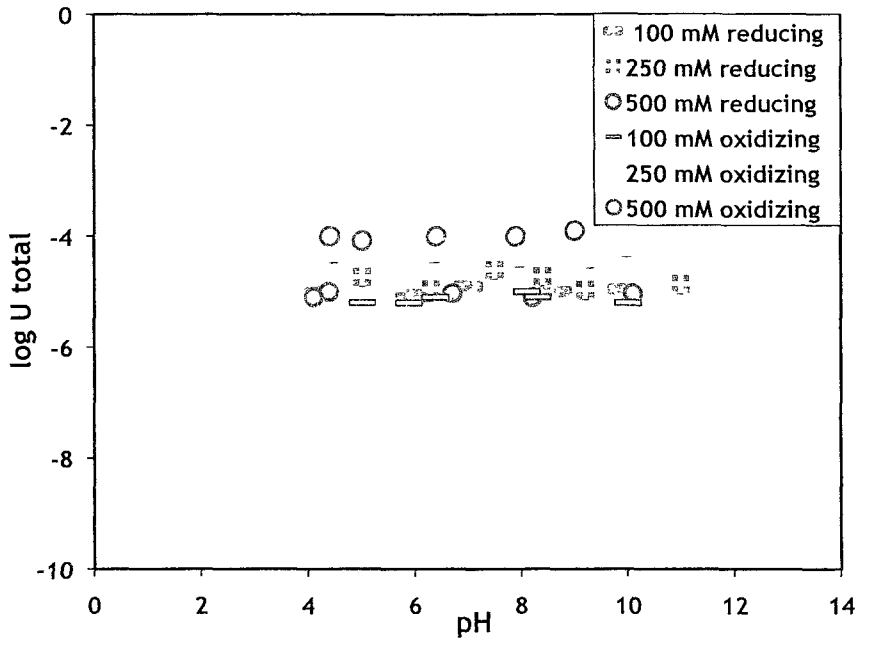

Figure 4.11. Exposure of UO_2 to ligands under ambient atmosphere (oxidizing) or in a glove box with $2.6 \cdot 10^{-3}$ M $Eu(II)Cl_2$ added (reducing) with 0.01 M NaCl and in the presence of varying concentrations of NTA.

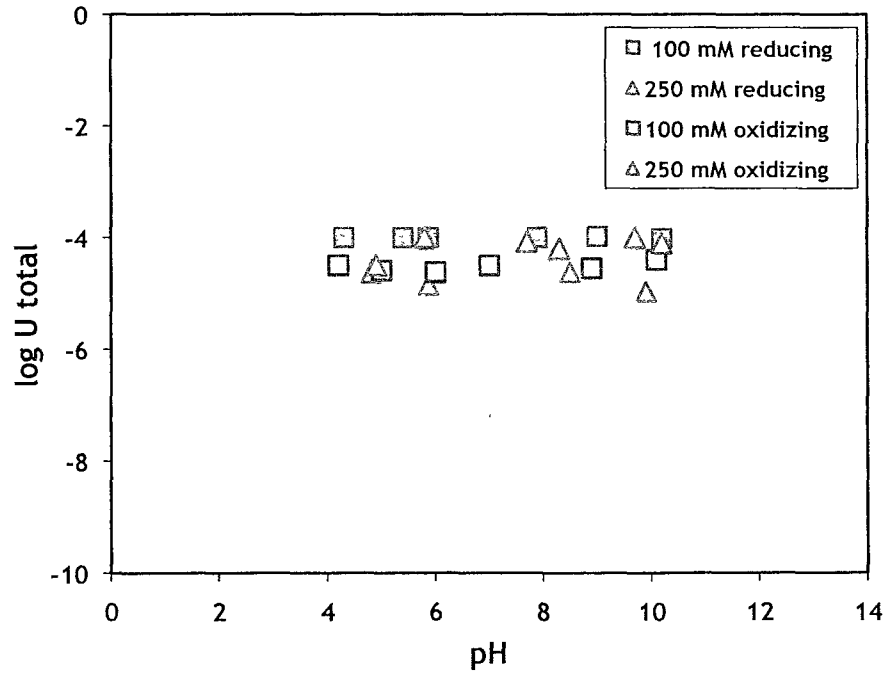

Figure 4.12. Exposure of UO_2 to ligands under ambient atmosphere (oxidizing) or in a glove box with $2.6 \cdot 10^{-3}$ M $Eu(II)Cl_2$ added (reducing) with 0.01 M NaCl and in the presence of varying concentrations of EDTA.

CHAPTER V

$UO_{2(s)}$ DISSOLUTION DISCUSSION

UO_2 solubility in the absence of ligands

The solubility of $UO_{2(s)}$ in the absence of organic ligands has been previously studied by several authors (Fuger 1993; Rai 1990, 2003; Neck and Kim 2001). However, particularly above a pH of 4, these investigators fail to obtain similar results. Studies attempting to define $U(IV)O_{2(s)}$ solubility constants have been performed by different authors, in different media, at different ionic strengths, at varying temperatures, from starting conditions of oversaturation and undersaturation, with different starting solid phases, and have been interpreted with different sets of species. This great diversity of experimental systems and conditions undoubtedly accounts for the tremendous disparity among reported K_{sp} values.

Maintenance of strictly reducing conditions during $UO_{2(s)}$ solubility experiments is likely a problem in many of the reported data. Rai (1990) conducted solubility experiments using Fe and Eu^{2+} to effectively eliminate O_2. The study was completed at room temperature, 1 bar, and a pH range of 2 to 12 and with solubility approached from the point of oversaturation and undersaturation. The starting solid was determined to be amorphous. Rai's (1990) work placed a much lower limit on U solubility compared to earlier studies. Whereas Rai (1990) used Fe and Eu^{2+} to control redox potentials, Bruno et al. (1987) used H_2 gas as the reductant and Pd as the catalyst. Results from Bruno et al. (1987) returned U activities that were four orders of magnitude above Rai's (1990)

findings. Bruno et al. (1987), in a very early attempt to elucidate U(IV) solubility, conducted their experiments in the presence of high O_2 fugacities, between $10^{-0.7}$ and 10^{-5}. Gayer and Leider (1957) obtained solubility results similar to Bruno et al. (1987), log U activities of ~ -4. The lower solubilities reported by Rai (1990) are in agreement with trends predicted from the solubility of other tetravalent actinides, suggesting that they most closely reflect the solubility of pure $U(IV)O_2$. However, Rai (1990) concluded that the disparity between the reported data could be attributed not only to ineffective controls on redox potential, but also to inadequate techniques for separating solids from solutions, and difficulties presented with the analytical detection of low U concentrations.

Rai (1990) used the solubility data obtained under strictly reducing conditions to constrain the first and fourth order hydrolysis reactions. The first order hydrolysis is represented by the reaction,

$$UO_2 \cdot xH_2O_{(am)} + 3H^+ \Leftrightarrow UOH^{3+} + (x+1)H_2O \qquad (4.1)$$

with a reported log K at zero ionic strength of 3.5 ± 0.8 (Figure 5.1). The fourth order hydrolysis was determined by Rai (1990) according to,

$$UO_2 \cdot xH_2O_{(am)} \Leftrightarrow U(OH)_4^0 + (x-2)H_2O \qquad (4.2)$$

and has a log K of -8 (Figure 5.1).

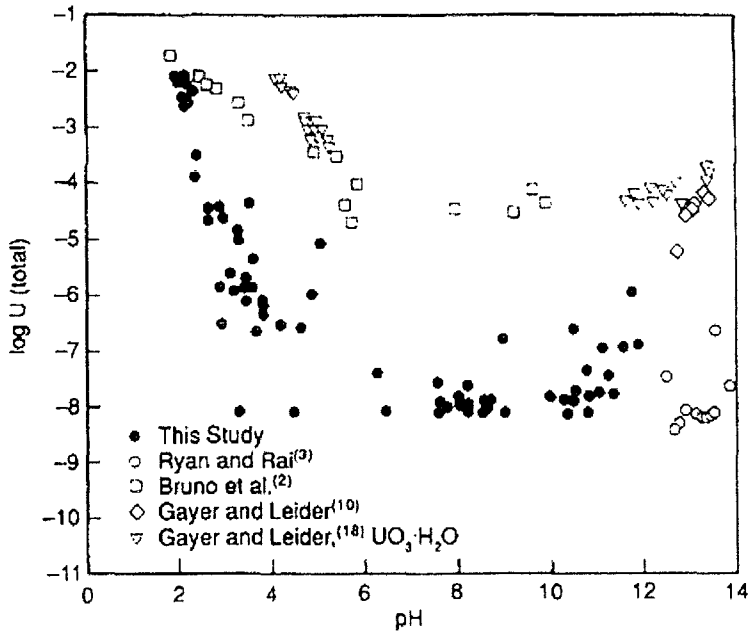

Figure 5.1. Comparison of aqueous U concentrations in equilibrium with $UO_2 \cdot xH_2O_{(am)}$ with previous literature (after Rai 1990). Rai used Fe and Eu^{2+} to eliminate O_2, and conducted experiments at room temperature and 1 bar (STP).

In 2001 Neck and Kim presented a critical review of $U(IV)O_2$ solubility that confirmed the conclusions of Rai (1990). They demonstrated that under strictly reducing conditions, log U activities should be approximately –8 for the fourth order hydrolysis reaction (Figure 5.2). Neck and Kim (2001) do not claim absolute control on oxidation occurs in the reviewed studies, but they argue that these tests have better controls on redox when compared to the studies of Bruno (1987) and Gayer and Leider (1957), which produced much higher solubilities. However, results from the investigations conducted under more strictly controlled redox still exhibited a distribution of solubility data that varied over several orders of magnitude. Neck and Kim (2001) suggest two possible causes for this scatter in the literature values: (1) a small and variable level of oxidation

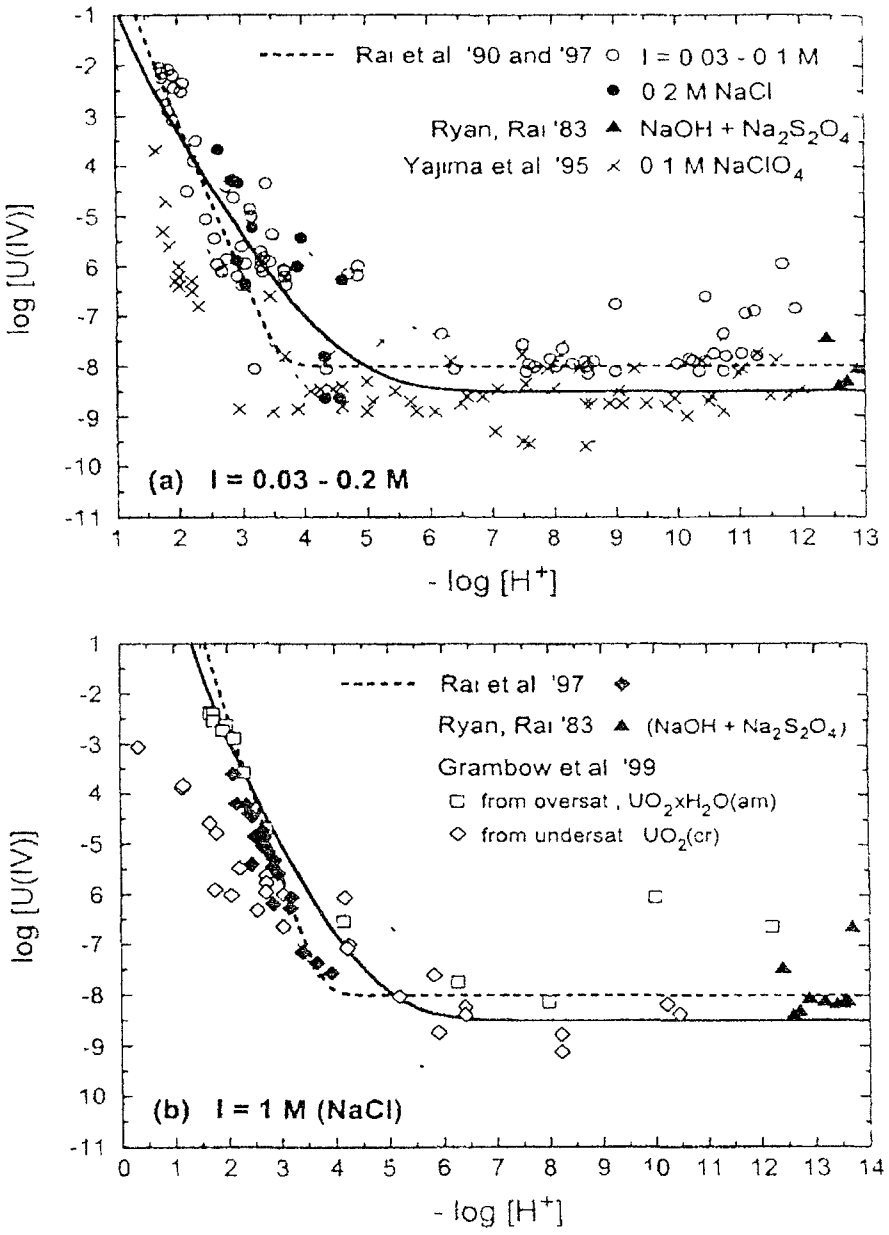

Figure 5.2. Review of $UO_{2(s)}$ solubility as a function of pH at 20-25°C and ionic strength of 0.03 -0.3 M (a) and 1 M (b) (after Neck and Kim 2001).

occurred and/or (2) significant variations in the solid phase used in the different experiments.

This highlights another important complication to consider when investigating $UO_{2(s)}$ solubility, the exact composition of the solid phase. Rai (1990) used amorphous $UO_{2(s)}$, whereas the solid in this study was determined by XRD to be crystalline. Neck and Kim (2001) compile data with distinct solid phases (Figure 5.2): amorphous UO_2 (Rai et al., 1990, 1997; Ryan and Rai 1983) and crystalline UO_2 (Yajima et al., 1995). Yajimia et al. (1995) approached equilibrium from the point of undersaturation and allowed a longer period of equilibration compared to other workers from the review. The longer equilibration time lead to an increase in crystallinity, resulting in lower solubilities than those observed in other studies (e.g., Rai et al, 1990; 1997; Ryan and Rai 1983). This comparison demonstrates the problematic inconsistencies among reported U(IV) solubility experiments. In addition, although Yajima et al. (1995) claim that the U activity in solution is in agreement with predicted $UO_{2(s)}$ solubility values, Neck and Kim (2001) take issue with this, stating that the crystalline solid used by Yajima et al. (1995) should result in log U activities several orders of magnitude lower than the reported values of –8. This assertion is based on the fact that the solubility products for all tetravalent crystalline actinides are known to differ by approximately eight orders of magnitude when compared to amorphous $UO_{2(s)}$ (Rai 1990; Neck and Kim 2001).

Neck and Kim (2001) call further attention to the disagreement between literature results for crystalline UO_2 and calculated predictions for tetravalent actinides using work from Parks and Pohl (1985). Parks and Pohl (1985) dissolved $UO_{2(cr)}$ at 100, 200 and 300°C and 1 bar in chloride solutions with $I < 0.1$ M and above pH 4, found log U

activities that ranged from log -9 to -10. Neck and Kim (2001) state that these values are higher than would be expected for crystalline tetravalent actinides, and furthermore, that at pH > 2 the reported U activity is more consistent with solubility of amorphous solids. Neck and Kim (2001) thus conclude that the solubility data of Parks and Pohl (1985), especially in the near neutral pH range do not reflect crystalline UO_2 dissolution, but instead are representative of dissolution of an amorphous surface layer. These studies highlight that oxidation of U(IV) in UO_2 is one pathway to enhanced solubilities, and a second possibility is the presence of an amorphous or partially amorphous solid phase.

$UO_{2(s)}$ hydrolysis in this study

Solubility experiments conducted outside of the chamber in this work resulted in a log U activity of ~ -4, suggesting that the solubility is influenced by the presence of U(VI) (Figure 4.6). These results are in agreement with expected values for ambient atmospheric conditions and conform well to work from Bruno (1987) and Gayer and Leider (1957; Figure 5.1). In contrast, experiments investigating the hydrolysis of $UO_{2(s)}$ under anaerobic conditions in the glovebox suggest that oxidation of U(IV) to U(VI) was not fully suppressed.

This is true in spite of the fact that several methods were used to eliminate U(VI) from the solid surface and control redox potentials in this study. The solid was washed with $NaHCO_3$, HCl and burned at high temperature to remove U(VI) from the surface. Results from the $NaHCO_3$ wash (Figure 4.3) and HCl wash (Figure 4.4) suggest that all labile U(VI) was removed from the surface. Deionized water used for solutions were sparged in the glovebox and Eu^{2+} was added to the experiments, as done by Rai (1990).

Nonetheless, the results suggest that even these extensive methods applied to the solid and solution did not entirely eliminate U(VI). Uranium activities for trials conducted under reduced conditions (Figure 4.5) remain several orders of magnitude above expected values from the work discussed above (Figures 5.1 – 5.3). Past work shows $U(IV)O_2$ solubility values spanning orders of magnitude, from log U of -7 to -10 (Rai 1990 and 1997; Yajima et al., 1995; Figures 5.1-5.3). These observations lead to the conclusion that the hydrolysis experiment in this study was contaminated with U(VI) because log U activities recovered from the hydrolysis were ~ -6. Furthermore, XRD demonstrates that the solid phase used in this experiment was crystalline, and the HCl and burn procedures would be expected remove any thin amorphous layers from the surface. With such thorough preparation methods, it is unlikely that the presence of an amorphous solid phase is responsible for high solubilities. Finally, solubility of the solid used in this study is well above that reported previously for $UO_{2(am)}$, which has an upper limit on log dissolved U of ~ -7. Therefore, contamination of the solid phase by U(VI) is almost certainly responsible for the elevated U activities observed relative to expectations under reducing conditions.

$U(IV)O_{2(s)}$ solubility promoted by ligands

Little work has been done to quantify the complexation of $U(IV)O_{2(s)}$ with organic acids (Hummel 2007, Pasilis and Pemberton 2003, Borkowski et al.,1996). Much of this work concerns the resulting aqueous U(IV)-ligand speciation and structure of U(IV)-ligand complexes in solution (Pasilis and Pemberton 2003, Bonin et al., 2009) and does not report the activity of U(IV) dissolved in solution. Due to the dearth of research

investigating the effects of organic acids on $U(IV)O_{2(s)}$ dissolution it is necessary to use $Th(IV)O_{2(s)}$ as a proxy. To provide better constraints on $U(IV)O_{2(s)}$ ligand-promoted solubility, prior work done with $Th(IV)O_2$ can be used to assess expected $U(IV)O_{2(s)}$ solubilities.

Thorium is an actinide, number 90 on the periodic table and is an element that is stable in the tetravalent state (Rai et al. 1997). This means that solubility experiments involving Th(IV) are not effected by oxidation with O_2, unlike those with U(IV)-bearing solids. Furthermore, because Th(IV) oxides can be expected to exhibit similar K_{sp} constants to U(IV) oxides they are excellent candidates to help place constraints on U(IV) solubility behavior. For example, the similarities in solubility between tetravalent actinide oxides have been demonstrated by Fuger (1993). A linear relationship links the log K of the solubility constant to the inverse square of the M^{4+} ionic radii (Figure 5.3). The work shows that although solubility varies over several orders of magnitude, there is a predictable trend between the two solids. Solubility work involving ThO_2 is used in this study to provide a broad comparison for $U(VI)O_{2(s)}$ complexation by ligands. Although solubility values between the two solids may not be the same, some of the general solubility behavior may be expected i.e. pH dependence, and enhancement or diminishment of solubility resulting from complexation.

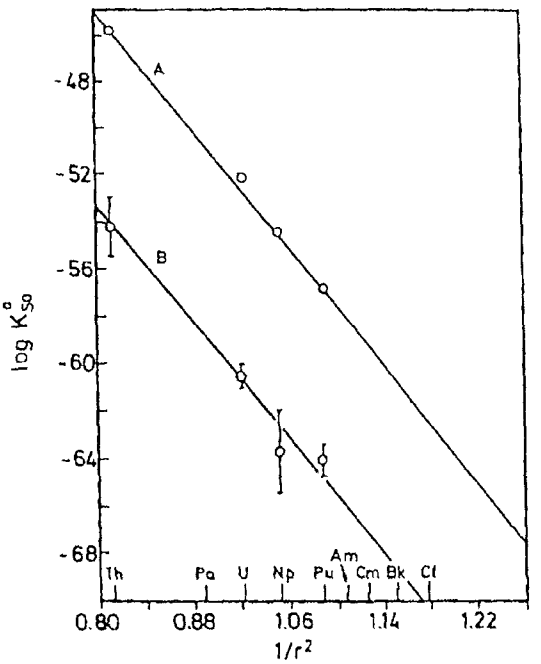

Figure 5.3. Variation of log solubility products of actinide dioxides (after Fuger 1993). Line A represents amorphous oxides and line B crystalline oxides.

To compare $ThO_{2(s)}$ solubility against results in this study, it is necessary to first define the activity of Th(IV) for the fourth order hydrolysis. Work by Neck and Kim (2003) shows experimental and calculated hydrolysis data for crystalline and amorphous phase $ThO_{2(cr)}$ at I = 0.5 M NaCl, STP. Above a pH of 4 the data plots between a log Th(IV) of -7 to -9. Although there is an order of magnitude elevation in Th(IV) activity compared to experiments with U(IV), the trends are similar to the hydrolysis results observed for $U(IV)O_2$. This comparison demonstrates that Th(IV) can be used as an approximate substitute for U(IV).

Work by Felmy et al. (2006) and Xia et al. (2003) investigating the dissolution of $ThO_{2(am)}$ in the presence of ligands (citrate or EDTA) can be expected to provide a meaningful comparison to the $UO_{2(s)}$ solubility experiments carried out in this study.

Their ThO_2 solubility studies were conducted under Ar atmosphere, approached from the point of undersaturation (0.1 g $ThO_{2(am)}$), using 0.01 -0.1 M ligand and varying ionic strengths (0.5 – 6.0 M $NaNO_3$). The results show that for $ThO_{2(am)}$, the addition of citrate and EDTA increased dissolution of the solid when compared to systems without organic acids (Figure 5.4(A)). For both ligands, Th(IV) activities were elevated six orders of magnitude, from approximately log Th(IV) of -8 to log Th(IV) of -2. For the $ThO_{2(s)}$ hydrolysis no pH dependence was observed between pH 4 and 8. In contrast, the addition of citrate or EDTA caused a strong correlation between pH and dissolution at pH > 8.

Citrate produced greater dissolution of $ThO_{2(am)}$ when compared to EDTA. The slope for the EDTA data under basic conditions was -1, whereas citrate was -3. Xia et al. (2003) attribute the shallow slope and low pH dependence of the EDTA system to the aqueous speciation; only one aqueous Th-EDTA complex dominates at all pH values ($ThEDTA_{aq}$). In contrast, citrate was determined to form aqueous complexes that hydrolyze ($Th(OH)_3(Cit)_3^{8-}$, $Th(OH)_3(Cit)_2^{5-}$) , resulting in a correlation of solubility enhancement with the change in OH^- concentrations at high pH.

The effect of varying citrate and EDTA concentrations ($1 \cdot 10^{-5}$ to $1 \cdot 10^{-2}$ M) on 0.01 g $ThO_{2(am)}$ has also been explored. It was found that small additions of either citrate or EDTA ($1 \cdot 10^{-5}$ M) do not result in enhanced solubility, presumably due to sorption of the ligand to the solid. For the citrate investigations, Felmy et al., (2006) theorized that only complexes with multiple citrates formed on the $ThO_{2(s)}$ surface, and that $ThO_{2(s)}$, dissolution depends strongly on specific metal/ligand ratios. Essentially, to solubilize $ThO_{2(s)}$ there must be a high concentration of citrate in solution relative to potential

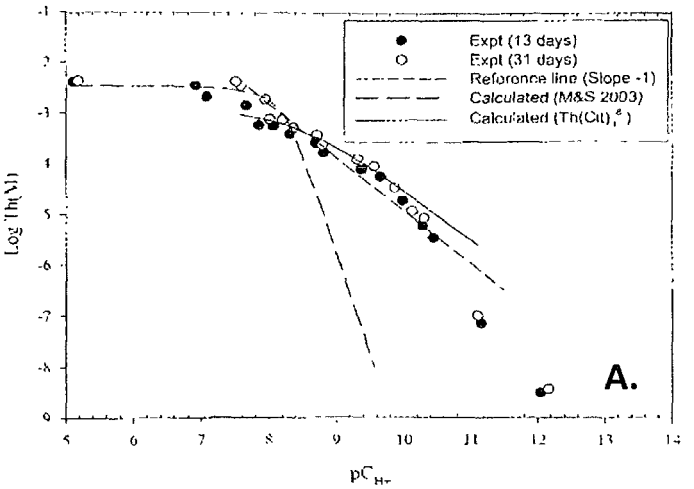

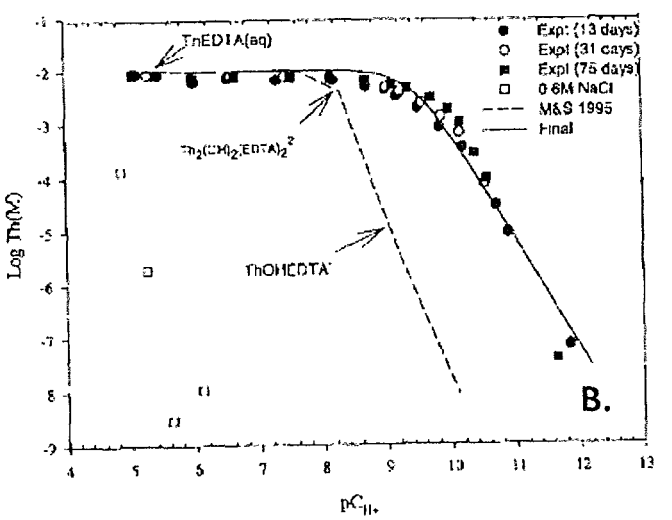

Figure 5.4. Solubility of $ThO_{2(am)}$ as function of pH in 0.5 M $NaNO_3$ in 10 mM (A) citrate (Felmy et al., 2006) and (B) EDTA (after Xia et al., 2003).

aqueous Th(IV). Similar observations were made by Xia et al. (2003), although they offered no explanation to explain the phenomenon. It is possible that a similar concentration-dependent relationship exists between Th and EDTA, and again an excess of ligand is needed to solubilize $ThO_{2(s)}$.

Similar work conducted in this study yielded very different results compared to those reported by Felmy et al. (2006) and Xia et al. (2003). Under reducing conditions, enhanced dissolution by citrate and NTA was not observed compared to the $UO_{2(cr)}$ hydrolysis in the absence of ligands (Figure 4.7 and 4.8). However, a two-order magnitude enhancement was seen for EDTA (Figure 4.6). In further contrast to Felmy et al. (2006), under reducing conditions, $UO_{2(s)}$ dissolution in the presence of citrate or NTA does not show a pH or ligand concentration dependence. Felmy et al. (2006) investigated a citrate concentration that ranged over several orders of magnitude, and found a strong dependence of solubility on the concentration of the ligand used. Because a smaller range of citrate and NTA was explored in this study, 100 – 500 mM, it may not be surprising that the ligand concentration dependence is not observed. However, the lack of pH dependence was also observed for experiments conducted under oxidizing conditions, pointing to possible interference by U(VI).

Experiments comparing the effect of ligands on $UO_{2(s)}$ dissolution under oxidizing versus reducing conditions resulted in fairly similar dissolved U activities (Figure 4.10 – 4.12), which were also similar to those for experiments completed in the absence of organic acids. It is very likely the $UO_{2(s)}$ in the organic acids experiments was tainted with U(VI), just as was concluded for the organic acid free experiments. In contrast to experiments conducted under anaerobic conditions, there is a small ligand concentration

dependence under ambient atmosphere. However, in contrast to $ThO_{2(s)}$ solubility experiments conducted in the presence of citrate (Felmy et al., 2006) or EDTA (Xia et al., 2003), there is little or no pH dependence for the U activities measured in this study. At least two potential explanations for the similarities in observed dissolved U activities under oxidizing and reducing conditions are: (1) the solid phase is contaminated by U(VI) or/and (2) interference by $Eu(II)Cl_2$ changes the U solubility in the reducing experiments.

Contamination of experiments with U(VI) may best explain the observed solubilities. However, a second consideration is the addition of Eu(II) to solutions in experiments conducted under reducing conditions. Extensive measures were taken to eliminate U(VI) from the solid surface. In solution, under STP conditions, up to $5.6 \cdot 10^{-4}$ M $O_{2(g)}$ can be dissolved into solution. To ensure control of oxidation potentials in solution $2.6 \cdot 10^{-3}$ M $Eu(II)Cl_2$ was added to suppress oxidation. It is possible that the high concentration of reductant resulted in a competing cation for ligand complexation, suppressing the dissolution of U.

CHAPTER VI

U(VI) SORPTION BACKGROUND

The potential migration of uranium waste away from storage facilities and into the biosphere necessitates a quantitative understanding of uranium speciation, precipitation, dissolution, sorption, and redox reactions in near surface environments. As was discussed in chapter 1, some major controls on the aqueous speciation of uranium in near surface settings are oxidation-reduction potential, and hence the valence state of U. The first portion of this work concerned $U(IV)O_{2(s)}$ dissolution in the presence of organic acids, in the second section, the focus now shifts to interactions of aqueous phase U(VI) with mineral surfaces. Under oxidizing conditions, uranium exists as the hexavalent U(VI) species (Murphy and Shock, 1999). To predict the migration of U(VI) through near surface systems, it is necessary to consider retention mechanisms, such as the sorption of aqueous U(VI) species by soil or sediment constituents, including clay minerals, oxides, carbonates, and organic matter. Sorption of U(VI) is established to be an important determinant of uranium bioavailability and mobility in the environment (Pabalan, 1988; Grenthe, 1989; Waite, 2000). This work investigates U(VI) sorption behavior onto the clay mineral kaolinite in the presence of organic acids.

The clay mineral kaolinite

Kaolinite, an aluminosilicate clay with a fairly simple chemistry ($Al_2Si_2O_5(OH)_4$) and structure (1:1 or "T:O"), is often used as a representative clay mineral in

experimental studies. Kaolinite is considered a secondary mineral because it is frequently formed by weathering or through hydrothermal alteration of aluminosilicates, especially feldspars Because it is a common product of rock weathering, it is found in many types of soils (Klein and Hurlbut, 1993).

Kaolinite is composed of repeating sheets of silica (SiO_2) tetrahedral (*t*) layers bonded to alumina (Al_2O_6) octahedral (*o*) layers. Individual *t-o* sheets are weakly held together by van der Waal forces (Figure 6.1; Klein and Hurlbut, 1993). Kaolinite does not experience interlayer swelling, because it does not contain an interlayer that can accommodate water, such as is present in smectite clays that posses a permanent negative charge. The alumina layer in kaolinite is similar to gibbsite, meaning that each aluminum atom is coordinated to six hydroxides in an octahedral pattern. Charge requirements result in one third of the Al cation sites being vacant. In this arrangement, one hydroxide is surrounded by 2 Al atoms resulting in a dioctahedral designation.

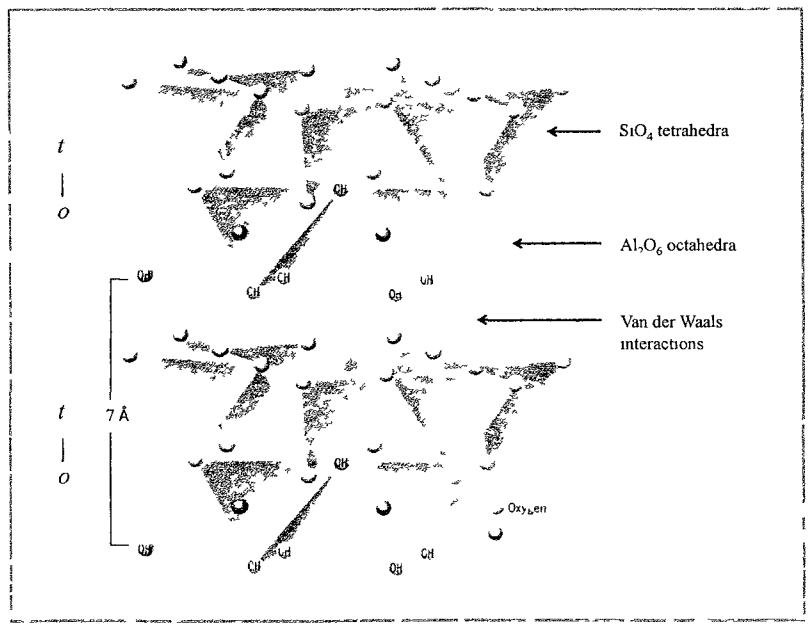

Figure 6.1. Kaolinite structure. Modified from Klein and Hurlbut (1993).

Sorption at mineral surfaces

Thermodynamically-based surface complexation models (SCMs) can be used to describe reaction stoichiometries and stability constants for equilibrium adsorption reactions (e.g. Stumm and Morgan, 1996). A double layer model (DLM) was used in this study to describe sorption of U(VI) to kaolinite. To characterize U(VI) complexation to the mineral surface, the DLM includes several assumptions, First, it is assumed that the mineral surfaces can be represented as a flat plane of hydroxylated sites, and that chemical reactions can be written to describe sorption at these sites. For example, the loss of a proton at the surface of a mineral would be described by the reaction,

$$>SOH \Leftrightarrow >SO^- + H^+ \qquad (1)$$

where >S represents a surface site. Second, it assumed that reactions at the surface are in a state of local equilibrium and can be described through mass law equations. Using the mass law equation, reaction 1 would be expressed as,

$$K^{int} = \frac{[>SO^- + H^+]}{[>SOH]} \qquad (2)$$

where the brackets [ ] indicate the activity of the species and K^{int} is the intrinsic thermodynamic equilibrium constant associated with the reaction. Finally it is assumed that such chemical reactions taking place can result in an overall positive or negative charge at the mineral surface. For example, equation 1 demonstrates that the deprotonation of the >SOH site results in a negatively charged $>SO^-$ site. The mineral surface exerts a variable electrical charge due to such reactions, and in response to this charge a diffuse layer of counterions will swarm the solid surface to balance the charge. The double layer model accounts for two layers of electric potential at the mineral surface

(Figure 6.2). The first layer has a constant potential, and the second layer possesses a potential that decays with distance from the surface.

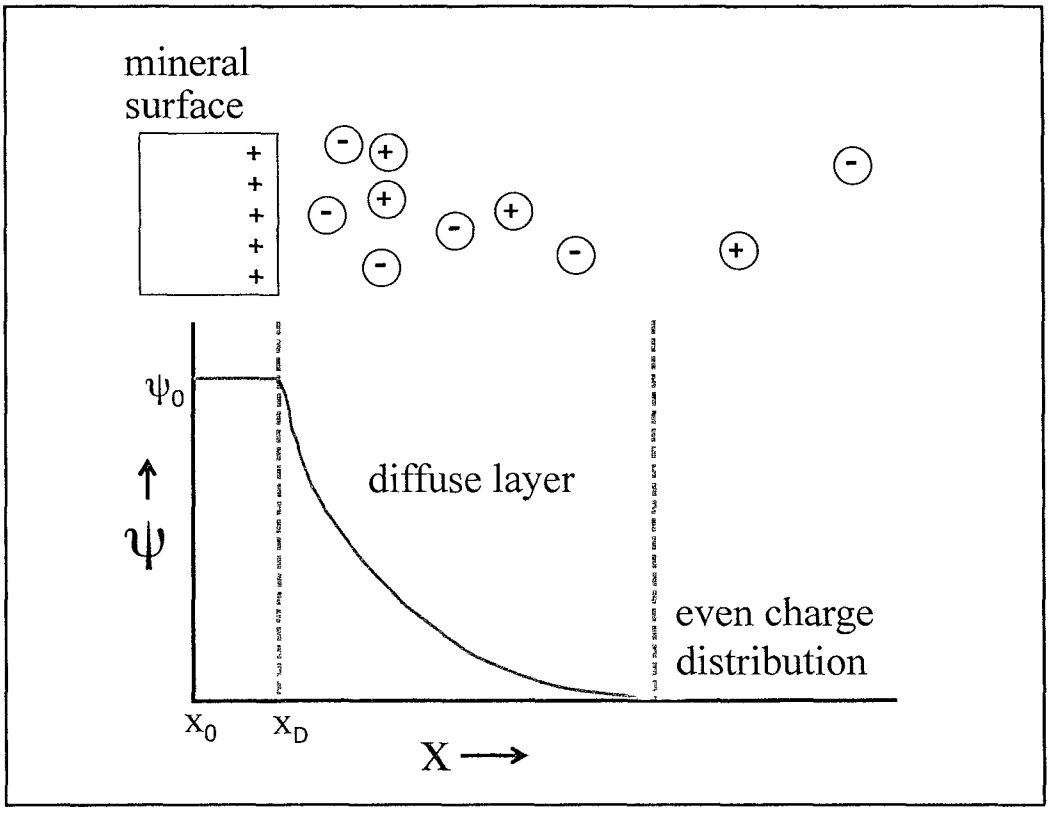

Figure 6.2. General form of the electric potential (ψ) versus distance (x) from the surface for the diffuse layer model.

By applying an electrostatic correction, such as the Coulombic correction factor (equation 3) the effect of surface charge on a measured equilibrium constant can be accounted for (Dzombak and Morel, 1990). For the DLM, Gouy-Chapman theory is used to derive the Coulombic correction factor:

$$\exp\left((-zF\psi(x))/RT\right) \qquad (3)$$

where z is the charge, F the Faraday constant, $\psi(x)$ the electric potential as a function of

the distance x from the surface, R the universal gas constant, and T the temperature. By applying equation 3 to account for effects of the electrostatic layer on surface complexation, the measured, or apparent, equilibrium constant (K^{app}) can corrected and the intrinsic equilibrium constant can be extracted (Koretsky 2000), according to:

$$K^{int} = K^{app} (\exp ((-zF\psi(x))/RT)) \quad (4)$$

Surface complexation modeling, in theory, provides a K^{int} that is independent of pH, concentration of the sorbate and solution composition (Koretsky 2000). The value only depends on the identity of the solid and the sorbing solute (and for some models, on ionic strength). The independence of chemical reactions and stability constants gained from the two-layer model is argued to be one of the better methods used to assist in predicting contaminant migration.

SCMs have been developed that are capable of correctly describing U(VI) sorption onto many potential sorbents under various pH, background electrolyte, carbonate concentrations, and sorbate/sorbent ratios (Pabalan and Turner, 1996; Waite et al., 2000; e.g., Pickryl, 2001; Villalobos et al., 2001; Payne et al., 2004; Catalano and Brown, 2005; Arda et al., 2006; Sachs and Bernhard, 2008; Sherman et al., 2008; Zhiwei et al 2009; Gao et al., 2010). Such reactions are crucial for accurate prediction of the fate and transport of U(VI) through soils and aquifers. Phyllosilicate minerals are an important constituent of nearly all sediments and soils (Brady and Weil, 1999). At the contaminated Hanford site, these have been shown to be the dominant solids responsible for immobilizing U(VI) in the deeper vadose zone (Catalano et al., 2006).

Brief review of U(VI) sorption onto kaolinite

Sorption of U(VI) on kaolinite has been demonstrated to be significant at circumneutral pH, under a variety of sorbate/sorbent ratios and in the presence of different background electrolytes (e.g., Payne et al., 2004; Arda et al., 2006; Sachs and Bernhard, 2008; Gao et al., 2010). Several diffuse layer surface complexation models (DLMs) have been developed that successfully describe sorption of U(VI) onto kaolinite as a function of pH, sorbate/sorbent ratio, background electrolyte, and in the presence of sulfate and phosphate (Payne et al., 2004; Arda et al., 2006; Gao et al., 2010). For example, Payne et al. (2004) conducted U(VI) adsorption experiments from a pH of 3 to 11 with 0.01 M $NaNO_3$ as a background electrolyte. Uranium adsorption was described using a nonelectrostatic model (NEM) with three surface species: $>TiOUO_2^+$, $>AlOUO_2OH$ and $>TiOUO_2CO_3^-$, where >AlOH indicates an aluminol site and >TiOH indicates a titanol site. The titanol sites are attributed to TiO_2 impurities in the natural clay specimens. In contrast, Arda et al. (2006) conducted batch sorption experiments from a pH of 2 to 5.4 in the presence of 0.01 M $NaClO_4$. The data was successfully parameterized using a DLM that described the U(VI) complexation to a variable charge edge site, $>SOUO_2^+$, and a permanent charge exchange site, X_2UO_2. A similar model was developed by Gao et al. (2010) to describe U(VI) sorption onto kaolinite as a function of pH (3 – 8) and sorbate/sorbent ratio and in the presence of 0.1 M NaCl. Gao et al. (2010) developed a DLM with three uranium surface species: one sorbed on a permanent charge or exchange site as X_2UO_2, and two sorbed on variable charge edge sites as $>SOUO_2^+$ and $>SO(UO_2)_3(OH)_5$.

Although several models have been developed to describe U(VI) sorption on kaolinite and other clays (Chisholm-Brause et al., 2001, Prikryl et al., 1994; Davis et al., 2004; Payne et al., 2004; Arda et al., 2006; Sherman et al., 2008; Gao et al., 2010) much less is known regarding the influence of organic acids on U(VI) complexation on kaolinite. It is well known that both naturally-occurring and synthetic ligands, such as citrate, oxalate, fulvic acid, humic acid, EDTA, and NTA form strong aqueous U(VI)-ligand complexes, which may significantly enhance U(VI) mobility (e.g., Wood, 1995; Del Cul et al., 2000; Lenhart et al., 2000; Knepper, 2003). For example, phytoextraction studies have shown that U(VI) can be effectively removed from contaminated soils via the formation of strong aqueous U(VI)-citrate complexes (Choy et al., 2006). Chelating agents such as NTA and EDTA, as well as complexing agents like citric acid, have been identified in mixed waste assemblages at the U.S. Department of Energy Hanford Site where they have been shown to increase tetravalent actinide mobility (Toste, 1995).

Although it is well established that many organic ligands may enhance U(VI) mobility through the formation of aqueous U(VI)-ligand complexes, it is also possible that U(VI) mobility may be diminished by organic acids via the formation of ternary U(VI)-ligand-clay complexes. For example, Sachs and Bernhard (2008) found that the presence of humic acid resulted in a significant enhancement of U(VI) sorption to kaolinite at low pH due to ternary complex formation, whereas sorption was slightly decreased at high pH by the formation of strong U(VI)-humic acid aqueous complexes. Most of the literature regarding U(VI)-organic acid interactions has focused on the formation of aqueous complexes; much less is known regarding the influence of organic acids on U(VI) sorption to clays. These effects are likely to be dependant on pH, pCO_2

and ionic strength conditions, and may be a significant control on uranium speciation in many natural sediments and soils.

Citric acid, fulvic acid and EDTA are three potentially important complexing ligands that may come into contact with actinide waste streams. In this study, the sorption of U(VI) onto kaolinite (KGa-1b) is investigated as a function of pH, ionic strength, pCO_2, and U(VI) concentration. The influence of varying concentrations of citric acid, fulvic acid and EDTA on U(VI) sorption onto kaolinite is also investigated, as well as sorption of the ligands onto the kaolinite surface. The results are quantified using a surface complexation model (NEM and DLM) approach.

CHAPTER VII

U(VI) SORPTION METHODS

U(VI) sorption to container walls, syringes or syringe filters

To investigate potential precipitation of U-bearing solids or loss of UO_2^{+2} by sorption to container walls, syringes or syringe filters, new 50 mL polypropylene tubes were prepared by first rinsing three times with DI water (>18 MΩ). The tubes were then immersed in 5% trace metal grade HNO_3 for 24 hours, rinsed three more times with DI water, and then air dried for 24 hours prior to use. Each cleaned tube was filled with a solution containing $1 \cdot 10^{-6}$, $1 \cdot 10^{-5}$, or $1 \cdot 10^{-4}$ M UO_2^{+2} in 0.01 M $NaNO_3$. These were agitated with a stir bar while the pH of each tube was adjusted to span a range of 3 to 10, at ~0.5 pH intervals, using small additions (~10 μL) of 0.001 to 0.1 M trace metal grade HNO_3 or NaOH. Once the desired pH was achieved, each tube was tightly capped and equilibrated for 24 hrs on a rotator, after which the pH was remeasured and recorded. Each tube was then centrifuged at 4000 rpm for 10 min and a 10 mL aliquot of the supernatant was withdrawn using new syringes, syringe-filtered through 0.45 μm nylon filters, and prepared with 5% nitric acid and an internal standard (1 ppm Y) for analyses of total U by ICP-OES with matrix matched calibration standards. UO_2^{+2} missing from solution was calculated by the difference between the UO_2^{+2} added and the concentration measured in the supernatant solution.

Potential sorption of UO_2^{+2} to the polypropylene tube wall was further investigated by pouring out all remaining solution, and inverting the tube on a Kimwipe

for ~2 min to assist in the removal of pendular moisture. The tube was then filled with 25 mL of a 0.5 M $NaHCO_3$ or 5% HNO_3 solution, tightly capped and rotated for 24 hours. At the conclusion of the equilibration period, a 10 mL aliquot of the solution was removed, acidified with 13% trace metal grade HNO_3 and an internal standard (1 ppm Y) for analysis of total U by ICP-OES was added. UO_2^{+2} sorbed onto the tube wall was assumed to be equal to the amount of U recovered in the wash solution of each aliquot.

U(VI) sorption to kaolinite in the presence and absence of organic acids

U(VI) sorption to kaolinite was similarly measured using batch reactors. Natural kaolinite (KGa-1b) was obtained from the Clay Minerals Society Source Clays. 0.1 g kaolinite (2 g/L) was weighed into each batch reactor and then 50 mL of a solution containing U(VI) ($1 \cdot 10^{-6}$ to $1 \cdot 10^{-4}$ M U) and background electrolyte (0.01 to 0.1 M $NaNO_3$) was added. A control 50 mL batch was set up with each experiment by adding the solution to a solid free tube and titrating to a pH of 3. Initially, several kinetics experiments were run at pH 6.5; these established that U(VI) uptake was rapid and reached a steady state within 2 hr. Reversibility of sorption was tested by dropping the pH to 3; 95% recovery of U(VI) was achieved within 4 hr. Therefore, subsequent sorption experiments were equilibrated for 24 hrs, which should be more than sufficient for equilibrium to be established.

Initial solutions of electrolyte and U(VI) used for the sorption experiments were typically preequilibrated for 30 min at pH ~6 under open atmosphere, then titrated and tightly capped once the desired pH was attained and remained stable for several minutes. Calculations completed using MINTEQ with an atmospheric concentration of 380 ppm

CO_2 yield an estimated $1.5 \cdot 10^{-5}$ M total aqueous CO_3^{-2} in solution at pH 6. Above pH 7.5, the concentration of aqueous CO_3^{-2} increases dramatically with increasing pH. However, the short period of exposure time (~1-10 min) during the titrations, prior to capping the vials, likely did not allow the dissolved carbonate levels to reach equilibrium in the individual reactors. To test this notion, an experiment was also conducted by spiking a volume of $NaHCO_3$ into each reactor prior to the titration calculated (using MINTEQ) to be sufficient to insure that the carbonate system reaches equilibrium. The results (see Chapter 8) suggest that carbonate exchange with the atmosphere does not reach equilibrium prior to capping the reactors in the unspiked experiments, thus, it was assumed in the modeling (see Chapter 8) that the total concentration of aqueous CO_3^{-2} remained at $1.5 \cdot 10^{-5}$ M in these experiments.

The influence of pCO_2 on U(VI) adsorption to kaolinite was also investigated using several additional experiments completed with 0 or 5% pCO_2 atmospheric conditions. These were conducted as described above, except that they were carried out under a controlled atmosphere inside a Coy (®) type B glove box anaerobic chamber. For experiments conducted under 0% pCO_2 a gas mixture of 95% N_2 and 5% H_2 was employed. Oxygen concentrations in the anaerobic chamber were monitored using an internal oxygen sensor and maintained below a working level of <10 ppm using catalytic desiccant packs combined with recirculating fans inside the chamber. CO_2 was eliminated by flushing the chamber thoroughly with the N_2/H_2 gas mix. A constantly stirred, open beaker of 500 mL saturated LiOH was also used to trap any remaining CO_2. Elevated pCO_2 experiments were carried out in a separate glovebox, and were achieved by titrating $CO_{2(g)}$ into the glovebox atmosphere and monitoring using a Bacharach CO_2 monitor

Model 2800 until 5% pCO_2 conditions were achieved. The elevated (5%) pCO_2 batch experiments were capped tightly immediately after titration, and thus likely did not fully equilibrate with the chamber atmosphere at pH > ~6. Therefore, these data are modeled assuming a constant concentration of $2.6 \cdot 10^{-3}$ M total aqueous CO_3^{-2} (calculated from 5% pCO_2 at pH 6 using MINTEQ).

Adsorption of U(VI) to kaolinite in the presence of fulvic acid (10 or 20 mg/L), EDTA ($1 \cdot 10^{-4}$ to $1 \cdot 10^{-2}$ M) and citric acid ($1 \cdot 10^{-4}$ and $1 \cdot 10^{-2}$ M) was also investigated using the methods described above. Fulvic acid (SRFAS1) was purchased from the International Humic Substances Society collection. EDTA solutions were made from NaEDTA solid (Fisher Scientific) and citric acid solutions were made from citrate monohydrate (Mallinckrodt Chemicals). For these experiments the organic acid was added to the solution of U(VI) and background electrolyte that was initially partitioned among the individual 50 mL batch reactors. This solution of U(VI), background electrolyte and organic acid was equilibrated under constant stirring for 30 minutes prior to addition to the centrifuge tubes containing kaolinite. Several experiments were also conducted with organic acids and kaolinite in the absence of U(VI), to assess their adsorption onto kaolinite as a function of pH. For these experiments the concentration of total organic carbon (TOC) in the supernatant was measured using a Shimadzu 5000 TOC.

CHAPTER VIII

U(VI) SORPTION RESULTS AND DISCUSSION

Control experiments

Glass, polycarbonate and polypropylene containers have all been observed to cause significant loss of radionuclides from solution (e.g., Lee et al., 2001). However, within the radionuclide sorption literature there is a great inconsistency of methods to account for the possible loss of U(VI) due to sorption onto reaction vessels. Methods that have been developed to correct for this artifact include: (1) using a single control or blank experiment to account for potential loss (Zuyi et al., 1999), (2) performing no-solid control experiments at a range of pH to account for potential loss as a function of pH and then correcting for the measured loss, (Prikryl 1994; Sachs and Bernhard 2008), (3) acknowledging the potential loss, but arguing that it is not possible to accurately quantify the effect (Turner and Sassman, 1996), (4) not discussing the issue at all (Davis et al, 2004; Garcia-Gonzalez 2010; Nebelung and Brendler 2010, Payne et al., 2004; Waite et al., 2000) and finally, (5) stating that the loss is insignificant (<5%), although typically without providing details regarding the methods used to determine this, and can therefore be ignored (Pathak and Choppin (2006); Gao et al., 2010). Given the evidence that significant loss of UO_2^{+2} may occur on container walls, syringes or syringe filters, properly accounting for this is crucial if accurate thermodynamic constants are to be derived from experimental data. Investigators who simply subtract U(VI) recovered from a wall rinse of a container lacking solid may overestimate the influence of the container,

because they fail to consider competitive sorption that will occur in the presence of a sorbent. It is necessary to confirm that the polypropylene wall is in fact sorbing U(VI) in the presence of the sorbent(s) under investigation. For example, when using polycarbonate tubes to investigate Ni^{2+}, Cs^{+} and Ln^{3+} sorption onto montmorillonite, Tertre et al. (2005) reported a 20% loss of metal to no-solid control container walls. To account for the competitive effects of the wall in the presence of clay, a 2% acid rinse was applied at the termination of sorption experiments. Results from the rinse proved that in the presence of montmorillonite a negligible concentration of metals was lost: <6% compared to up to 20% in the absence of the clay.

In this study, possible loss of U(VI) via sorption to the polypropylene container wall, syringes or syringe filters was first quantified using no-solid control experiments. Results from the no-solid tests demonstrate a significant loss of U(VI) for all U(VI) concentrations explored with the loss strongly dependent on pH and U(VI) concentration (Figure 8.1). At circumneutral pH, experiments containing $1 \cdot 10^{-5}$ and $1 \cdot 10^{-4}$ M U(VI) show over 90% loss from solution; U(VI) sorption reaches 100% for $1 \cdot 10^{-6}$ M U(VI) experiments. Less U(VI) is lost in all experiments at higher or lower pH values, although for $1 \cdot 10^{-6}$ M U(VI) experiments between ~40 to 50% remains sorbed across the entire pH range tested (3-10). Speciation calculations completed using MINTEQ predict that up to 40% of aqueous U(VI) will precipitate as schoepite in a narrow pH range of 7.4 to 8.6 for experiments with 10^{-6} M U(VI) (Figure 8.1). Greater loss is calculated for $1 \cdot 10^{-5}$ and $1 \cdot 10^{-4}$ M U(VI) experiments, reaching up to 90 and 100% respectively, in the circumneutral range. U(VI) loss from solution, particularly for the low concentration experiments was considerably greater than this. To explore potential sorption to the container wall, the

tubes were rinsed with 0.5 M $NaHCO_3$ or 5% HNO_3 after removal of the initial solution. This should complex and remove any U(VI) bound onto the polypropylene container walls. The wash solution typically released quantities of U(VI) equivalent to, or slightly less than, those lost in the no-solid experiments, demonstrating that U(VI) loss is mainly due to wall sorption. Lower recoveries, such as observed for $1 \cdot 10^{-5}$ M U(VI) experiment at circumneutral pH (Figure 8.2), may be due to some loss of U(VI) as a fine precipitate removed with the initial supernatant and subsequently captured on the syringe filters. After confirming that a significant potential for both precipitation and wall sorption was present for the experimental conditions used in the adsorption experiments, methods described by Tertre et al. (2005) were applied to determine if significant U(VI) loss would still occur in the presence of kaolinite. In the presence of kaolinite, negligible (<5%) U(VI) was recovered after bicarbonate or nitric acid washing of the container walls (Figure 8.3). It should also be noted that the extractions may overestimate U(VI) loss, because any fine clay particulates remaining in the tube after removal of the initial slurry would not be readily distinguished from U(VI) sorbed to the wall. The negligible quantity of U(VI) extracted from the container walls at the conclusion of the kaolinite sorption experiments allows the effect of the wall to be disregarded in the experimental results described and modeled below.

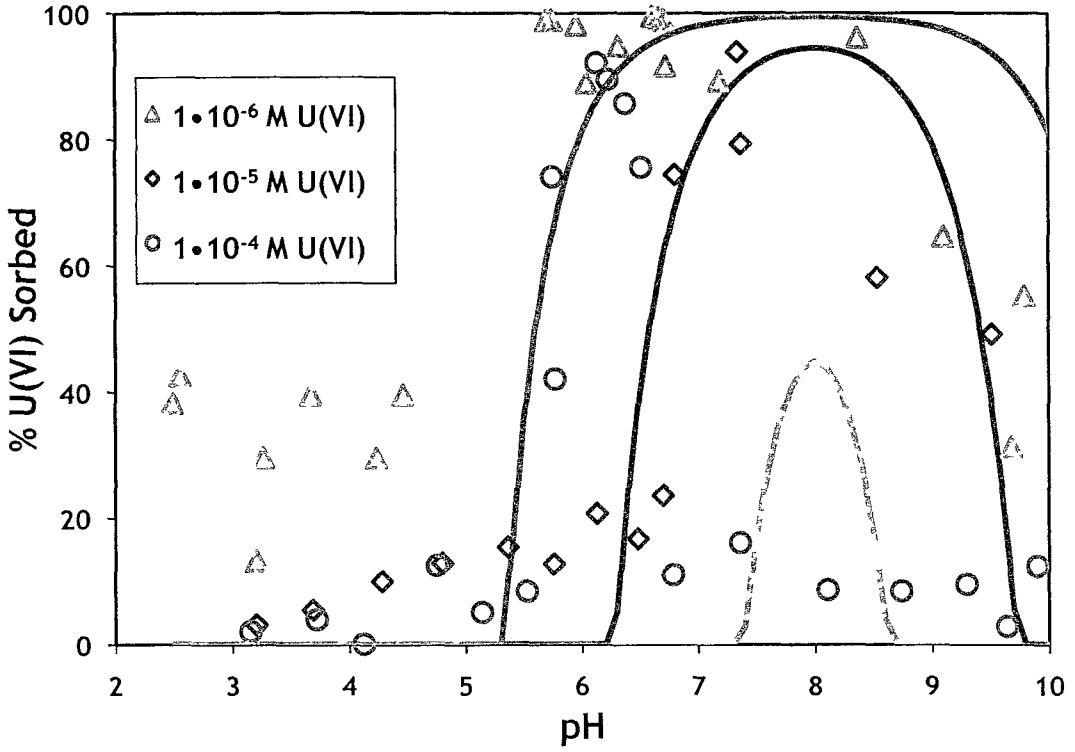

Figure 8.1. Loss of U(VI) from control experiments in 0.01 M $NaNO_3$, under $1.52 \cdot 10^{-5}$ M pCO_2 and in the absence of kaolinite. Lines indicate calculated precipitation of U(VI) using the speciation code MINTEQ.

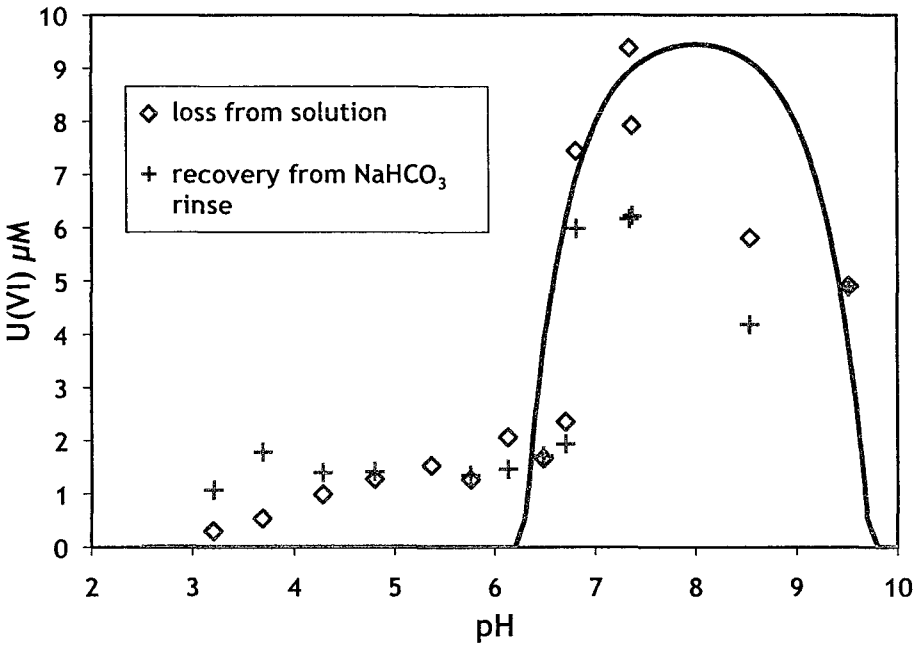

Figure 8.2. Comparison of $1 \cdot 10^{-5}$ M U(VI) loss with U(VI) recovered from 0.5 M $NaHCO_3$ wall rinse.

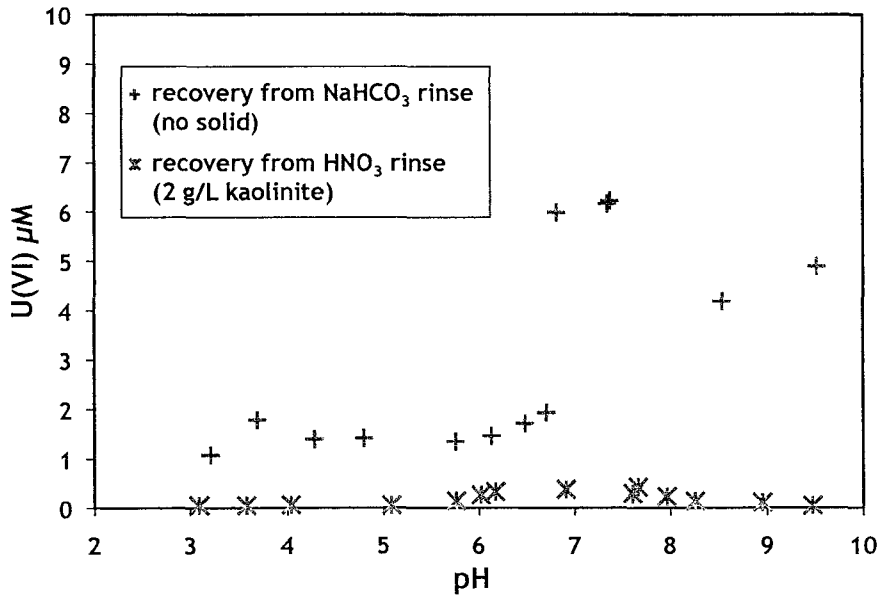

Figure 8.3. Comparison of 10^{-5} M U(VI) loss in the presence of 2 g/L kaolinite with U(VI) recovered from 5% HNO_3 wall rinse.

U(VI) sorption to kaolinite in the absence of organic ligands

U(VI) sorption on kaolinite increases from pH ~3 to 7, reaching near 100% at pH 8, and at higher pH, sorption decreases slightly (Figure 8.4). Little ionic strength dependence is observed; increasing ionic strength from 0.01 to 0.1 M $NaNO_3$ produces only a slight decrease in U(VI) sorption. In contrast, U(VI) sorption is greatly effected by pCO_2 concentrations (Figure 8.5). In the absence of pCO_2 and under atmospheric conditions with tightly closed tubes and without addition of sodium carbonate to insure equilibrium with respect to atmospheric pCO_2 at all pH values, U(VI) sorption is near ~100% from pH 8 to 9. In contrast, in experiments completed under atmospheric conditions and spiked with $NaHCO_3$ to ensure carbonate equilibrium, U(VI) sorption increases from pH 3 to 7 and decreases above a pH of ~7.5. In the presence of 5% pCO_2 U(VI) sorption peaks at 45% between pH 5 and 7 and decreases dramatically at higher pH.

Payne et al. (2004) developed a non-electrostatic surface complexation model (NEM) to describe adsorption of $1 \cdot 10^{-6}$ or $1 \cdot 10^{-5}$ M U(VI) on 4 or 40 g/L kaolinite (KGa-1b) in the presence of 0.01 M $NaNO_3$. Sorption was assumed to occur on kaolinite aluminol edge sites (>AlOH) and on titanol sites (>TiOH) of titanium dioxide impurities. These surface sites were chosen based on transmission electron microscopy (TEM) data, which showed that U(VI) tended to preferentially associate with fine-grained anatase and rutile (TiO_2) impurities. Payne et al. (2004) calculated aluminol and titanol site densities from TEM observations by assuming the formation of 1:1 U-surface complexes on the kaolinite and titanium dioxide particles (Table 8.1). Payne et al. (2004) assumed that U(VI) sorption occurs via the formation of three surface species: $>TiOUO_2^+$,

>$AlOUO_2OH$ and >$TiOUO_2CO_3$ (Table 8.2; Figure 8.6). Formation of a monodentate U(VI) complex on a titanol site,

$$>TiOH + UO_2^{+2} \Leftrightarrow >TiOUO_2^{+} + H^{+} \quad (1)$$

is consistent with their TEM observations highlighting the important role of anatase in binding U(VI). Acidity constants and U(VI) binding on kaolinite were described using aluminol, rather than silanol, sites for the kaolinite based on previous work, by Borovec (1981), Kohler et al. (1992), and Turner and Sassman (1996) demonstrating that the aluminol site (>AlOH) in the gibbsite-type layer preferentially sorbs U(VI) compared to the silanol sites in the siloxane layer of kaolinite. Due to the increasing hydrolysis of the U(VI) ion at higher pH, they assumed formation of a monodentate U(VI) hydroxide on the aluminol site to account for U(VI) sorption at circumneutral pH values, according to

$$>AlOH + UO_2^{+2} + H_2O \Leftrightarrow >AlOUO_2OH + 2H^{+} \quad (2)$$

Finally, to improve the model fit at high pH a U(VI)-carbonate complex sorbing onto a titanol site was included, according to

$$>TiOH + UO_2^{+2} + CO_3^{2-} \Leftrightarrow >TiOUO_2CO_3^{-} + H^{+} \quad (3)$$

Without this species, the model overestimated U(VI) sorption at high pH. Furthermore, the presence of U(VI)-carbonato ternary surface complexes on phyllosilicates has been confirmed by EXAFS (Catalano and Brown, 2005).

The SCM parameters for U(VI) adsorption described by Payne et al. (2004) were used together with the NEA thermodynamic database provided with the speciation code Visual MINTEQ (Table 8.3), to model the data for the conditions used in this study. A relatively good fit to the experimental data is achieved over a wide range of conditions, i.e. varying ionic strength, and pCO_2 (Figure 8.4, and 8.5). At low pH (3 to 5), the NEM produces good predictions for varying ionic strength conditions; at high pH behavior is underestimated. For varying pCO_2 the NEM again results in a good simulation of the data at low pH, and underpredicts sorption at high pH for 0 and $1.52 \cdot 10^{-5}$ M aqueous pCO_3^{-2}; whereas for open-atmosphere and 5% pCO_2 conditions, good fits are observed.

Although the NEM produces reasonably good fits to the U(VI) adsorption data, it does not adequately reproduce U(VI) sorption behavior in the presence of organic acids (see below), which may indicate that interactions with the electrical double layer must be included explicitly in the model. Therefore, a diffuse layer model (DLM) was also developed and tested, first in the absence of the ligands. For the DLM, a relatively simple model with only a single surface site type, in contrast to the two used by Payne et al. (2004), was used. The site density and acidity constants were taken from Sverjensky and Sahai (1996). These authors argue that sorption of cations onto oxides is best described using internally-consistent set of parameters, i.e. 10 sites/nm^2 and acidity constants based on properties of the solid (dielectric constants and Pauling bond strengths), allowing for a minimization of the number of experimentally derived constraints within a model (Table

8.2). Surface complexation stability constants for U(VI) adsorption were optimized using FITEQL4.0 (Herblin and Westall, 1999). Aqueous reactions and stability constants from Visual MINTEQ were used in all models and activity corrections were included in the calculations (Table 8.3). Optimizations in FITEQL4.0 were completed using edges from all pCO_2 conditions simultaneously to derive best-fit stability constants over the full range of conditions. Total carbonate concentrations were either assumed to be constant (closed cap experiments) or pH-dependent values calculated using MINTEQ and assuming equilibrium with respect to the atmosphere were used (experiments pre-spiked with $NaHCO_3$).

To choose surface reaction stoichiometries, the U(VI) aqueous speciation at conditions of $1 \cdot 10^{-5}$ M U(VI) and 0.01 M $NaNO_3$ (Figure 8.7) was considered. Under fully equilibrated atmospheric pCO_2 conditions, U(VI) dominates the speciation at low pH; from a pH of 5 to 8 hydrated U(VI) species are the most abundant aqueous complexes, shifting to U(VI)-carbanato species at higher pH. Because sorption reaches a maximum in the circumneutral pH range and the aqueous speciation is dominated by hydroxide complexes from pH 5 to 8, a single $>XOUO_2OH$ complex was tested according to the reaction,

$$>XOH + UO_2^{+2} + H_2O \Leftrightarrow >XOUO_2OH + 2H^+ \quad (4)$$

with a resulting stability constant of -6.1. This DLM provides a good fit to the measured data, yielding a WSOS/DF of 3.54. In contrast to the Payne et al. (2004) model, the DLM overestimates U(VI) adsorption at pH 5-7 for atmospheric pCO_2 and tends to

underestimate sorption at low pH and low pCO_2, and across the measured pH range for data measured under 5% pCO_2 (Figure 8.4, 8.5). A variety of other reaction stoichiometries were also explored when constructing the DLM. These included bidentate complexes ($>(XO)_2UO_2$, $>(XO)_2UO_2OH$)), as well as other monodentate complexes ($>XOUO_2^+$, $>XOUO_2(OH)_2^-$, $>XOUO_2(OH)_4^{-3}$, $>XOUO_2(OH)_7^{-6}$), however, none of these resulted in lower WSOS/DF values compared to the $>XOUO_2OH$ complex.

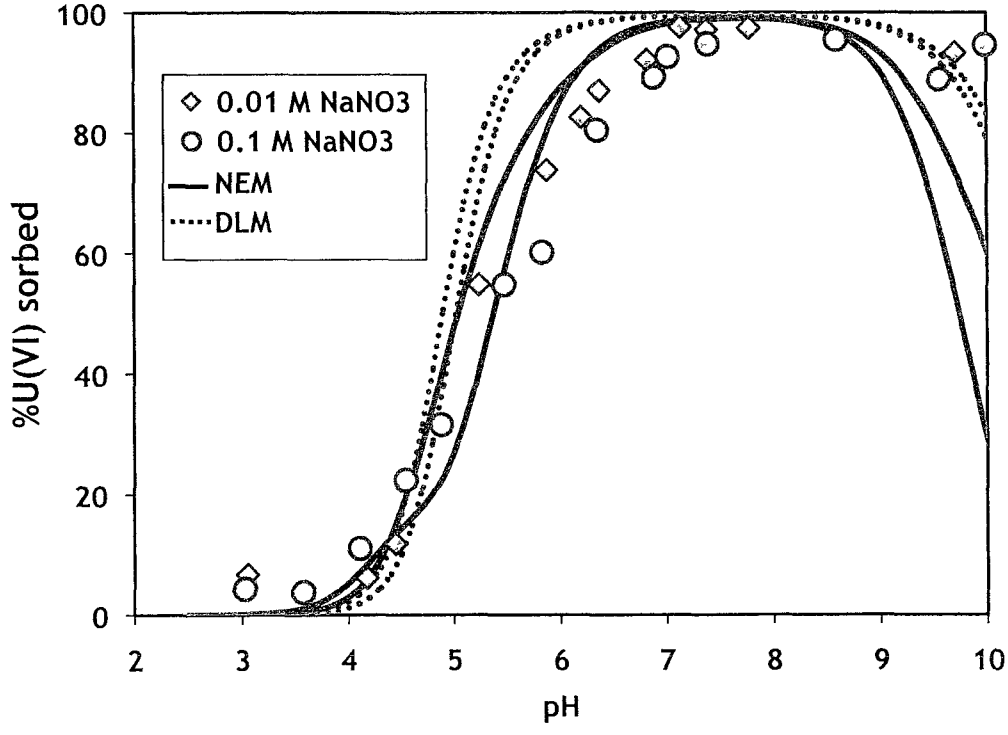

Figure 8.4. $1 \cdot 10^{-5}$ M U(VI) sorption on 2 g/L kaolinite with 0.01 M $NaNO_3$ as a function of ionic strength with tightly capped tubes (assumed total $CO_3^{-2}{}_{(aq)} = 1.52 \cdot 10^{-5}$ M).

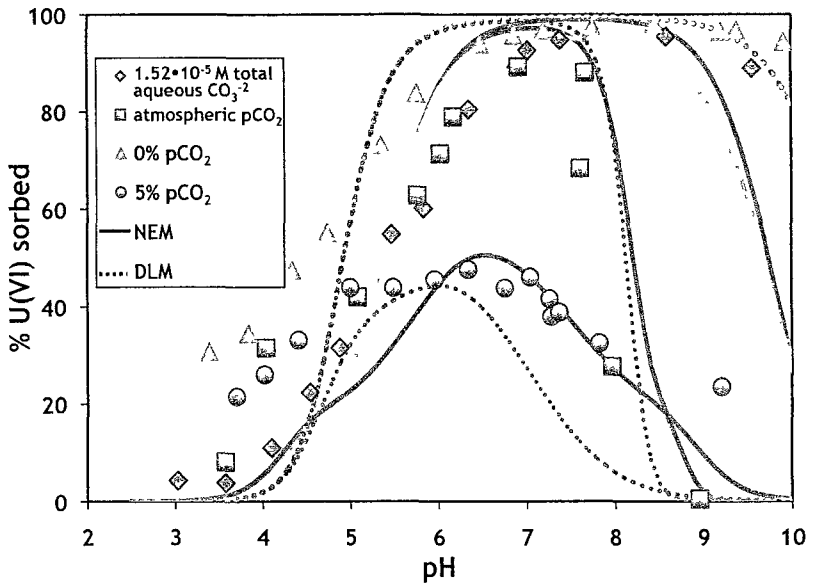

Figure 8.5. $1 \cdot 10^{-5}$ M U(VI) sorption on 2 g/L kaolinite with 0.01 M $NaNO_3$ as a function of varying pCO_2. Lines indicate model fits calculated using the Payne et al. (2004) NEM (solid lines) or the DLM (dotted) developed in this study (assumed total $CO_3^{-2}{}_{(aq)}$ = $1.52 \cdot 10^{-5}$ M).

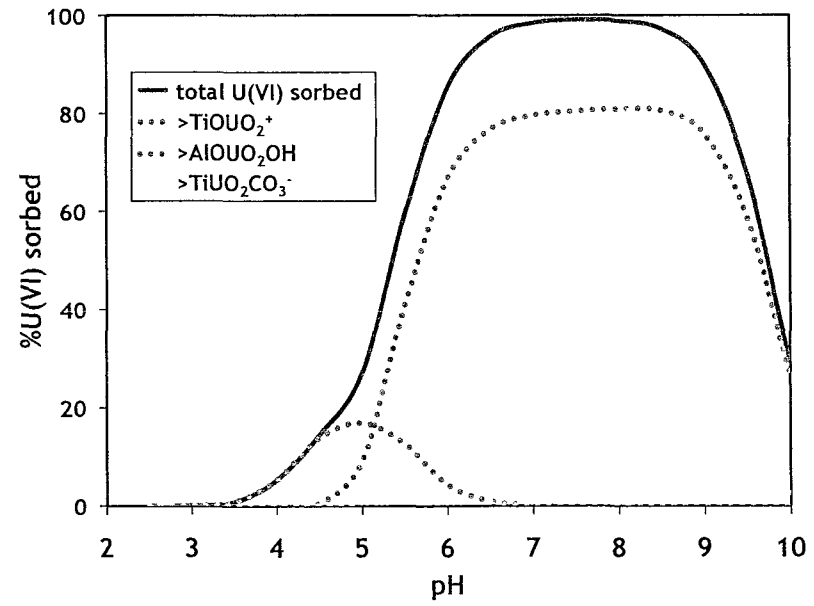

Figure 8.6. Distribution of U(VI) sorbed predicted by the NEM for $1.52 \cdot 10^{-5}$ M total $CO_3^{-2}{}_{(aq)}$ (assumed total $CO_3^{-2}{}_{(aq)} = 1.52 \cdot 10^{-5}$ M).

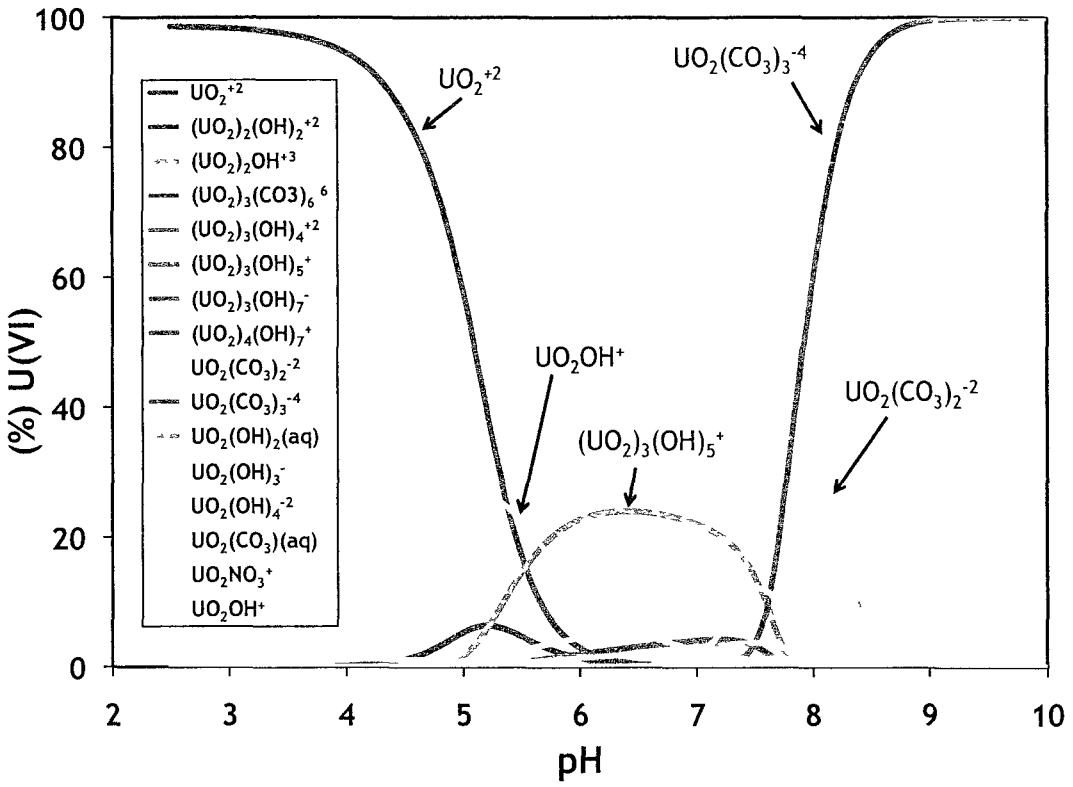

Figure 8.7. Aqueous speciation of U(VI) as a function of pH calculated for $1 \cdot 10^{-5}$ M U(VI) in 0.01 M $NaNO_3$, fully equilibrated with atmospheric pCO_2 in the absence of solid using MINTEQ with the NEA thermodynamic database (Table 8.3).

Table 8.1. Surface area, surface site types and surface site densities used in surface complexation model calculations.

Model	Solid	Surface area (m^2/g)	Site types	Site density ($umol/m^2$)
NEM	Kaolinite	13.6	>AlOH	0.18
NEM	Kaolinite	13.6	>TiOH	0.03
DLM	Kaolinite	13.6	>XOH	16.6

Table 8.2. Reaction stochiometries and stability constants used in surface complexation models.

Model	Surface	Reaction	Log K
NEM	Kaolinite	$>AlOH + H^+ \Leftrightarrow >AlOH_2^+$	6.3
NEM	Kaolinite	$>AlOH \Leftrightarrow >AlO^- + H^+$	-8.7
NEM	Kaolinite	$>AlOH + UO_2^{+2} + H_2O \Leftrightarrow >AlOUO_2OH + 2H^+$	-4.14
NEM	Ti-oxide	$>TiOH + H^+ \Leftrightarrow >TiOH_2^+$	4.9
NEM	Ti-oxide	$>TiOH \Leftrightarrow >TiO^- + H^+$	-7.5
NEM	Ti-oxide	$>TiOH + UO_2^{+2} \Leftrightarrow >TiOUO_2^+ + H^+$	1.76
NEM	Ti-oxide	$>TiOH + UO_2^{+2} + CO_3^{-2} \Leftrightarrow TiOUO_2CO_3^- + H^+$	12.0
DLM	Kaolinite	$>XOH + H^+ \Leftrightarrow >XOH_2^+$	2.1
DLM	Kaolinite	$>XOH \Leftrightarrow >XO^- + H^+$	-8.1
DLM	Kaolinite	$>XOH + UO_2^{+2} + H_2O \Leftrightarrow >XOUO_2OH + 2H^+$	-6.18
DLM	Kaolinite	$>XOH + UO_2^{+2} \Leftrightarrow >XOUO_2^+ + H^+$	-1.05

U(VI) sorption to kaolinite in the presence of EDTA

All experiments investigating the sorption of U(VI) onto kaolinite in the presence of organic acids were conducted under atmospheric conditions (an assumed $1.5 \cdot 10^{-5}$ M total CO_3^{-2}) with 10^{-5} M U(VI) and 2 g/L KGa-1b in 0.01 M $NaNO_3$. The addition of $1 \cdot 10^{-4}$ to $1 \cdot 10^{-2}$ M EDTA results in a pronounced decrease in U(VI) sorption (up to 80% drop) between pH 4 and 11 (Figure 8.8). TOC data does not show a strong concentration dependence on EDTA loss from solution and suggests that under all of the experimental conditions less than 10% of the EDTA sorbs onto the kaolinite surface (Figure 8.9).

The NEM and DLM described above were used, together with aqueous U(VI)-EDTA reactions and stability constants in the default MINTEQ thermodynamic database (Table 8.3), to simulate U(VI) sorption in the presence of EDTA. For these calculations, it was first assumed that EDTA does not interact with the kaolinite surface. This results in an underprediction of U(VI) sorption at pH < 6 or 7 for both the NEM and the DLM (Figure

Table 8.3. Aqueous complexation reactions and stability constants.

Reaction	Log K
$Na^+ + NO_3^- \Leftrightarrow NaNO_{3(aq)}$	-0.55
$UO_2^{+2} + NO_3^- \Leftrightarrow UO_2NO_3^+$	0.3
$UO_2^{+2} + H_2O \Leftrightarrow UO_2OH^+$	-5.25
$2UO_2^{+2} + H_2O \Leftrightarrow (UO_2)_2OH^{+3} + H^+$	-2.7
$UO_2^{+2} + 2H_2O \Leftrightarrow UO_2(OH)_{2(aq)} + 2H^+$	-12.15
$2UO_2^{+2} + 2H_2O \Leftrightarrow (UO_2)_2(OH)_2^{+2} + 2H^+$	-5.62
$H_2O \Leftrightarrow OH^- + H^+$	-13.997
$UO_2^{+2} + 2CO_3^{-2} \Leftrightarrow UO_2CO_{3(aq)}$	9.94
$UO_2^{+2} + 3H_2O \Leftrightarrow UO_2(OH)_3^- + 3H^+$	-20.25
$3UO_2^{+2} + 4H_2O \Leftrightarrow (UO_2)_3(OH)_4^{+2} + 4H^+$	-11.9
$3UO_2^{+2} + 5H_2O \Leftrightarrow (UO_2)_3(OH)_5^+ + 5H^+$	-15.55
$UO_2^{+2} + 2CO_3^{-2} \Leftrightarrow UO_2(CO_3)_2^{2-}$	16.61
$4UO_2^{+2} + 7H_2O \Leftrightarrow (UO_2)_4(OH)_7^+ + 7H^+$	-21.9
$3UO_2^{+2} + 7H_2O \Leftrightarrow (UO_2)_3(OH)_7^- + 7H^+$	-32.2
$UO_2^{+2} + 3CO_3^{-2} \Leftrightarrow UO_2(CO_3)_3^{4-}$	21.84
$UO_2^{+2} + 4H_2O \Leftrightarrow UO_2(OH)_4^{-2} + 4H^+$	-32.4
$3UO_2^{+2} + 6CO_3^{-2} \Leftrightarrow (UO_2)_3(CO_3)_6^{-6}$	54
$CO_3^{-2} + Na^+ \Leftrightarrow NaCO_3^-$	1.27
$CO_3^{-2} + Na^+ + H^+ \Leftrightarrow NaHCO_{3(aq)}$	10.029
$Na^+ + H_2O \Leftrightarrow NaOH_{(aq)} + H^+$	-13.897
$CO_3^{-2} + 2H^+ \Leftrightarrow H_2CO_{3(aq)}$	16.681
$CO_3^{-2} + H^+ \Leftrightarrow HCO_3^-$	10.329
$EDTA^{-4} + H^+ \Leftrightarrow HEDTA^{-3}$	10.98
$EDTA^{-4} + 2H^+ \Leftrightarrow H_2EDTA^{-2}$	17.221
$EDTA^{-4} + 3H^+ \Leftrightarrow H_3EDTA^-$	20.339
$EDTA^{-4} + 4H^+ \Leftrightarrow H_4EDTA_{(aq)}$	22.552
$EDTA^{-4} + 5H^+ \Leftrightarrow H_5EDTA^+$	24.052
$EDTA^{-4} + 6H^+ \Leftrightarrow H_6EDTA^{+2}$	23.94
$EDTA^{-4} + Na^+ \Leftrightarrow NaEDTA^{-3}$	1.64
$UO_2^{+2} + EDTA^{-4} + H^+ \Leftrightarrow UO_2HEDTA^{-3}$	19.63
$2UO_2^{+2} + EDTA^{-4} \Leftrightarrow (UO_2)_2EDTA_{(aq)}$	20.43
$2UO_2^{+2} + EDTA^{-4} + H_2O \Leftrightarrow (UO_2)_2OHEDTA^- + H^+$	15.423
$Citrate^{-3} + H^+ \Leftrightarrow HCitrate^{-2}$	6.396
$Citrate^{-3} + 2H^+ \Leftrightarrow H_2Citrate^-$	11.157
$Citrate^{-3} + 3H^+ \Leftrightarrow H_3Citrate_{(aq)}$	-2.7
$Citrate^{-3} + Na^+ \Leftrightarrow NaCitrate^{-2}$	1.39
$2UO_2^{+2} + 2Citrate^{-3} \Leftrightarrow (UO2)_2Citrate_2^-$	21.3
$UO_2^{+2} + Citrate^{-3} \Leftrightarrow UO_2Citrate^-$	8.69

8.8) . In contrast, at higher pH, the models both greatly overpredict U(VI) sorption in the presence of the EDTA (Figure 8.4A). The underprediction of U(VI) sorption at low pHsuggests formation of U(VI)-EDTA-kaolinite ternary complexes. Previous studies have proposed that metal-EDTA ternary complexes form on a variety of oxides at low pH (e.g., Zachara et al., 1995; Nowack et al., 1996; Friedly et al., 2002;). For example, Nowack et al. (1996) successfully described the adsorption of Ni^{2+} or Fe^{2+} on several oxide minerals (goethite, HFO, lepidocrocite, δ-Al_2O_3 and γ-Al_2O_3) in the presence of EDTA with a DLM or constant capacitance model (CCM) by including ternary complexes. Similarly, Friedly et al. (2002) produced reactive transport simulations to represent Ni, Zn and Ca mobilization through a quartz sand aquifer by including metal-EDTA-solid ternary complexes in their model. A study by Zachara et al. (1995) demonstrated the ability of EDTA to enhance the adsorption of Co-60 to goethite in a pH range where cobalt, in the absence of EDTA, does not appreciably adsorb.

To resolve the differences between model and data at low pH, the U(VI) aqueous speciation at low pH was used to infer likely ternary complex stoichiometries. Between pH 3 to ~7, nearly all U(VI) in solution is chelated as a UO_2HEDTA^- complex (Figure 8.10). Therefore, FITEQL was used to optimize stability constants for individual U(VI) sorption edges in the presence of EDTA using the Payne et al. (2004) NEM with each of the following ternary complexes: $>SOUO_2EDTA^{-3}$, $>SO(UO_2)_2HEDTA$, or $>SOUO_2HEDTA^{-2}$, where >SOH represents either a titanol (>TiOH) or an aluminol (>AlOH) site. Optimization of individual surface complexes as well as combinations of two or three complexes were attempted, for example simultaneously fitting for stability

constants of U(VI)-EDTA complexes on both the titanol and aluminol sites. Because of the large size of the EDTA molecule, bidentate complexes ($>(TiO)_2UO_2EDTA^{-4}$, $(>(AlO)_2UO_2EDTA^{-4})$ were also tested, together with several combinations of mono- and bidentate species, but all of these resulted in higher WSOS/DF values compared to optimizations with a single surface species. Optimization of stability constants for each single surface species tested was possible for the U(VI) edges measured under lower EDTA concentrations, but FITEQL failed to converge for optimizations of the $1 \cdot 10^{-2}$ M EDTA edge, so for this dataset stability constants were instead optimized by eye in MINTEQ. Of the ternary complexes tested, the $>TiOUO_2EDTA^{-3}$ species resulted in the best fit to the full suite of data at low pH, per the reaction,

$$>TiOH + EDTA^{-4} + UO_2^{+2} \Leftrightarrow >TiOUO_2EDTA^{-3} + H^+ \quad (5)$$

with a median stability constant of 15.3. The loss of EDTA from solution occurring due to formation of this ternary complex is between 0.1 and 10% of total EDTA for the $1 \cdot 10^{-4}$ to $1 \cdot 10^{-2}$ M EDTA experiments. The TOC data are not sensitive enough to detect this low level of EDTA absent from solution. Thus, formation of this ternary complex cannot be confirmed or dismissed based on the TOC data. The addition of the $>TiOUO_2EDTA^{-3}$ ternary complex provides a better fit to the data at low pH, but with the addition of only this complex, the NEM continues to overestimate U(VI) sorption above pH ~7. At high pH, EDTA speciation in the aqueous phase is dominated by the formation of $NaEDTA^{-3}$ (Figure 8.10). MINTEQ calculations show that the concentration of $NaEDTA^{-3}$ is an order of magnitude greater than aqueous U(VI)-EDTA complexes at high pH.

Furthermore, when modeling Co sorption to goethite in the presence of EDTA, Zachara et al. (1995) observed a decrease in Co adsorption and attributed the suppression to competition by a Ca^{2+} species. Therefore, a second ternary complex (>SONaEDTA^{-4}) was considered as a possible explanation for the decrease in U(VI) sorption onto kaolinite at high pH. Simultaneous optimization of >TiONaEDTA^{-4} and >AlONaEDTA^{-4} stability constants failed to converge in FITEQL. Optimizations using only >TiONaEDTA^{-4} also failed to converge. Stability constant optimization could only be achieved for formation of >AlONaEDTA^{-4}, according to:

$$>AlOH + EDTA^{-4} + Na^{+} \Leftrightarrow >AlONaEDTA^{-4} + H^{+} \quad (6).$$

It is not surprising that a stability constant could not be optimized for formation of a ternary complex on the titanol site, but could be optimized using the aluminol site. The acidic titanol site has a low point of zero charge (pH_{pzc}) relative to aluminol causing it to be more negatively charged than the aluminol site at a given pH, and NaEDTA^{-3} does not exist appreciably in solution below pH ~7. In addition, the stability constant for formation of the >TiOUO$_2$EDTA^{-3} complex using the low pH data results in saturation of the titanol site, thus precluding sorption of NaEDTA^{-3}. It is not possible to include formation of both ternary complexes on this site and produce an acceptable fit of the data across the measured pH range.

Stability constants for reactions 5 and 6 were optimized concurrently in FITEQL, producing good fits for individual experiments with $1 \cdot 10^{-4}$ and $1 \cdot 10^{-3}$ M EDTA. However, optimizations for sorption edges measured with the highest EDTA concentration

conditions would not converge in FITEQL, so these were again fit by eye using MINTEQ. The median stability constants from the simultaneous optimizations, shown in Table 8.4, improve the overall fits, reproducing the general trends observed in the measured edges for U(VI) sorption in the presence of EDTA (Figure 8.11). However, at low pH the model reproduces only the average sorption for all EDTA conditions explored and does not correctly capture the observed spread of the experimental edges. The relatively high stability constant, a log K of 15.3, for the $>TiOUO_2EDTA^{-3}$ required to produce good fits at low pH loads the titanol surface with U(VI)-EDTA at all pH values. Because the titanol site is fully saturated with the U(VI)-EDTA ternary complex across the pH range, at high pH the model overestimates sorption for high EDTA conditions (Figure 8.12). In the circumneutral pH range, additional U(VI) sorption onto the aluminol site results in an overestimation of total U(VI) sorption for the NEM.

The model prediction that all titanol sites are complexed by the UO_2EDTA^{-3} from pH 5 – 11 (Figure 8.12) is consistent with the observation of Payne et al. (2004) that rutile and anatase impurities have greater surface area and greater reactivity compared to

Table 8.4. Ternary complexes.

Model	Surface	Reaction	Log K
DLM	Kaolinite	$>XOH + Citrate^{-3} \Leftrightarrow >XOHCitrate^{-3}$	8
DLM	Kaolinite	$>XOH + Citrate^{-3} + UO_2^{2+} \Leftrightarrow >XOUO_2Citrate^{-2} + H^+$	8.9
NEM	Kaolinite	$>AlOH + EDTA^{-4} + Na^+ \Leftrightarrow >AlONaEDTA^{-5} + H^+$	15.3
NEM	Ti oxide	$>TiOH + EDTA^{-4} + UO_2^{2+} \Leftrightarrow >TiOUO_2EDTA^{-3} + H^+$	1.07
NEM	Kaolinite	$>AlOH + H^+ + Citrate^{-3} \Leftrightarrow >AlOH_2Citrate^{-2} + H^+$	14.7
NEM	Kaolinite	$>AlOH + 2H^+ + Citrate^{-3} \Leftrightarrow >AlOH_2Citrate^{-2} + H^+$	19.7
NEM	Ti-oxide	$>TiOH + 2H^+ + Citrate^{-3} \Leftrightarrow >TiOH_2Citrate^{-2}$	21
NEM	Kaolinite	$>(AlOH)_2 + UO_2^{2+} + Citrate^{-3} \Leftrightarrow >(AlO)_2UO_2Citrate^{-3} + 2H^+$	10
NEM	Ti-oxide	$>(TiOH)_2 + UO_2^{2+} + Citrate^{-3} \Leftrightarrow >(TiO)_2UO_2Citrate^{-3} + 2H^+$	18

aluminol sites on kaolinite. Thus, U(VI) saturates the titanol surface sites before binding to the kaolinite. From pH ~7 to 9 the aluminol surface sites begin to take up UO_2OH^+. At higher pH, as the $NaEDTA^{-3}$ concentration in solution increases, the competition for the aluminol sites causes a decrease in the sorption of UO_2OH^+. Above pH ~9 $NaEDTA^{-3}$ saturates all available aluminol surface sites, leaving U(VI) bound exclusively to the titanol sites. Although an improved fit to the high pH was provided by the addition of competitive $NaEDTA^{-3}$ complexes to the aluminol sites, the predicted loss of EDTA from solution is not consistent with the TOC results. The total amount of EDTA removed from solution due to formation of $>TiOUO_2EDTA^{-3}$ and $>TiONaEDTA^{-4}$ surface species is predicted to be 0.2, 2 and 20% for $1 \cdot 10^{-4}$, $1 \cdot 10^{-3}$ and $1 \cdot 10^{-2}$ respectively. A loss of 0.2 to 2% cannot be discerned from TOC results, but a loss of 20% would be evident within the uncertainty of the data. This discrepancy demonstrates that this NEM is not correctly describing the reaction stoichiometries, and some other process must result in the lower than expected sorption of U(VI) ion at high pH in the presence of EDTA. One possibility is that the model does not fully capture the U(VI) sorption behavior because the NEM does not take into account electrostatic effects at the mineral surface.

To determine whether explicit accounting for electrostatic effects would provide a better fit to the data, a DLM was developed using a similar approach to that described above for the NEM: aqueous U(VI)-EDTA surface complexes were included to increase sorption at low pH, and at high pH the formation of $>XONaEDTA^{-4}$ was included to decrease U(VI) sorption. The addition of U(VI)-EDTA complexes increases model

predictions of U(VI) sorption at low pH, however, at high pH the addition of $>XONaEDTA^{-4}$ does not effect the sorption edges. Because the site density in the DLM is two order of magnitude greater than in the NEM, there are enough >XOH sites to accommodate all U(VI) and Na-EDTA species. Thus, the addition of Na-EDTA surface complexes to the DLM does not result in the same competitive effect observed for the NEM. This suggests that the internally consistent parameters advocated by Sverjensky and Sahai (1996) are either physically unrealistic, and thus hinder development of accurate models of competitive effects for limited sites, or, that another process is responsible for the inability of the model to correctly simulate the diminished U(VI) sorption at high pH.

The inability of both the NEM and the DLM models to fit this data might be explained by at least three other phenomena: (1) incorrect descriptions of carbonate equilibria, (2) inaccuracies in the predicted U(VI) aqueous speciation in the presence of EDTA or (3) inadequate descriptions of electrostatic effects. The EDTA experiments were conducted under atmospheric conditions. However, as described above, it is clear that at high pH, carbonate did not fully equilibrate before the batch experiments were sealed. Thus, a fixed concentration of $1.5 \cdot 10^{-5}$ M total aqueous CO_3^{-2} is assumed for all atmospheric experiments. However, the true concentration of CO_3^{-2} is unknown and this estimate may be in error. A higher concentration of CO_3^{-2} would result in less sorption at the high pH range, where the SCMs perform poorly (Figure 8.11, dotted lines). It is possible that the actual pCO_3^{-2} concentration lies somewhere between$1.5 \cdot 10^{-5}$ M and fully equilibrated conditions, if this is the case the fit of the modeled edges to the measured data would be greatly improved. Another potential source of error is uncertainty with

respect to the predicted U(VI)-EDTA aqueous speciation. The formation of stronger than predicted aqueous U(VI)-EDTA complexes at high pH would result in the observed lower sorption. Finally, it is possible that the complexity of the system, with formation of ternary surface complexes, necessitates a more sophisticated description of the electrical double layer, such as a triple layer model or a CD-MUSIC approach.

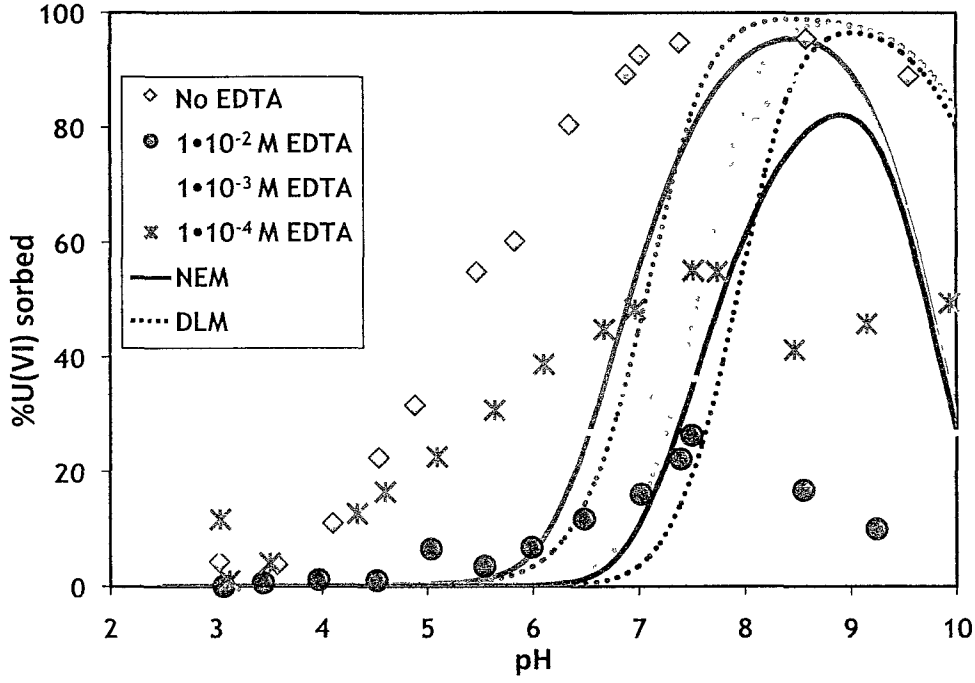

Figure 8.8. Sorption of $1 \cdot 10^{-5}$ M U(VI) on 2 g/L kaolinite in 0.01 M $NaNO_3$ with varying concentrations of EDTA (assumed total $CO_3^{-2}{}_{(aq)} = 1.52 \cdot 10^{-5}$ M).

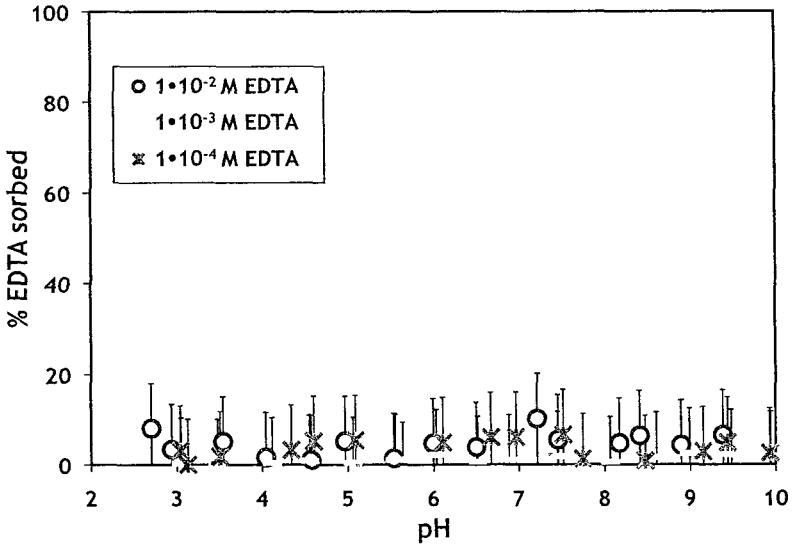

Figure 8.9. EDTA sorbed as a function of pH and EDTA concentration for experiments conducted with 2 g/L kaolinite in 0.01 M $NaNO_3$, and in the absence of U(VI) (assumed total $CO_3^{-2}{}_{(aq)} = 1.52 \cdot 10^{-5}$ M).

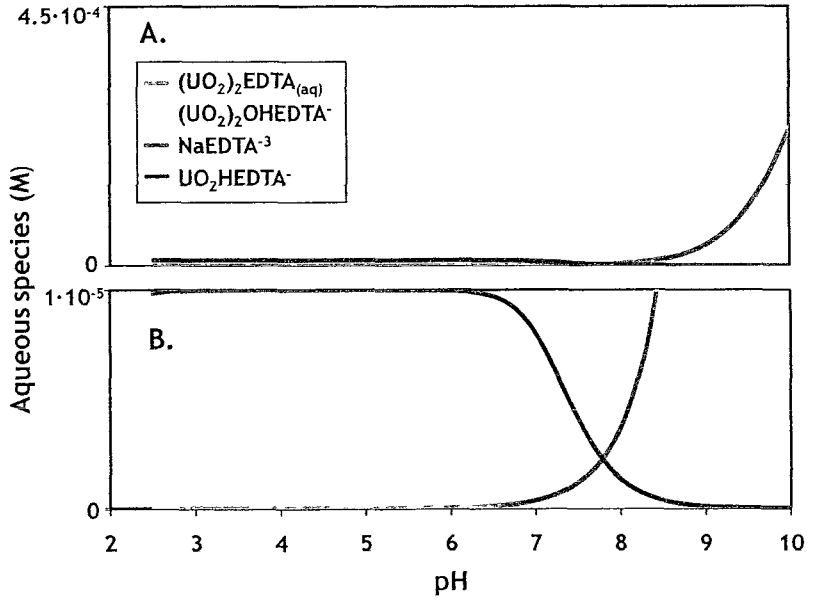

Figure 8.10. Aqueous speciation of U(VI) and EDTA calculated in MINTEQ with the NEA thermodynamic database (Table 8.3) for $1 \cdot 10^{-5}$ M U(VI) and 0.01 M EDTA in 0.01 M $NaNO_3$ with $1.52 \cdot 10^{-5}$ M $CO_3^{-2}{}_{(aq)}$ with (A) full range of concentration and (B) expanded scale to more clearly show U(VI) speciation.

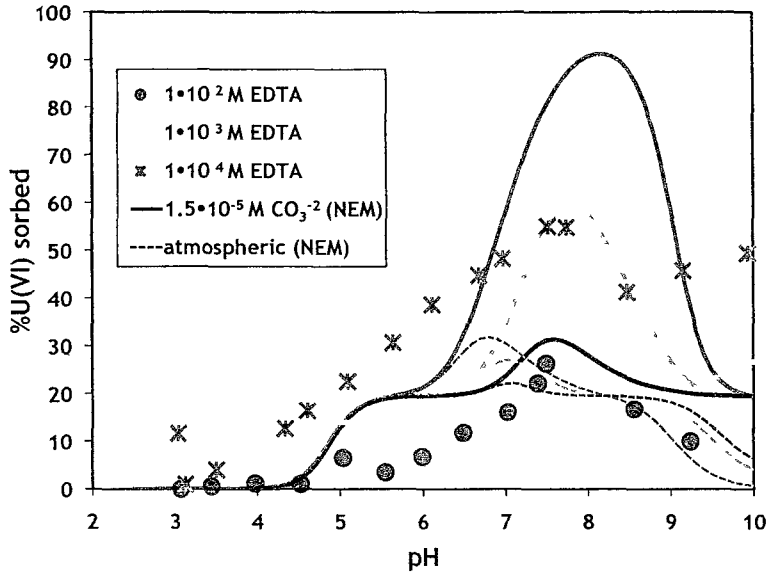

Figure 8.11. Sorption of $1 \cdot 10^{-5}$ M U(VI) on 2 g/L kaolinite in 0.01 M $NaNO_3$ with varying concentrations of EDTA. Lines indicate U(VI) sorption calculated using the NEM with ternary complexes shown in Table 8.4 and assuming $1.52 \cdot 10^{-5}$ M $CO_3^{-2}{}_{(aq)}$ (solid lines) or full equilibration with atmospheric pCO_2 as a function of pH (dotted lines).

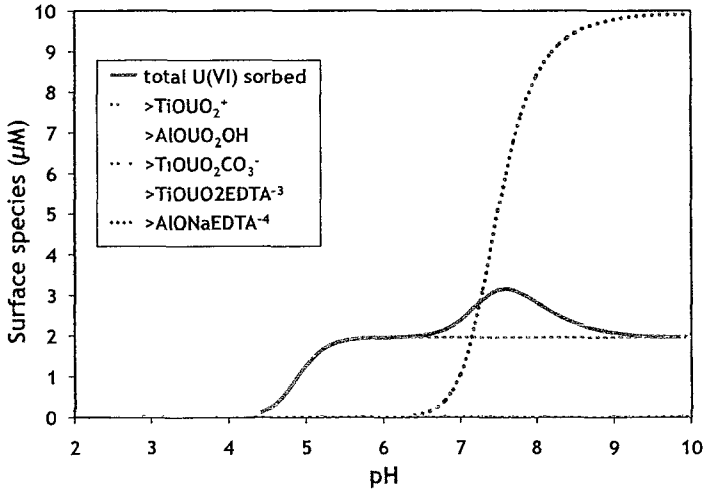

Figure 8.12. Surface species as a function of pH calculated using the NEM for $1 \cdot 10^{-5}$ M U(VI) on 2 g/L kaolinite in 0.01 M $NaNO_3$ with $1.52 \cdot 10^{-5}$ M $CO_3^{-2}{}_{(aq)}$ and 0.01 M EDTA with reaction stoichiometries, stability constants, aqueous stability constants and solid parameters shown in Tables 8.1-8.4.

U(VI) sorption to kaolinite in the presence of citrate

The addition of $1 \cdot 10^{-4}$ M citric acid results in a ~10% enhancement of U(VI) sorbed from pH 3 to ~5, and above pH 5 up to 20% decrease in U(VI) sorbed occurs compared to the experiments without organic acids. Addition of $1 \cdot 10^{-2}$ M citric acid results in approximately 60% U(VI) sorbed with essentially no dependence on pH (Figure 8.13). Redden et al. (1998) investigated a similar system, exploring the effects of $2.7 \cdot 10^{-7}$ to $1.6 \cdot 10^{-5}$ M citrate on the sorption of $1 \cdot 10^{-6}$ M U(VI) onto 1.2 g/L kaolinite (KGa-1b) in the presence of 0.1 M NaCl (Figure 8.14). Addition of $2.7 \cdot 10^{-7}$ M citrate has little effect on U(VI) sorption, but $2.7 \cdot 10^{-6}$ M citrate results in a slight enhancement at low pH, and ~10% decrease in sorption between pH 5-7, comparable to the influence of $1 \cdot 10^{-4}$ M citric observed in this study. Redden et al. (1998) report decreased U(VI) sorption across pH with the addition of $1.6 \cdot 10^{-6}$ M citrate (Figure 8.14).

TOC data for $1 \cdot 10^{-2}$ M citrate conditions suggest a 0 to ~15% loss of citrate from solution (Figure 8.15), and $1 \cdot 10^{-4}$ M citrate results in up to 20% loss of TOC from solution, with the most pronounced losses at circumneutral pH. These results agree well with those for citric acid sorbed onto kaolinite reported by Redden et al. (1998). At low citrate concentrations ($2.7 \cdot 10^{-7}$ M) the ligand was fully sorbed in typical anion fashion, reaching ~100% uptake at low pH and fully desorbing above pH 9. Greater additions of citric acid ($1.6 \cdot 10^{-6}$ M) led to only ~20% of the ligand being complexed to the solid. These results suggest that surface sites on the mineral are limiting under high citrate concentrations. Citrate concentrations in this study were two to four orders of magnitude

greater than those explored by Redden et al. (1998). Under such conditions, the expected small relative loss of citrate is likely close to the TOC instrumental error.

To construct a model that would better describe U(VI) sorption behavior in the presence of citrate, citrate sorption data from Redden et al. (1998) were used to parameterize citrate-kaolinite reaction stoichometries and stability constants. Citrate edges were fit using both a DLM and NEM. A single-site DLM was developed by considering several surface complexes, including: $>SOHCitrate^{-3}$, $>SOH_2Citrate^{-2}$, $(>SOH)_2Citrate^{-3}$, $(>SOH_2^+)_2Citrate^-$, $(>SOH)_3Citrate^{-3}$, and $(>SOH_2^+)_3Citrate$. Complexation of citrate to any neutrally charged surface sites, i.e. $>SOHCitrate^{-3}$, $(>SOH)_2Citrate^{-3}$, $(>SOH)_3Citrate^{-3}$, could simulate the data equally well. In the absence of spectroscopic data to rule out any of these, the monodentate complex, according to:

$$>SOH + Citrate^{-3} \Leftrightarrow >SOHCitrate^{-3} \quad (7)$$

was chosen for simplicity (Figure 8.15). Very good simulations of the citrate data from Redden et al. (1998) are obtained with this reaction stoichiometry. A slight (~10%) overestimation of citrate sorption occurs at very low pH for $2.7 \cdot 10^{-7}$ M and $1.6 \cdot 10^{-6}$ M citrate experiments. The model parameterized using only citrate edges from Redden et al. (1998) produces very good predictions, well within the measured data range, for experiments with $1 \cdot 10^{-4}$ and $1 \cdot 10^{-2}$ M citrate from this study (Figure 8.15).

The DLM was used with the citrate-kaolinite and U(VI)-kaolinite surface reaction stoichiometries and stability constants derived for the individual binary systems to calculate U(VI) sorption for the kaolinite-U(VI)-citrate systems (Figures 8.13 and 8.14).

These initial predictions do not agree well with the measured U(VI) sorption data. Sorption is underestimated at low pH and overestimated at high pH, particularly in the presence of higher concentrations of citrate. In order to achieve a better fit to the data, ternary complexes were included in the model to increase the calculated uranyl sorption at low pH. Aqueous speciation calculations were used as a guide for composing possible ternary surface complexes. Calculations completed using MINTEQ show that in the presence of citrate three additional metal-ligand complexes are formed in solution, $UO_2Citrate^-$, $(UO_2)_2(Citrate)_2^{-2}$ and $NaCitrate^{-2}$ with the concentration of $NaCitrate^{-2}$ up to four orders of magnitude greater than that of U(VI)-Citrate complexes (Figure 8.16). Five ternary complexes, $>XOHUO_2Citrate^-$, $>(XOH)_2UO_2Citrate^-$, $>XOH_2UO_2Citrate$, $>XOUO_2Citrate^{-2}$, and $>(XO)_2UO_2Cit^{-3}$ were added to the DLM. However, FITQEL would not converge for optimizations of the stability constants of any of these five species, therefore, MINTEQ was used to fit these by eye. The best fit to the experimental data was found using a monodentate species according to the reaction,

$$>XOH + Citrate^{-3} + UO_2^{+2} \Leftrightarrow >XOUO_2Citrate^{-2} + H^+ \quad (8)$$

For low citrate concentrations (Figure 8.17) the model predictions are improved with the inclusion of this ternary complex, but still fail to correctly simulate the enhanced uranyl sorption at low pH. At high pH the model fails to accurately predict the loss of U(VI) from the surface for all but the edge with the lowest citrate concentration. As the concentration of citrate increases to $1 \cdot 10^{-4}$ and $1 \cdot 10^{-2}$ M citrate (Figure 8.18), model predictions become very poor across the entire pH range. Uranyl sorption is still

underestimated at low pH and overestimated at high pH, compelling consideration of other reactions to better describe U(VI) surface complexation in this system. Because the DLM failed to provide acceptable fits to the data across the entire range of measured data, and because the NEM provided superior fits for the EDTA system, additions of ternary complexes to the NEM were also attempted.

For the NEM, six different surface complexes and combinations of these were tested to account for the sorption of citric acid onto kaolinite in the absence of U(VI): $>SOHCitrate^{-3}$, $>SOH_2Citrate^{-2}$, $(>SOH)_2Citrate^{-3}$, $(>SOH_2^+)_2Citrate^-$, $(>SOH)_3Citrate^{-3}$, and $(>SOH_2^+)_3Citrate$ where >S represents either a titanol or an aluminol site. The best fit to the data was achieved with the following species: $>TiOH_3Citrate^-$, $>AlOH_3Citrate^-$ and $>AlOH_2Citrate^{-2}$, but the NEM fit to the TOC data underpredicts citrate sorption at low pH. In the circumneutral pH range the model generally describes the data well for all concentrations with the exception of the $2.7 \cdot 10^{-6}$ M citrate experiment, for which citrate adsorption is overestimated by ~10%. At high pH the model again slightly underestimates citrate sorption across the concentration range.

Initial NEM calculations of uranyl adsorption for the kaolinite-citrate-uranyl system completed using the species derived for the kaolinite-uranyl or kaolinite-citrate systems fail to correctly describe the ternary system edges (Figure 8.13 and 8.14). For high concentration citrate experiments ($1 \cdot 10^{-4}$ and $1 \cdot 10^{-2}$ M), the model greatly underestimates uranyl sorption. For the conditions of Redden et al. (1998), uranyl sorption is underestimated at low pH and overestimated at high pH for low concentrations of citrate. For greater additions of citrate (e.g., $1.6 \cdot 10^{-5}$ M citrate), a closer

approximation of the uranyl behavior is achieved at low pH, but sorption is overestimated at high pH.

To better fit the experimental data, ternary complexes were fit using the NEM. At the highest citrate concentration ($1 \cdot 10^{-2}$ M citrate), ~60% of the U(VI) is sorbed regardless of pH (Figure 8.13). For the NEM parameters, this is equivalent to half of all available sites, suggesting that bidentate uranyl-citrate species might be significant. As pointed out by Redden et al. (1998), citric acid, a ligand with three functional groups, is unlikely to bind to single surface sites to form monodentate complexes. Rather, a single sorbed ligand is likely to block multiple sites because each carboxyl group can potentially block a different site on the surface. For example, Cornell and Schindler (1980) used spectroscopic data to demonstrate that citrate can bind to goethite with multiple orientations, including as complexes that block several sites.

Bidentate citrate-uranyl species were also attempted for the DLM, but in contrast to the NEM, the addition of these complexes did not produce an improved fit compared to monodenate complexes. The disparity in behavior of the two models is due to the large difference in site densities. The DLM site density is four orders of magnitude greater than that used in the NEM. Thus, the addition of bidentate species to the NEM exhausts all of the available sites for high citrate concentrations, limiting the amount of U(VI) that may sorb onto the solid. In contrast, addition of bidentate complexes to the DLM, does not limit U(VI) sorption because there are enough sites for all of the bidentate uranyl-citrate complexes to bind at the surface.

Attempts to simulate U(VI) sorption behavior by including bidentate ternary complexes in the NEM failed to converge in FITEQL, therefore, MINTEQ was used to fit

stability constants for these complexes by eye. Two bidentate surface complexes (>$(TiO)_2UO_2$Citrate and >$(AlO)_2UO_2$Citrate with stability constants shown in Table 8.4), do provide an improved description of U(VI) sorption, but not a good fit overall. When applied to the data from Redden et al. (1998), the general trend of increased U(VI) sorption at low pH is correctly described for the $2.7 \cdot 10^{-7}$ and $2.7 \cdot 10^{-6}$ M citrate experiments, however, the total increase in uranyl sorption is overestimated (Figure 8.17). At pH above ~5, the model underestimates uranyl sorption in the presence of $2.7 \cdot 10^{-7}$ M citrate and greatly overestimates sorption with the addition of $2.7 \cdot 10^{-6}$ M citrate. The $1.6 \cdot 10^{-5}$ M citrate edge is not well described; uranyl sorption is greatly overestimated at all pH values. For $1 \cdot 10^{-4}$ and $1 \cdot 10^{-2}$ M citrate experiments, the model again falls short with sorption underpredicted at low pH and overpredicted at high pH (Figure 8.18).

Both the NEM and DLM fail to correctly simulate U(VI) sorption onto kaolinite in the presence of citrate over a broad range of conditions. Although some of the general trends are approximated, the individual edges cannot be simulated with the models tested in this study. Several issues may be responsible for the poor fits. These include: (1) the U(VI)-citrate stoichiometry changes with increasing citrate concentrations, and therefore a single set of ternary reactions does a poor job of predicting the citrate behavior over large variations in ligand concentration. Indeed, the same conclusion was drawn by Min (2006) for studies of 35 mg/L Cd sorption on kaolinite in the presence of 0 to 5 mM citric acid. An increase in Cd sorption was observed with small additions of citrate, however, at concentrations > 3 mM the amount of Cd sorbed was minimal. (2) Citrate may bind onto the solid with multiple surface configurations (i.e. monodentate, bidentate, tridentate),

with the predominant complex dependent on the citrate concentration. (3) With greater additions of citric acid, kaolinite dissolution might cause an increase of dissolved Si and Al that can compete for surface sites at high pH (>~8). In the absence of spectroscopic data, the configurations of metal and citrate at the kaolinite surface in this study remain speculative. Although the SCMs can be used to rule out species that are completely inconsistent with the experimental data, the many possible combinations of reaction stoichiometries make it difficult or impossible to constrain a unique set of reactions without complementary spectroscopic data.

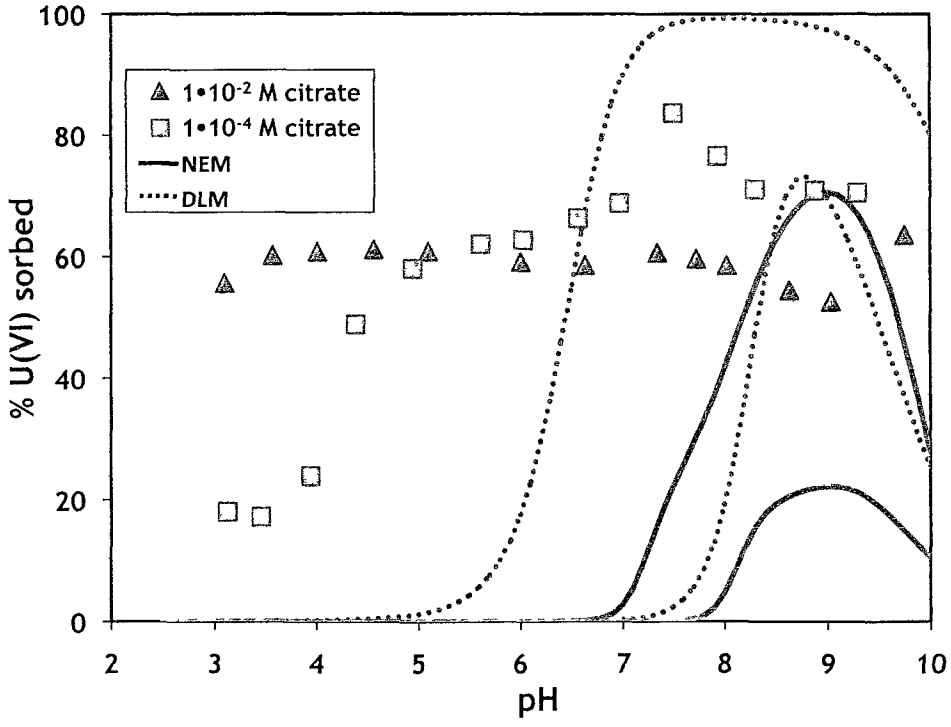

Figure 8.13. Sorption of $1 \cdot 10^{-5}$ M U(VI) on 2 g/L kaolinite in 0.01 M $NaNO_3$ with varying concentrations of citric acid. Lines indicate predicted U(VI) sorption with the NEM (solid) and DLM (dotted) assuming all citric acid remains in solution (assumed total $CO_3^{-2}{}_{(aq)} = 1.52 \cdot 10^{-5}$ M).

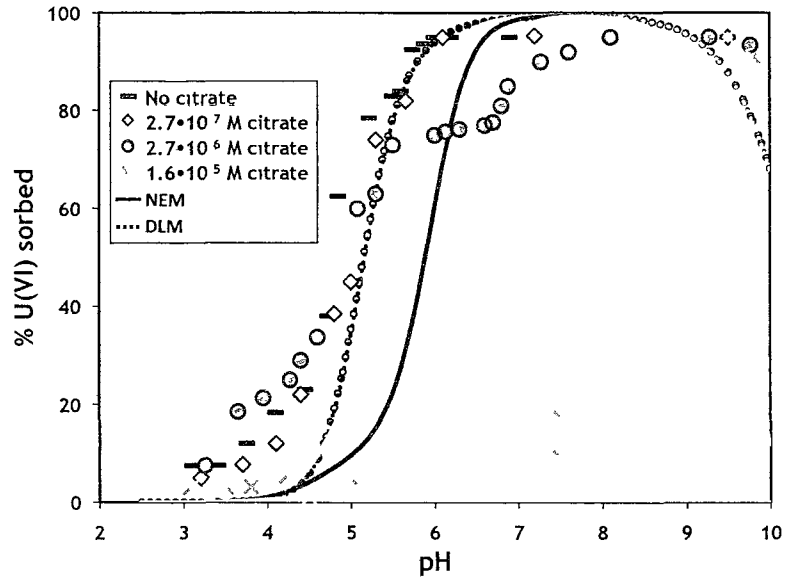

Figure 8.14. Citric acid sorbed as a function of pH and citrate concentration for experiments from Redden et al. (1998). Lines indicate predicted U(VI) sorption with the NEM (solid) and DLM (dotted) assuming all citric acid remains in solution (assumed total $CO_3^{-2}{}_{(aq)} = 1.52 \cdot 10^{-5}$ M).

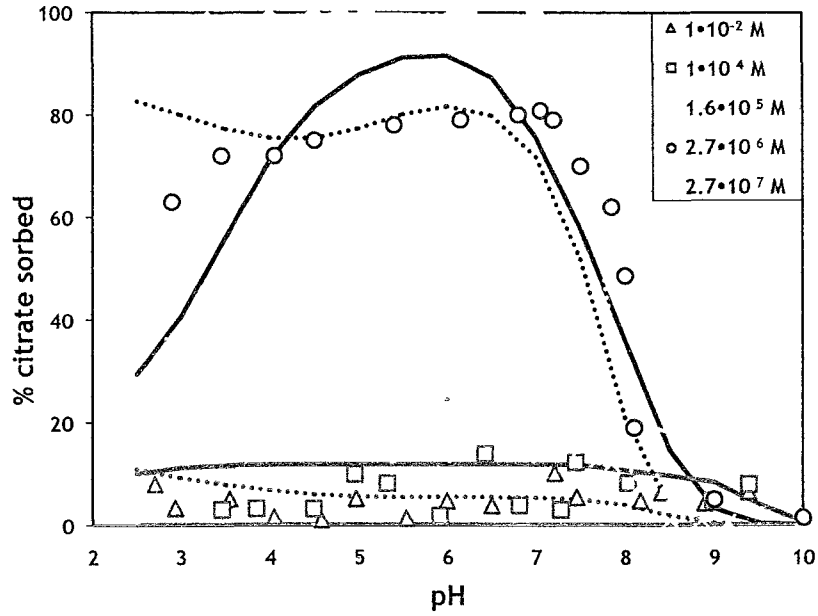

Figure 8.15. Citrate sorbed onto kaolinite, taken from Redden et al. (1998) and TOC results from this study. Lines indicate citrate sorption with the NEM (solid) and DLM (dotted) assuming all citric acid remains in solution (assumed total $CO_3^{-2}{}_{(aq)} = 1.52 \cdot 10^{-5}$ M).

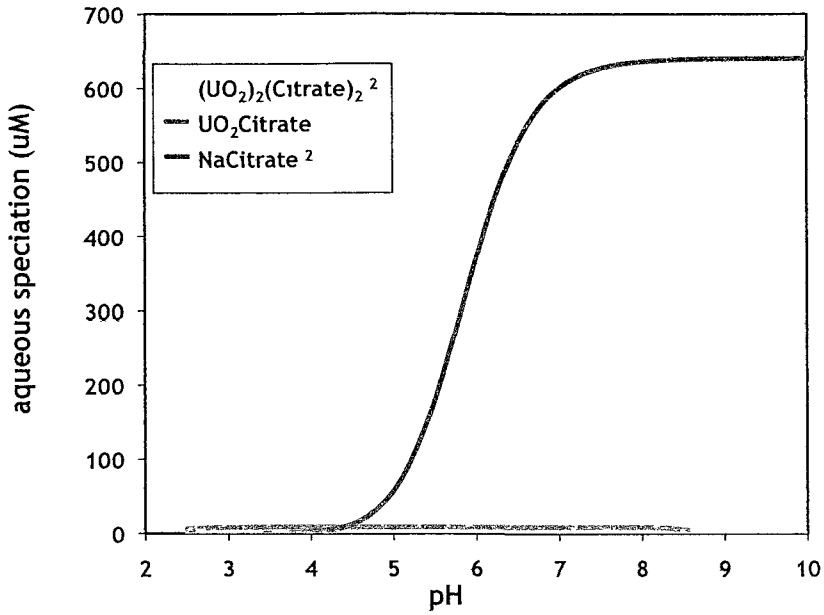

Figure 8.16. Speciation of citric acid as a function of pH calculated using MINTEQ with the NEA thermodynamic database (Table 8.3) for $1 \cdot 10^{-5}$ M U(VI), 0.01 M $NaNO_3$, 1.52 10^{-5} M $CO_3^{-2}{}_{(aq)}$ and 0.01 M citrate.

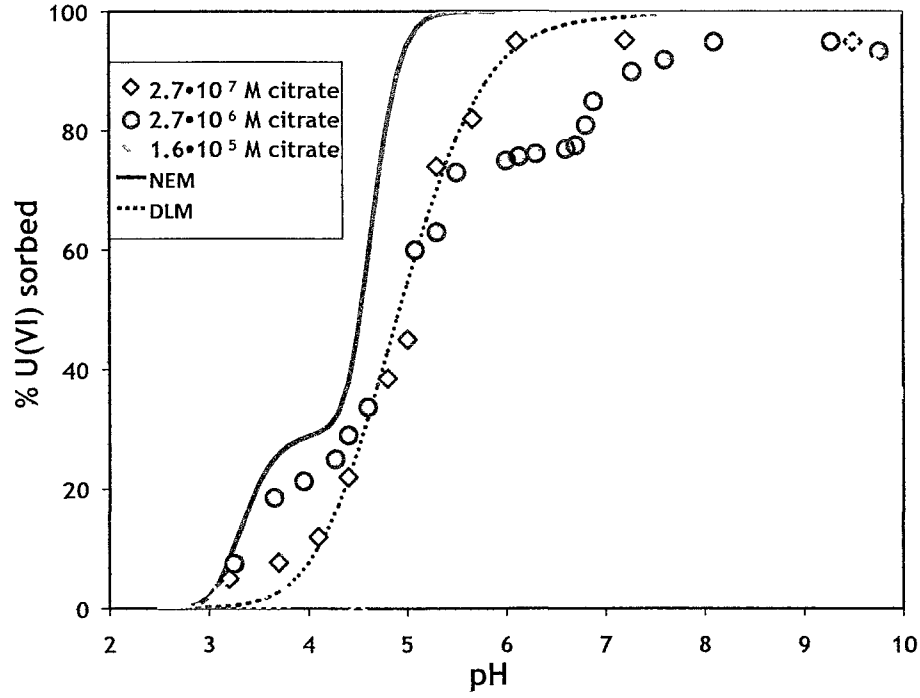

Figure 8.17. Sorption of citrate onto kaolinite from Redden et al., (1998) with NEM and DLM model fits (assumed total $CO_3^{-2}{}_{(aq)} = 1.52 \cdot 10^{-5}$ M).

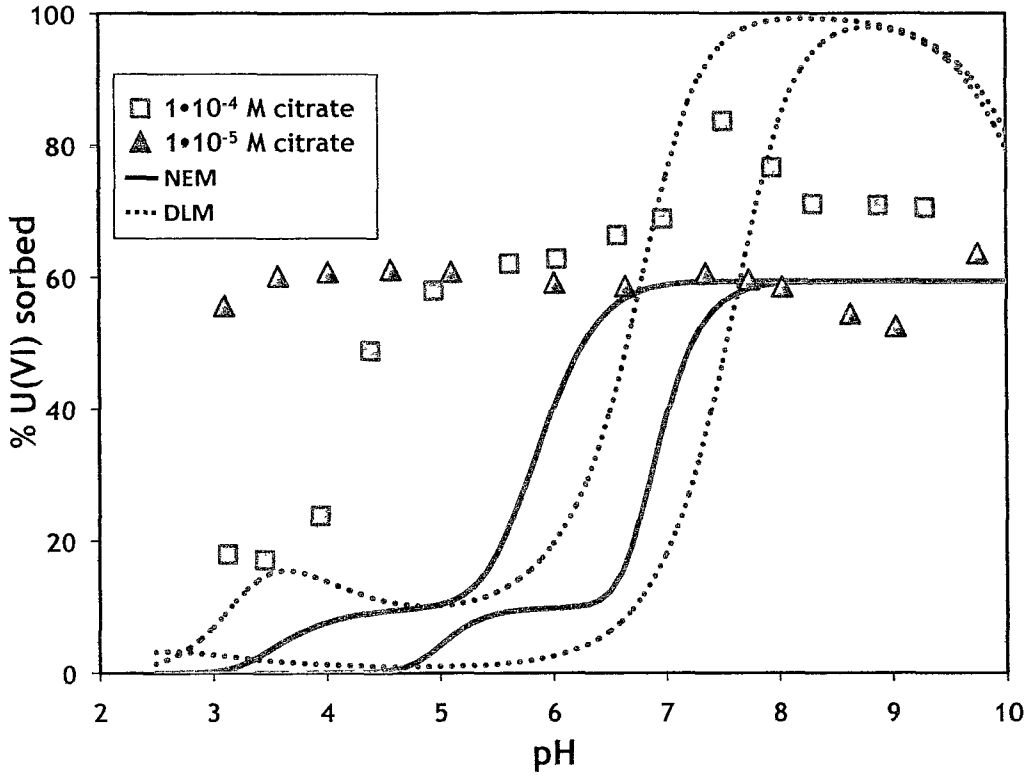

Figure 8.18. Data from this study, citrate sorbed as a function of pH and citrate concentration for experiments conducted with 2 g/L kaolinite in 0.01 M $NaNO_3$ and in the absence of U(VI). Experiments were completed under atmospheric conditions with tightly capped reactors (assumed total $CO_3^{-2}{}_{(aq)} = 1.52 \cdot 10^{-5}$ M).

U(VI) sorption to kaolinite in the presence of fulvic acid

Addition of fulvic acid leads to an increase in U(VI) sorbed from pH 3 to ~5 or 5.5 for 20 mg/L and 10 mg/L addition, respectively (Figure 8.19). 10 mg/L fulvic acid decreases U(VI) sorption by ~10%. In contrast, doubling the amount of fulvic acid added decreases sorption by up to 40% at pH ~7-9. TOC results show that ~50% of the 10 mg/L fulvic acid is lost from solution at low pH, and as pH increases the concentration of

ligand in solution increases. Similarly, TOC results for 20 mg/L fulvic acid demonstrate a 30% loss at low pH decreasing to levels below detection at high pH (Figure 8.20). These results are in good agreement with similar work done by Ren et al. (2010) and Zuyi et al. (2000) using other substrates. Ren et al. (2010) studied the effects of adding 10 or 20 mg/L fulvic acid (SRFA) to bentonite clay (MX-80) in 0.01 M $NaClO_4$ with $8.33 \cdot 10^{-5}$ M U(VI). A small increase in U(VI) sorption was observed below pH 5, but above pH 5 a 10 to 20% decrease in sorption took place. A similar effect was seen by Zuyi et al. (2000) for sorption of $3.2 \cdot 10^{-5}$ M U(VI) onto Al_2O_3 in 0.01 M $NaNO_3$ with the addition of 50 or 100 mg/L fulvic acid (extracted from weathered coal in Henan Province, P.R. China). Zuyi et al. (2000) observed up to a 10% increase in sorption at low pH and above pH ~7 a small decrease in U(VI) sorbed. Enhancement of metal sorption on clays in the presence of natural organic matter at low pH has been attributed to the formation of ternary complexes and diminished sorption at high pH is explained by the formation of aqueous U(VI)-fulvic acid species (Murphy et al., 1998; Zuyi et al., 2000; Ren et al., 2010). The formation of ternary complexes at low pH in this study is also consistent with TOC data, which demonstrate a loss of fulvic acid from solution as a function of pH, with more ligand removed from solution at low pH, presumably due to sorption onto the kaolinite surface. As the solid surface becomes increasingly negatively charged, a corresponding diminishment of fulvic acid loss from solution occurs as the ligand is released back into solution. Greater additions of fulvic acid result in a smaller pH range of enhanced U(VI) sorption and a more pronounced loss of U(VI) from the solid at high pH. For comparison, Krepelova et al. (2008) investigated the effects of 10 mg/L humic acid (HA) addition on $1 \cdot 10^{-4}$ M U(VI) sorption onto 4 g/L kaolinite (KGA-1b) in the presence of 0.1 M $NaClO_4$

over a pH range of 5 to 8 using XAS. They found U-O_{ax} distances of 1.78 Å, confirming the formation of U(VI)-HA-kaolinite ternary complexes.

The speciation of U(VI) in the presence of fulvic acid was calculated with the initial assumption that all of the fulvic acid remains in solution. Complexation of U(VI) to the fulvic acid was predicted using the default MINTEQ thermodynamic database with the NICA-Donnan method, and complexation of the U(VI) to kaolinite was calculated using either the DLM or NEM described above. These calculations suggest that the amount of U(VI) complexed to fulvic acid will increase with pH, from ~15 to 40% at pH 2.5, to 50 to 100% at ~4 to 6 (Figure 8.21). Above pH 6, aqueous U(VI)-fulvic complexes become less prevalent. With the first-order approximation that fulvic acid does not bind to the kaolinite surface, the NEM and DLM both predict a loss of U(VI) from the solid surface due to the formation of competitive aqueous U(VI)-fulvic acid species. Predictions of U(VI) sorption with the addition of fulvic acid are more reasonable at high pH using this assumption, but the model greatly underpredicts U(VI) sorption at low pH. This is not surprising, given that the TOC data shows significant loss of fulvic acid from solution at low pH. Using the pH-dependent concentration of U(VI) bound to fulvic acid predicted using the NICA-Donnan model, together with the fraction of fulvic acid bound to the solid surface from the TOC data, a simple calculation provides a rough estimate of U(VI) sorption via ternary complexes in the presence of fulvic acid. A simple linear fit to the TOC data was used to calculate the percentage of fulvic acid complexed to the kaolinite as a function of pH (Figure 8.20), and it was assumed that the U(VI) calculated to be bound to the fulvic acid using the Nica-Donnan model also sorbs to the surface. This approach neglects changes in U(VI) complexation at the surface

resulting from blockage of sites or changes to the electrical double layer caused by the sorbed fulvic acid, and it also neglects changes in the U(VI) aqueous speciation that would result from the additional binding of U(VI) to the kaolinite surface as ternary complexes. Nonetheless, it is clear that even this very simple calculation produces a better estimate of the U(VI) sorption edges at low pH (Figure 8.22). The remaining underestimation of sorption may in part be due to the crude method applied that cannot fully account for changes in U(VI) aqueous speciation in the presence of fulvic acid and the consequences these complexes would have for U(VI) interactions at the solid surface.

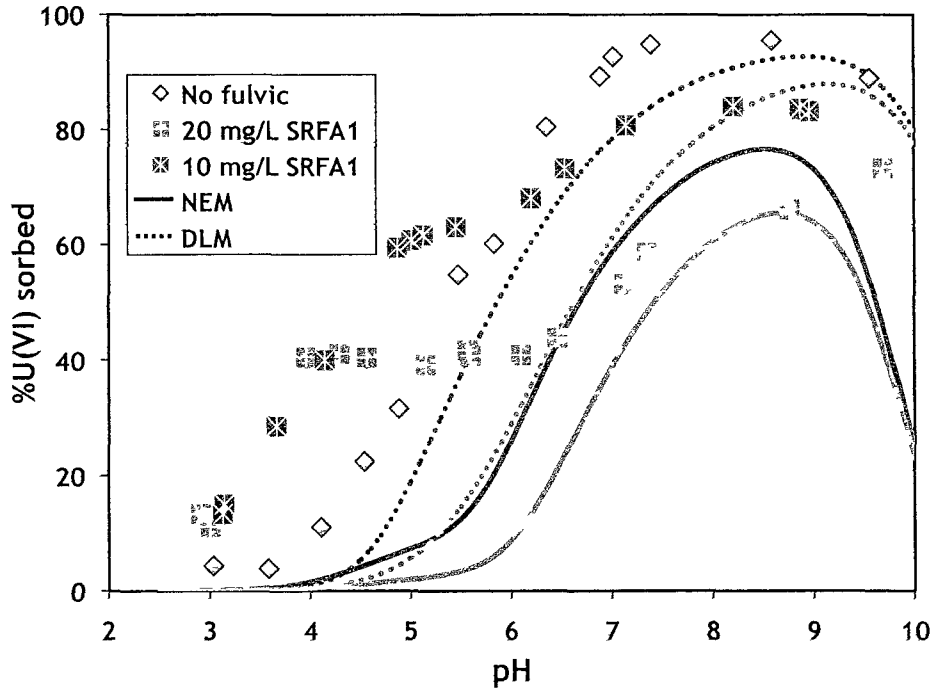

Figure 8.19. Sorption of $1 \cdot 10^{-5}$ M U(VI) on 2 g/L kaolinite in 0.01 M $NaNO_3$ with varying concentrations of fulvic acid. Lines indicate U(VI) sorption calculated with MINTEQ using the DLM (solid) or NEM (dotted) and the NICA-Donnan model to account for U(VI)-fulvic acid aqueous complexation, and assuming that all fulvic acid remains in solution with constant $1.52 \cdot 10^{-5}$ M $CO_3^{-2}{}_{(aq)}$.

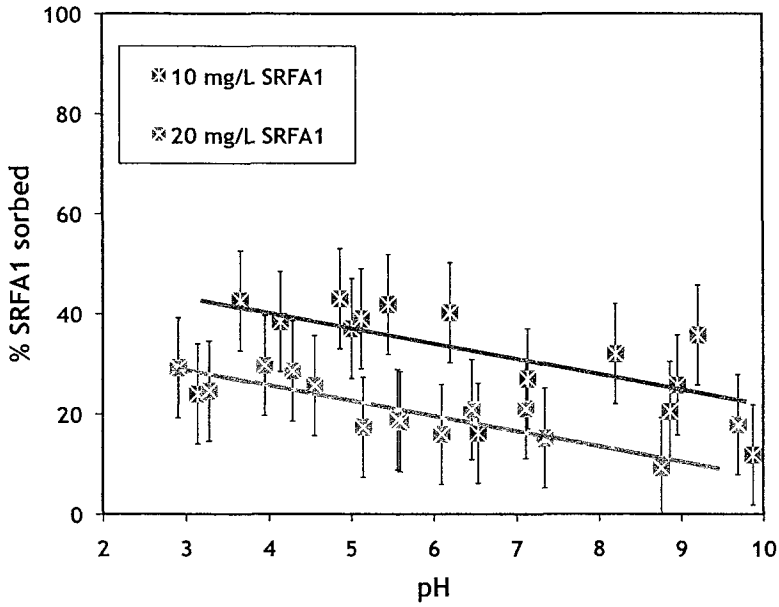

Figure 8.20. Fulvic acid sorbed as a function of pH and fulvic concentration for experiments conducted with 2 g/L kaolinite in 0.01 M $NaNO_3$, and in the absence of U(VI). Experiments were completed under atmospheric conditions with tightly capped reactors.

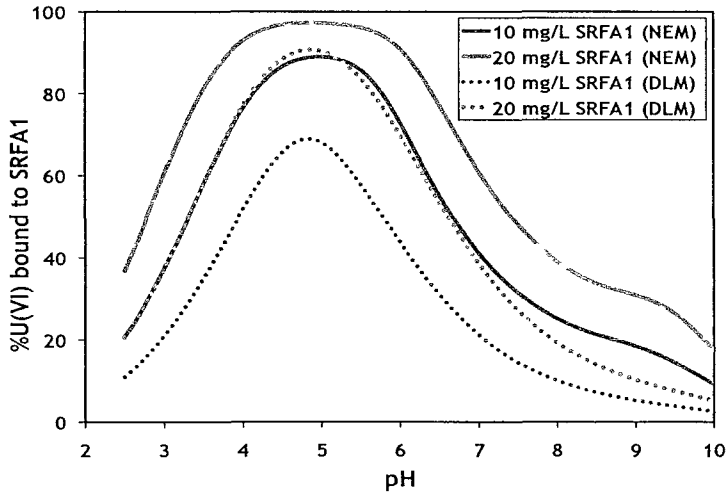

Figure 8.21. Percentage of U(VI) bound to fulvic acid as a function of pH calculated in MINTEQ using the NEM (solid lines) or DLM (dotted lines) with the NICA-Donnan default database to account for U(VI)-fulvic acid complexation in solution and assuming $1.52 \cdot 10^{-5}$ M total $CO_3^{-2}{}_{(aq)}$.

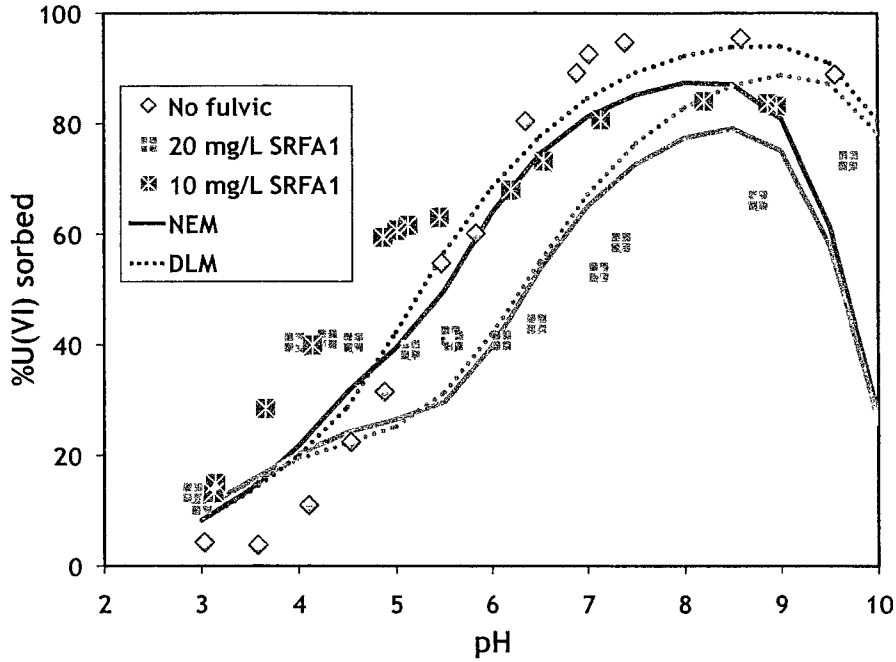

Figure 8.22. Sorption of 10^{-5} M U(VI) on 2 g/L kaolinite in 0.01 M $NaNO_3$ with varying concentrations of fulvic acid. Lines indicate U(VI) sorption calculated with MINTEQ using the DLM (solid) or NEM (dotted) and the NICA-Donnan model to account for U(VI)-fulvic acid aqueous complexation. Fulvic acid, together with complexed U(VI), is assumed to bind to the surface as a linear function of pH derived from TOC data.

CHAPTER IX

CONCLUSIONS AND FUTURE WORK

$U(IV)O_{2(s)}$ dissolution

Hydrolysis of $UO_{2(s)}$ performed under oxidizing conditions resulted in U activities that were in agreement with past literature values for U in the hexavalent state. Hydrolysis of $UO_{2(s)}$ under reducing conditions was shown to produce lower U activities when compared to oxidizing conditions, however solubility was still higher than those established by past workers. For no-ligand experiments, the presence of U(VI) is almost certainly responsible for the elevated U activities observed.

$UO_{2(s)}$ solubilization experiments conducted in the presence of citrate, NTA or EDTA under anaerobic conditions did not result in enhanced dissolution when compared to the hydrolysis results. Under ambient atmosphere, UO_2 dissolution is slightly higher when compared to data obtained under reducing conditions. The similarity between the data obtained for the two redox conditions again suggests that U(VI) is present. In addition, the lack of pH dependence observed for all experiments is reflective of U(VI) hydrolysis. Experiments may also have been influenced by the presence of Eu(II), which may have provided a competing cation, suppressing complexation of U by the organic ligands.

Although the effects of citrate, NTA and EDTA on UO_2 dissolution were not clearly elucidated by this work, these experiments are nonetheless valuable, because they demonstrate the significant challenges involved in maintaining pure $U(IV)O_2$. These

experiments help to isolate methods that are not effective under experimental conditions, and also suggest that under most environmentally relevant conditions, some U(VI) is likely to be present at the surface of $U(IV)O_2$, with significant ramifications for the reactivity of the solid. To better investigate U(IV) complexation with ligands under reducing conditions, the following methods are suggested:

(1) Extend the pH range investigated to include the first order hydrolysis. By investigating solubility at low pH (2-4), more controls would be gained and better interpretations could be determined. A secondary confirmation regarding the presence or absence of U(VI) could be made.

(2) Potential complications from the reductant, Eu(II), are uncertain. The concentration of Eu(II) added was two orders of magnitude greater than the expected O_2 concentration in solution. The concentration of Eu(II) could be reduced.

(3) Experiments could be approach from the point of oversaturation, which would eliminate problems with U(VI) on the solid surface. However, lengthy equilibration periods are needed to precipitate crystalline, rather than amorphous UO_2.

(4) To better investigate the effect of ligands it is suggested that the concentration of ligands be increased by at least an order of magnitude. This study considered a relatively small concentration range (100 – 500 mM); to better discern the effects of ligand promoted dissolution experiments covering multiple orders of magnitude in ligand concentration might be useful.

U(VI) sorption on kaolinite

Significant loss of U(VI) from no-solid control experiments shows that sorption to polypropylene container walls can potentially skew experimental results. However, uranyl loss to the container does not occur significantly in the presence of KGa-1b under the specific conditions used in this study, and thus competitive effects of the container wall can be ignored. Nonetheless, the control experiments demonstrate the significant potential for U(VI) to be lost to vessel walls, and it is emphasized that for other systems extraction of U(VI) from the container should be performed to ensure that any loss of U(VI) is insignificant.

Sorption of U(VI) to kaolinite (KGa-1b) shows little ionic strength dependence, but is strongly effected by pH, with 100% sorption in the circumneutral range. This shows that clay minerals may be an important impediment to U(VI) mobilization in the subsurface. By increasing pCO_2 to levels commonly found in soils and subsurface sediments, a large decrease in U(VI) sorbed, particularly at pH > 6, is observed and attributed to the increase in aqueous U(VI)-carbonato complexes. A NEM developed by Payne et al. (2004) was used to successfully simulate U(VI) sorption behavior as a function of pH, pCO_2 and ionic strength. To account for possible electrostatic effects, especially in the presence of organic ligands, a single-site DLM was also developed. The DLM was equally capable of describing U(VI) sorption for varying pCO_2, pH and ionic strength.

The addition of EDTA, citric or fulvic acid had a significant influence on U(VI) sorption to kaolinite, suggesting that these ligands may provide important controls on U(VI) mobility and bioavailability in the environment. Consistent with prior work using

other sorbates and sorbents, this study suggests that U(VI)-ligand-kaolinite complexes form at low pH. All three organic acids tended to decrease U(VI) sorption at high pH, with more pronounced effects observed with increasing concentrations of the organic acids. Addition of the organic acids enhances U(VI) sorption at low pH, presumably due to the formation of kaolinite-organic ligand-U(VI) ternary complexes. This could be simulated reasonably well in the NEM and DLMs developed for both EDTA and citric acid additions through inclusion of ternary surface complexes. The poor model fits over broad ranges in solution pH could reflect inaccuracies in estimates of the total CO_3^{-2} in solution, or in the aqueous speciation of U(VI) in the presence of the organic ligands. Furthermore, the site density postulated by Sverjensky and Sahai (1996) does not allow competition to occur between U(VI) and sodium for surface sites at high pH, because the large surface site density allows accommodation of both U(VI) and Na-EDTA surface complexes. This suggests that either a more sophisticated description of the electrostatics is required, or that there are inaccuracies in the predicted U(VI) aqueous speciation in the presence of the organic acids. The lack of full equilibration with ambient pCO_2 may also have contributed to the lack of good fits achieved with either the NEM or the DLM over the broad range of tested solution composition. TOC data helped to constrain the choice of models, however, more spectroscopic data (e.g. XAS) would also be useful to provide more constraints on the SCM descriptions of U(VI) sorption in the presence of these organic acids.

REFERENCES

Abdelouas, A: Uranium mill tailings: geochemistry, mineralogy, and environmental impact. *Elements* 2006, 2: 335-351.

Abdelouas A, Lutze W, Nuttall E: Uranium contamination in the subsurface: Characterization and remediation. *Reviews in Mineralogy, Uranium: Geochemistry and the Environment* 1999, 434-473.

Aiken GR, McKnight DM, Wershaw RL, McCarthy P: Humic substances in soil, sediment and water. Wiley, New York, p: 692.

Arda D, Hizal R, Apak R: Surface complexation modeling of U(VI) adsorption onto kaolinite based clay minerals using FITEQL 3.2. *Radiochimica Acta* 2006, 94:835-844.

Blanpain P, Capus G, Palussiere JC: Nuclear fuel cycle front end chemistry. *Chimia* 2005, 59: 849-897.

Bonin L, Guillaumont D, Jeanson A, Den Auwer C, Grigoriev M, Berthet JC, Hennig C, Scheinost A, Moisy PH: Thermodynamic and structure of actinide(IV) complexes with nitrilotriacetic acid. *Inorganic Chemistry* 2009, 48: 3943-3953.

Borkowski M, Lis S, Choppin GR: Complexation study of NpO_2^+ and UO_2^{2+} ions in several organic ligands in aqueous solutions of high ionic strength. Radiochemica Acta 1996, 74: 117-121.

Borovec Z: The adsorption of uranyl species by fine clay. *Chemical Geology*, 1981, 32:45-58.

Brady NC, Weil RR: *The Nature and Properties of Soils, fourteenth edition.* Pearson Prentice Hall 1999, 317-319.

Bruno J, Casas I, Lagerman B, Munoz M: The determination of the solubility of amorphous UO2(s) and the monoduclear hydrolysis constats of uranium(IV) at 25C *Materials Research Society Proceedings* 1987, 153-160.

Burns PC: The crystal chemistry of uranium. *Reviews in Mineralogy, Uranium: Geochemistry and the Environment* 1999, 23-90.

Casey WH, Ludwig C: Silicate mineral dissolution as a ligand-exchange reaction. *Reviews in Mineralogy Volume 31: Chemical weathering rates of silicate minerals* 1995, (31) 88-117.

Catalano JG, McKkinley JP, Zachara JM, Heald SM, Smith SC, Brown Jr GE: Changes in uranium speciation through a depth sequence of contaminated Hanford sediments. *Environmental Science and Technology* 2006, 40:2517-2524.

Catalano JG, Brown Jr GE: U(VI) adsorption onto montmorillonite: evaluation of binding sites and carbonate complexation. *Geochimica et Cosmochimica Acta* 2005, 69:2995-3005.

Chisholm-Brause CJ, Berg JM, Matzner RA, Morris DE: Uranium (VI) sorption complexes on montmorillonite as a function of solution chemistry. *Journal of Colloid and Interface Science* 2001, 233:38-49.

Choy CC, Korfiatis GP, Meng X: Removal of depleted uranium from contaminated soils. *Journal of Hazardous Materials* 2006, 136:53-60.

Clark DL, Hobart DE, Neu MP: Actinide carbonate complexes and their importance in actinide environmental chemistry. *Chemical Reviews* 1995, 95:25-48.

Cordfunke EHP: The chemistry of uranium: Including its applications in nuclear technology 1969, 23-65.

Cornell RM, Schindler PW: Infrared study of the adsorption of hydroxycarboxylic acids on alpha-FeOOH and amorphous Fe(III) hydroxide. *Colloid and Polymer Science* 1980, 258:1171-1175.

Cotton S: Introduction to the actinides. *Lanthanide and Actinide Chemistry* 2006, 145-152.

Davis JA, Meece DE, Kohler M, Curtis GP: Approaches to surface complexation modeling of uranium (VI) adsorption on aquifer sediments. *Geochimica et Cosmochimica Acta.* 2004, 68:3621-3641

Del Cul GD, Toth LM, Bond WD, Williams DF: Evaluation of processes that might lead to separation of actinides in waste storage tanks under alkaline conditions. *Separation Science and Technology* 2000, 35:2127-2141.

Drever JI, Stillings LL: The role of organic acids in mineral weathering. *Colloids and Surfaces* 1997, 120: 167-181.

Drever JI, Vance GF: Role of soil organic acids in mineral weathering processes. *Organic Acids in Geologic Processes* 1994, 116-138.

Dzomback DA, Morel FMM: The generalized two-layer model. *Surface Complexation Modeling: Hydrous Ferric Oxide* 1989, 9-42.

Eby, GN: Equilibrium thermodynamics and kinetics. *Principles of Environmental Geochemistry* 2004, 27-58.

Ewing RC: Radioactivity and the 20th century. *Reviews in Mineralogy, Uranium: Geochemistry and the Environment* 1999, 38:1-19.

Felmy AR, Cho H, Dixon DA, Xia Y, Hess NJ, Wang Z: The aqueous complexation of thorium with citrate under neutral to basic conditions. *Radiochemica Acta* 2006, 94: 205-212.

Finch R, Murakami T: Systematics and paragenesis of uranium minerals. *Reviews in Mineralogy, Uranium: Geochemistry and the Environment* 1999, 92-179.

Francis AJ, Dodge CJ, Gillow JB, Cline JE: Microbial transformations of uranium in wastes. Radiochemica Acta 1991, 52(3): 311-316.

Friedly, JC, Kent DB, Davis JA: Simulation of the mobility of metal-EDTA complexes in groundwater: The influence of contaminant metals. *Environmental Science and Technology* 2002, 36:355-363.

Fuger J: Problems in the thermodynamics of the actinides in relation with the back-end of the nuclear-fuel cycle. Journal of Nuclear Materials 1993, 201: 3-14.

Gao L, Yang Z, Shi K: U(VI) sorption on kaolinite effects on pH, U(VI) concentration and oxyanions. *Journal of Radioanalytical and Nuclear Chemistry* 2010, 284:519-526.

Gayer KH, Leider H: The solubility of uranium(IV) hydroxide in solutions of sodium hydroxide and perchloric acid at 25-degrees-C. Canadian Journal of Chemistry 1957, 35: 5-7.

Garcia-Gonzalez N, Ordonez-Regil E, Simoni E, Barrera-Diaz E: Effects of organic acids on sorption of U(VI) ions in solution onto ZrP_2O_7. *Journal of Radioanalytical and Nuclear Chemistry* 2010, 283:409-415.

Grenthe I: Thermodynamics in Migration Chemistry. *Radiochimica Acta* 1991, 52/53: 425-432.

Herblin AL, Westall J: FITEQL – a computer program for determination of chemical equilibrium constants from experimental data. Department of Chemistry, Oregon State University, Corvallis, OR, Rep 1999.

Huang FH: Container materials in environments of corroded spend nuclear fuel. *Journal of Nuclear Materials* 1996, 231: 74-82.

Hummel W, Puigdomenech I, Rao L, Tochiyama O: Thermodynamic data of compunds. and complexes of U, Np, Pu and Am with selected organic ligands. *Chimie* 2007, 10: 948-958.

Jiang GCT, Aschner M: Neurotoxicity of depleted uranium. *Biological Trace Element Research* 2005, 110: 1-6.

Jones DL: Organic acids in the rhizosphere – a critical review. *Plant and Soil* 1998, 205: 24-44.

Klein C, Hurlbut CS Jr: Systematic mineralogy part IV: Silicates. *Manual of Mineralogy 21st Edition* 1985, 440-557.

Knepper TP: Synthetic chelating agents and compounds exhibiting complexing properties in the aquatic environment. *Trends in Analytical Chemistry* 2003, 23: 708-724.

Kohler M, Wieland E, Leckie JO: Metal-ligand-surface interactions during sorption of uranyl and neptunyl on oxides and silicates. In: *Water-Rock Interactions (VII)*: Edited by: Kharaka YK, Maest AS. Rotterdam: Balkema; 1992, 51-54.

Koretsky C: The significance of surface complexation reactions in hydrologic systems: a geochemist's perspective. *Journal of Hydrology* 2000, 230: 127-171.

Krepelova A, Rech T, Sachs S, Drebert J, Bernhard G: Structural characterization of U(VI) surface complexes on kaolinite in the presence of humic acid using EXAFS spectroscopy. *Journal of Colloid and Interface Science* 2008, 319:40-47.

Landry CJ, Koretsky CM, Lund TJ, Schaller M, Das S: Surface complexation modeling of Co(II) adsorption on mixtures of hydrous ferric oxide, quartz and kaolinite. *Geochimica et Cosmochimica Acta* 2009, 73:3723-3737.

Langmuir D: Aqueous environmental geochemistry. Prentice Hall, Upper Saddle River, NJ, 1997, 600.

Lee KY, Yoon YY, Lee SG, Lee DH, Kim YJ, Woo NM: Sorption of radionuclides on the container wall during batch migration studies. *Journal of Radioanalytical and Nuclear Chemistry* 2001, 249:271-278.

Lenhart JJ, Cabaniss SE, MacCarthy P, Honeyman BD: Uranium(VI) complexation with citric, humic and fulvic acids. *Radiochimica Acta* 2000, 88:345-353.

Min L: Effects of organic acids on adsorption of cadmium onto kaolinite, goethite and bayerite. *Pedosphere* 2006, 16:185-191.

McKeague JA, Cheshire MV, Andreux F, Berthelin J: Organo-mineral complexes in relation to pedogenesis. *Interactions of Soil Minerals with Natural Organics and Microbes* 1986, 17: 549-592.

Morel FMM, Herring JG: Solid dissolution and precipitation: Acquisition and control of alkalinity. *Principles and Applications of Aquatic Chemistry* 1993, 236-318.

Morrison SJ, Spangler RR: Extraction of uranium and molybdenum from aqueous solutions: A survey of industrial materials for use in chemical barriers for uranium mill tailings remediation. *Environmental Science and Technology* 1992, 26: 1922-1931.

Murphy RJ, Lenhart JJ, Honeymon BD: The sorption of thorium (IV) and uranium (VI) to hematite in the presence of natural organic matter. *Colloids and Surfaces* 1999, 157:47-62.

Murphy WM, Shock EL: Environmental aqueous geochemistry of actinides. *Reviews in Mineralogy, Uranium: Mineralogy, Geochemistry and the Environment* 1999, 38:221-253.

Nebelung C, Brendler V: U(VI) sorption on granite: prediction and experiments. *Radiochimica Acta* 2010, 98:621-625.

Neck V, Kim JI: Solubility and hydrolysis of tetravalent actinides. *Radiochemica Acta* 2001, 89: 1-16.

Nowack B, Lutzenkirchen J, Behra P, Sigg L: Modeling the adsorption of metal-EDTA complexes onto oxides. *Environmental Science and Technology* 1996, 30: 2397-2405.

Oburger E, Kirk GJD, Wenzel WW, Puschenreiter M, Jones DL: Interactive effects of organic acids in the rhizosphere. *Soil Biology & Biochemistry* 2009, 41:449-457.

Pabalan R, Turner D, Bertetti P, Prikryl JD: Uranium(VI) sorption onto selected mineral surfaces. In: *Adsorption of metals by geomedia; variables, mechanisms, and model applications* 1997, 99-130.

Parks GA, Pohl DC: Hydrothermal solubility of uraninite. *Geochemica Cosmochimica Acta* 1988, 52: 863.

Pasilis SP, Pemberton JE: Speciation and coordination chemistry of uranyl(VI)-citrate complexes in aqueous solution. Inorganic Chemistry 2003, 42 (21): 6793-6800.

Pathak PN, Choppin GR: Sorption of U(VI) ion on hydrous silica: effects of ionic strength and ethylenediaminetetraacetic acid (EDTA). *Journal of Radioanalytical and Nuclear Chemistry* 2007, 272:37-43.

Payne TE, Davis JA, Lumpkin GR, Chisari R, Waite TD: Surface complexation model of U(VI) sorption on Georgia kaolinite. *Applied Clay Science* 2004, 26:151-162.

Pittman ED, Lewman MD: Introduction to the role of organic acids in geologic processes. *Organic Acids in Geologic Processes* 1994, 1-21.

Prickryl JD, Jain A, Turner DR, Pabalan RT: UraniumVI sorption behavior on silicate mineral mixtures. *Journal of Contaminant Hydrology* 2001, 4:241-253.

Prikryl JD, Pabalan RT, Turner DR, Leslie BW: Uranium sorption on α-alumina: effects of pH and surface-area/solution-volume ratio. *Radiochimica Acta* 1994, 66/67: 291-296.

Rai D, Yui Mikazu, Moore DA: Solubility and solubility product at 22°C of UO2(c) precipitated from aqueous U(IV) solutions. Journal of Solution Chemistry 2003 32: 1-17.

Rai D, Felmy AR, Sterner SM, Moore DA, Mason MJ, Novak CF: The solubility of Th(IV) and U(IV) hydrous oxides in concentrated NaCl and MgCl2 solutions. Raidochemica Acta 1997, 79: 239.

Rai D, Felmy AR, Ryan JL: Uranium(IV) hydrolysis constants and solubility product of $UO_2 \cdot xH_2O$(am). *Inorganic Chemistry* 1990, 29: 260-264.

Redden, Li, Leckie: Sorption of U(VI) and citric acid on kaolinite. *In: Adsorption of metals by geomedia: variables, mechanisms, and model applications* 1998, 90-311.

Ren X, Wang S, Yang S, Li J: Influence of contact time, pH, soil humic/fulvic acids, ionic strength and temperature on sorption of U(VI) onto MX-80 bentonite. *Journal of Radioanalytical and Nuclear Chemistry* 2010, 283:253-259.

Ryan JL, Rai D: The solubility of uranium(IV) hydrous oxide in sodium hydroxide solutions under reducing conditions. *Polyhedron* 1983, 2: 947.

Sachs S, Bernhard G: Sorption of U(VI) onto an artificial humic substance-kaolinite associate. *Chemosphere* 2008, 72:1441-1447.

Sherman DM, Peacock CL, Hubbard CG: Surface complexation of U(VI) on goethite (α-FeOOH). *Geochimica et Cosmochimica Acta* 2008, 72:298-310.

Shock EL, Sassani DC, Betz H: Uranium in geologic fluids: Estimates of standard partial molal properties, oxidation potentials, and hydrolysis constants at high temperatures and pressures. *Geochimica et Cosmochimica Acta*, 1997, 61 (20):4245-4266.

Shoesmith DW: Fuel corrosion processes under waste disposal conditions. *Journal of Nuclear Materials* 2000, 282: 1-31.

Stevenson FJ: Organic acids in soil. *Soil biochemistry* 1967, 1: 119-146.

Strobel BW: Influence of vegetation on low-molecular-weight carboxylic acids in soil solution – a review. *Geoderma* 2001, 99: 169-198.

Stumm W, Morgan JJ: *Aquatic Chemistry: Chemical equilibria and rates in natural waters, 3rd edition.* New York: Wiley; 1996.

Sverjensky, D. Sahai, N: Theoretical prediction of single-site surface-protonation equilibrium constants for oxides and silicates in water. *Geochimica et Cosmochimica* 1996, 60:3773-3797.

Tertre E, Berger G, Castet S, Loubet M, Giffaut, E: Experimental sorption of Ni^{2+}, Cs^{+} and Ln^{3+} onto a montmorillonite up to 150°C. *Geochimica et Cosmochimica*, 2005, 69:4937-4989.

Toste AP, Osborn BC, Polach KJ, Lechner-Fish TJ: Organic analyses of an actual and simulated mixed waste: Hanford's organic complexant waste revisited. *Journal of Radioanalytical and Nuclear Chemistry* 1995, 194 (1): 25-34.

Turner DR, Sassman SA: Approaches to sorption modeling for high-level waste performance assessment. *Journal of Contaminant Hydrology* 1996, 21:311-332.

Uijt de Haag PAM, Smetsers RCGM, Witlox HWM, Krus HW, Disenga AHM: Evaluating the risk from depleted uranium after the boeing 747-258F crash in Amsterdam, 1992. *Journal of Hazardous Materials* 2000, A76: 39-58.

Villalobos M, Trotz MA, Leckie JO: Surface complexation modeling of carbonate effects on the adsorption of Cr(VI), Pb(II), and U(VI) on goethite. *Environmental Science and Technology* 2001, 35:3849-3856.

Waite TD, Davis JA, Fenton BR, Payne TE: Approaches to modeling uranium (VI) adsorption on natural mineral assemblages. *Radiochimica Acta* 2000, 88:687-693.

Wood SA: The role of humic substances in the transport and fixation of metals of economic interest (Au, Pt, Pd, U, V). *Ore Geology Reviews* 1996, 11:1-31.

Wronkiewicz DJ, Buck EC: Uranium mineralogy and the geologic disposal of spent nuclear fuel. *Reviews in Mineralogy, Uranium: Geochemistry and the Environment* 1999, 38: 475-494.

Xia Y, Felmy AR, Rao L, Wang Z, Hess N. Thermodynamic model for the solubility of $ThO_{2(am)}$ in the aqueous Na^{+}-H^{+}-OH^{-}-NO_3^{-}-H_2O-EDTA system. *Radiochemica Acta* 2003, 91: 751-760.

Yajima T, Kawamura Y, Ueta S: Uranium(IV) solubility and hydrolysis constants under reduced conditions. *Materials Research Society Proceedings.* 1995, 353: 1137.

Zachara JM, Smith SC, Kuzel LS: Adsorption and dissociation of Co-EDTA complexes in iron oxide-containing subsurface sands. *Geochimica et Cosmochimica Acta* 1995, 59:4825-4844.

Zhiwei N, Qiaohui F, Wenhua W, Junzheng X, Lei C, Wangsuo W: Effect of pH, ionic strength and humic acid on the sorption of uranium (VI) to attapulgite. *Applied Radiation and Isotopes* 2009, 67:1582-1590.

Zuyi T; Taiwei C, Jinzhoiu D, XiongXin D, Yingjie, G: Effect of fulvic acids on sorption of U(VI), Zn, Yb, I and Se(IV) onto oxides of aluminum, iron and silicon. *Applied Geochemistry* 2000, 15:133-139.